Energy & Environmental Science

ROYAL SOCIETY OF CHEMISTRY

REVIEW

View Article Online
View Journal | View Issue

Cite this: *Energy Environ. Sci.*, 2022, **15**, 2690

Hydrogen liquefaction: a review of the fundamental physics, engineering practice and future opportunities

Saif ZS. Al Ghafri, [ab] Stephanie Munro,[a] Umberto Cardella,[c] Thomas Funke,[d] William Notardonato,[e] J. P. Martin Trusler,[f] Jacob Leachman,[g] Roland Span, [h] Shoji Kamiya,[i] Garth Pearce, [j] Adam Swanger,[k] Elma Dorador Rodriguez,[a] Paul Bajada,[a] Fuyu Jiao,[a] Kun Peng,[a] Arman Siahvashi,[a] Michael L. Johns [ab] and Eric F. May *[ab]

Received 12th January 2022,
Accepted 20th April 2022

DOI: 10.1039/d2ee00099g

rsc.li/ees

Hydrogen is emerging as one of the most promising energy carriers for a decarbonised global energy system. Transportation and storage of hydrogen are critical to its large-scale adoption and to these ends liquid hydrogen is being widely considered. The liquefaction and storage processes must, however, be both safe and efficient for liquid hydrogen to be viable as an energy carrier. Identifying the most promising liquefaction processes and associated transport and storage technologies is therefore crucial; these need to be considered in terms of a range of interconnected parameters ranging from energy consumption and appropriate materials usage to considerations of unique liquid-hydrogen physics (in the form of *ortho–para* hydrogen conversion) and boil-off gas handling. This study presents the current state of liquid hydrogen technology across the entire value chain whilst detailing both the relevant underpinning science (*e.g.* the quantum behaviour of hydrogen at cryogenic temperatures) and current liquefaction process routes including relevant unit operation design and efficiency. Cognisant of the challenges associated with a projected hydrogen liquefaction plant capacity scale-up from the current 32 tonnes per day to greater than 100 tonnes per day to meet projected hydrogen demand, this study also reflects on the next-generation of liquid-hydrogen technologies and the scientific research and development priorities needed to enable them.

Broader context

The global trade of fossil fuels amounts to over 3200 million tonnes of coal and oil and more than 850 billion cubic metres of gas each year. Average global atmospheric carbon dioxide levels have exceeded 410 parts per million and are higher than at any point in the past 800 000 years. Amidst growing pressure for countries to decarbonise their economies, future energy trading will increasingly include low- and zero-emissions production. There is a growing international consensus that hydrogen will play a key role in the world's transition to a sustainable energy future. Transportation of hydrogen over long distances will likely require both liquefaction and intermediate storage. However, hydrogen liquefaction has not yet been deployed at a scale necessary to supply projected liquid hydrogen demand. As a fluid that is not well understood at cryogenic temperatures and high pressures, liquid hydrogen presents a variety of technical, economic, and commercial challenges. This paper identifies the key research challenges that must be addressed over the course of the next decade in each of these areas.

[a] *Fluid Science and Resources Division, Department of Chemical Engineering, University of Western Australia, Crawley, WA 6009, Australia. E-mail: eric.may@uwa.edu.au*
[b] *Future Energy Exports Cooperative Research Centre, 35 Stirling Hwy, Crawley, WA 6009, Australia*
[c] *HS Kempten, 87435 Kempten (Allgäu)*
[d] *FormFactor GmbH, Süss Straße 1, Registergericht Dresden HRB 3021, 01561 Thiendorf, Germany*
[e] *MitaVista, the Space Life Science Lab Suite 201C, 505 Odyssey Way, Exploration Park, FL 32953, USA*
[f] *Department of Chemical Engineering, Imperial College London, South Kensington Campus, London SW7 2AZ, UK*
[g] *Hydrogen Properties for Energy Research (HYPER) Laboratory, School of Mechanical and Material Engineering, Washington State University, USA*
[h] *Lehrstuhl für Thermodynamik, Ruhr-Universität Bochum, D-44780 Bochum, Germany*
[i] *Kawasaki Heavy Industries, Ltd, 1-1, Kawasaki-cho, Akashi-City, 673-8666, Japan*
[j] *School of Mechanical and Manufacturing Engineering, The University of New South Wales, Sydney, NSW 2052, Australia*
[k] *NASA Kennedy Space Center, Cryogenics Test Laboratory, UB-G, KSC, FL 32899NASA, USA*

1 Introduction

There is increasing consensus that hydrogen will be essential for a global transition to a sustainable energy economy. This transition is becoming increasingly important in light of both ambitious international climate goals and record-breaking carbon dioxide levels realised in 2019.[1–5] Hydrogen can both enable the decarbonisation of sectors that are energy-intensive, including long-haul transport, industrial chemicals, and mineral processing,[6–8] and be paired with renewables to store energy and overcome the challenges of intermittency.[9] It can also be used as an energy carrier to export renewable energy from regions of abundant renewable resources to nations with limited energy resources.[2]

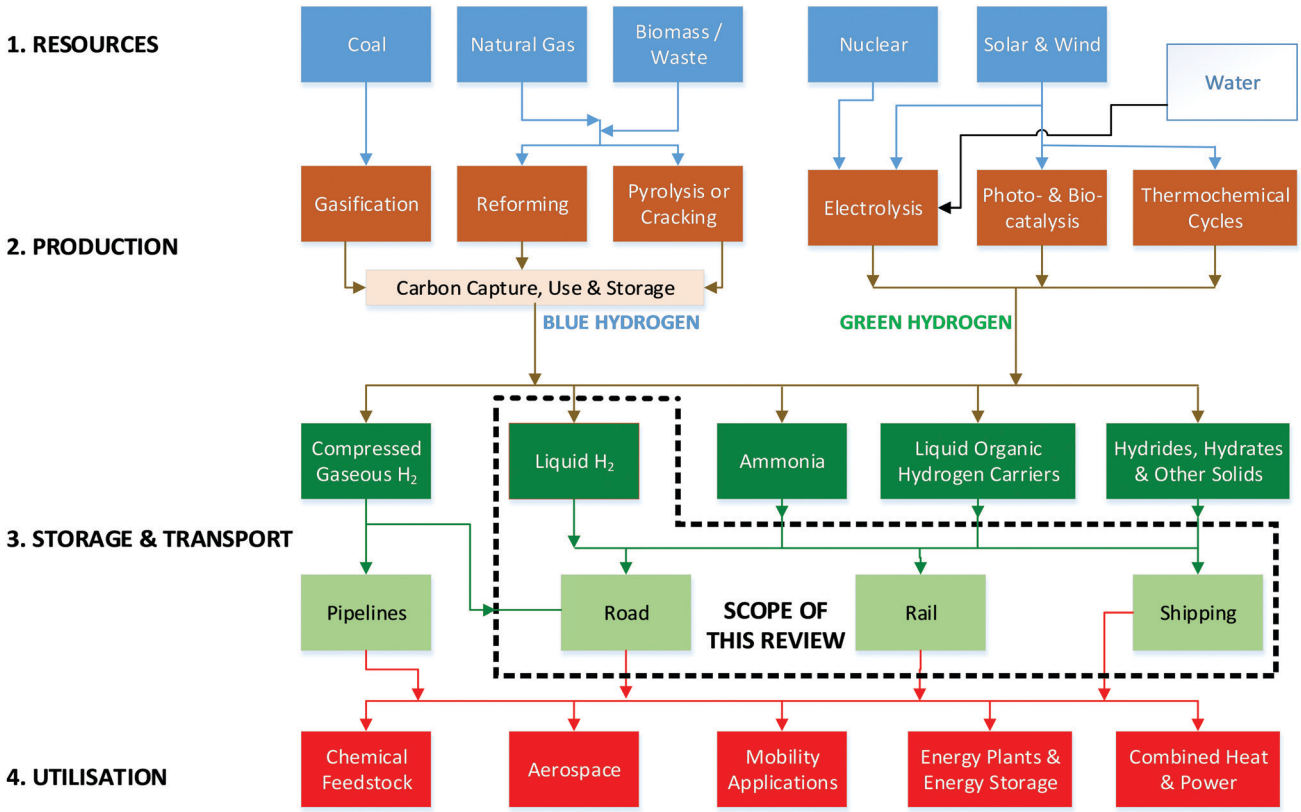

Fig. 1 The hydrogen value chain and its relation to the focus of this review into hydrogen liquefaction.

Such a transition will, however, require the development of Hydrogen value chains that are both sustainable and substantial in scale. Consequently, hydrogen road maps have been outlined for regions and countries such as the United States,[10] European Union,[11,12] Japan,[13,14] Australia,[15] Germany[16] and the United Kingdom.[17] Fig. 1 shows a block diagram representing the hydrogen value chain comprising four primary stages, labelled here as (1) resources, (2) production, (3) storage & transport, and (4) utilisation. Each of these stages can be realised using one of multiple possible options resulting, therefore, in a relatively large number of pathways by which the complete hydrogen value chain can be traversed. In addition to technical merit and cost, the selection of an option within a given stage of the value chain is influenced by both previous and subsequent stages. These inter-stage interactions mean that the hydrogen value chain can be considerably more complicated than other comparable energy value chains.[18–20]

Primary energy sources are either carbon-based (natural gas, coal, biomass) or non-carbon based (wind, solar, nuclear). Water is another resource that can be critical to the first stage of the hydrogen value chain, particularly if the primary energy is produced in electrical form. These resources are then converted into hydrogen-containing materials through a variety of processes[21–56] during the production stage. Production of H_2 today is dominated by the use of fossil fuels[57] because this is the cheapest way of manufacturing, for example, the fertiliser needed for food production. However, this does not account for the latent cost associated with the substantial emissions of CO_2 resulting from such H_2 production.

Table 1 presents comparative data for the current costs of producing H_2 with low or no CO_2 emissions. Pairing hydrogen produced from fossil fuels with carbon capture and storage (CCS)[5] (to produce so-called blue hydrogen) can increase the associated cost by up to 54% while reducing CO_2 emissions.[37] However, the scale of CCS† [23] needed for blue H_2 production technologies could represent a significant constraint on the role it can play within decarbonised energy supply chains. Green hydrogen production technologies[38–56] (from renewable energy sources together with electrolysis, solar thermochemical splitting and biochemical processes) also face significant challenges as they are still limited in scale,‡ [58] and their energy consumption is not yet cost-competitive. Nevertheless, the improving efficiencies and cost-reductions occurring in renewable energy generation and green hydrogen production suggest a cost curve trajectory that may bring them into line with blue hydrogen in the coming decade.[59]

Storage and Transport is crucial to the establishment of a hydrogen value chain. The focus of this review, liquid hydrogen, is one of many technologies[63–82] likely to play a significant role in

† Global capture and storage capacity of projects currently operating or under construction is around 40 million tonnes per annum (Mtpa).

‡ The largest PEM electrolyser currently in use has a capacity of 20 MW. This is equivalent to a hydrogen production capacity of 8 TPD, assuming a power consumption of 66 kWh $kg_{H_2}^{-1}$.

Table 1 Summary of low carbon or carbon neutral hydrogen production processes. All data sourced are from base case scenarios. Efficiencies are expected to increase with time

Production process	Ref.	Feedstock	Power req. [kWh $kg_{H_2}^{-1}$]	H_2 capacity [TPD]	Capex [M$]	Opex[a] [M$ per $year^{-1}$]	Cost [US$ per kg_{H_2}]	Capacity factor[b]
SMR with CCS[c]	25, 37, 60 and 61	Natural gas	44–50	210–341	226–463	16.1	1.63–1.99	90–95%
CG with CCS[d]	37, 61 and 62	Coal	47.2	277–500	546–677	27.6	1.63–2.26	85%
Solar PV-Electrolysis[e]	46 and 47	Water	55	10	134–260[f]	4.30–8.32[g]	6.22–12.1	20–31%[h]
Wind-Electrolysis[i]	48 and 49	Water	44.7–53.4	50	185–500[f]	9.13–25.3	2.37–5.69	41–55%[h]

[a] Variable costs excluded. [b] Capacity factor of the hydrogen production method. Capacity factor is the unitless ratio of an actual electrical energy output over a given period of time to the maximum possible electrical energy output over that period. For Solar PV and Wind electrolysis, the operation of the electrolyser is dependent on the renewable energy source and as such, the system has a similar capacity factor. For SMR and CG with CCS, the capacity factor is affected by maintenance requirements. [c] Feedstock cost ranges from: 5.76–10.5 US$ per GJ. [d] Feedstock cost: 1.15–2.16 US$ per GJ. [e] Studies were conducted 5 years apart, 2015 and 2020. Variance in costs and capacity factor are attributed to significant developments within the solar photovoltaic industry made during that time. [f] Renewable energy with feedstock cost included in plant capital. [g] Shaner *et al.* estimates yearly Opex for electrolyser to be 3.2% of the Capex. Neither study states other Opex values. [h] Assuming the electrolyser is off-grid and powered solely by the renewable energy source. This value is location dependent. If connecting to the grid is possible, the electrolysers may operate at their maximum capacity, increasing the capacity factor to 97%. However, as most grids are currently fossil-fuel derived, CO_2 emissions would be emitted. [i] Data retrieved from conceptual study investigating near, mid and long-term production costs associated with a 50 tonnes per day (TPD) standalone wind-hydrogen system. Stated costs is the range between the near and long-term scenarios for when the system is not connected to the grid.

the international trade of hydrogen. While the production stage usually generates gaseous H_2, storing and transporting the associated energy over long time scales and distances requires the implementation of a physical or chemical conversion process within the 3rd stage of the value chain to achieve a viable energy density. The choice of which hydrogen vector to select to this end is strongly coupled to the mode of transport best-suited, both technically and from a cost perspective, to the intended end-use of the hydrogen with distance and the infrastructure available at both ends of the supply-chain being additional considerations.§

The final stage of the hydrogen value chain is utilisation, which is currently dominated by chemical feedstock[83] (*e.g.* fertilisers, oil-refining, plastics, semi-conductors) and aerospace applications (rocket fuel).[84–86] However, while global hydrogen production is now approximately 75 million tonnes per year,[87] annual global demand is projected to reach 621 million tonnes, with the majority being used in the transportation sector.[88] Certain hydrogen vectors are chemically incompatible with particular utilisation options, and thus the cost of converting them back to a compatible form must be factored in to any analysis used for vector selection. The very-high purity requirements of H_2 fuel cell vehicles are similar to those needed and achieved during the hydrogen liquefaction process. For this reason, liquid hydrogen is expected to play a significant role within the supply chains needed to meet projected global demand.

Liquid hydrogen's role in the value chain

While liquid hydrogen's strengths as a vector include purity, end-use versatility, and ease of gasification, it also suffers from disadvantages relative to other possible vectors. Table 2 presents a summary of key properties of the primary hydrogen vectors available for storage and transport. These properties, together with an analysis of the costs associated with each stage of the liquid hydrogen supply chain, help with assessments of (i) applications for which it is most suited relative to other possible vectors, and (ii) technology gaps that need to be addressed to improve economic viability.

An additional advantage of liquid hydrogen over other possible vectors include its relatively high volumetric hydrogen density (80% greater than gaseous H_2 compressed to 70 MPa, and 50% greater than methylcyclohexane). The energy costs of producing ammonia and methanol per unit mass of hydrogen are comparable with liquid hydrogen yet the latter has no energy cost associated with dehydrogenation, which is required for fuel cell applications. For direct combustion, dealing with the greenhouse gases and other pollutants that can be emitted by liquid vectors (CO_2 for methanol, NO_x and N_2O for ammonia) can also be a significant issue.

Nevertheless, liquid hydrogen is characterised by several appreciable limitations and challenges that restrict its current use. These include:

- Economics: hydrogen liquefaction is an energy-intensive process. Current processes have specific energy consumptions (SEC¶) of between (11.9 and 15) kWh $kg_{LH_2}^{-1}$ which is (35 to 45)% of the lower heating value of hydrogen.[124–126] This contributes significantly to the current specific liquefaction cost (SLC‖) range of (2.5–3.0) US$ per kg_{LH_2}.[124–127]
- Cryogenic loss: boil-off loss associated with the storage, transportation and handling of liquid hydrogen can consume up to 40% of its available combustion energy.[83] For example, the NASA Space Shuttle program carried out from 1977 to 2011 purchased over 24 500 tonnes of liquid hydrogen, of which

§ Recently, BMW Group developed cryo-compressed hydrogen storage technology, involves storing gaseous hydrogen at low temperature on board the vehicle at a pressure of up to 35 MPa. This offers 50% more hydrogen storage capacity than the 70 MPa storage tanks. Liquid hydrogen is typically stored in insulated tankers at near atmospheric pressure. However, heat ingress is hard to avoid, owing to the temperature gradient between the liquid hydrogen and the external environment. This causes liquid hydrogen to evaporate to enter the vapor phase. This evaporated gas is usually called boil-off gas (BOG).

¶ Specific energy consumption is defined as the actual specific work that is required by the hydrogen liquefaction process. SEC (kWh $kg_{LH_2}^{-1}$) = (P_{net}/m_{LH_2}). Net power consumption, P_{net}, is defined as the difference between the total power consumption and total power recovered (by the turbine expanders).

‖ Specific liquefaction cost is defined as the total cost to produce 1 kg of liquid hydrogen. This include CAPEX, OPEX and Operation & Maintenance (OP) cost.

Table 2 At-a-glance summary of the properties of various hydrogen vectors, including LNG for comparison[a]

		CGH_2	CGH_2	LH_2	NH_3	MeOH	LOHC	LNG
		Ref. 37, 89 and 90	Ref. 89–91	Ref. 37, 89 and 92–110	Ref. 60, 98 and 111–115	Ref. 92 and 116–118	Ref. 92, 98, 111 and 119–121	Ref. 122 and 123
Vector properties	p/MPa	35	70	0.1	0.1	0.1	0.1	0.1
	T/K	298	298	20.3	240.1	298	240.1	111.5
Volumetric density[b]	[kg m^{-3}]	23.3	39.2	70.9	682	786	769	423
Gravimetric hydrogen content	[wt%]	100	100	100	17.8	12.5	6.16	—
Volumetric H_2 density	[kg_{H_2} m^{-3}]	23.2	39.2	70.9	121	99	47.3	—
Specific energy [mass][c]	[kWh $kg_{carrier}^{-1}$]	33.3	33.3	33.3	5.93	4.20	2.05	15.3
Specific energy [volume][c]	[kWh $L_{carrier}^{-1}$]	0.78	1.31	2.36	4.04	3.30	1.58	6.67
Energy to produce carrier	[kWh $kg_{carrier}^{-1}$]	1.67–4.4	6.7	6–15[d]	2–4[e]	2.06–2.83[f]	0.04–0.07[g]	0.33–0.7[h]
Energy to produce carrier	[kWh $kg_{H_2}^{-1}$]	1.67–4.4	6.7	6–15[d]	11.2–22.5	10.9–15[f]	0.967	—
Energy for dehydrogenation	[kWh $kg_{H_2}^{-1}$]	—	—	—	7.94	6.7–15.4 [i]	9.7–11.2[j]	—
End product consumed[k]	[%]	5–13.2	20	18.2–45.5	57.4–90.4	52.8–91.2	32–36.5	2.2–4.6
LCOP[l]	[US$ per kg]	0.22–0.28[m]	2.83[n]	0.5–3[o]	1–2.17[p]	2–4.17[q]	0.58–1.56[r]	0.03–0.21[s]

[a] CGH_2 – compressed hydrogen gas, LH_2 – liquid hydrogen, NH_3 – ammonia, MeOH – methanol, LOHC – methylcyclohexane. [b] Volumetric density is obtained using reference thermodynamic models implemented in REFPROP 10. [c] Excluding LNG, specific energy refers to amount of hydrogen available, in kWh equivalent terms, within one unit of carrier. LHV of hydrogen used: 120 MJ kg^{-1} and LHV of LNG [methane] used: 50 MJ kg^{-1} to calculate values. Molecular mass taken from the National Centre for Biotechnology Information. [d] Includes current industrial hydrogen liquefaction plant technology and conceptual studies for a range of plant capacities, from 5 TPD to >50 TPD. 6 kWh kg^{-1} has been demonstrated in conceptual studies for plant capacities > 50 TPD. The specific energy consumption of liquefiers operated in the USA is stated to range between 12.5 and 15 kWh $kg_{H_2}^{-1}$ for capacities between 5.4 and 32 TPD. [e] Value calculated from the energy requirements for ammonia synthesis only. [f] Electricity consumption to synthesise methanol from CO_2. This value includes energy requirement for water electrolysis to produce hydrogen. The study evaluates 2 different scenarios, transporting CO_2 and placing the CO_2 recovery facility nearby to the electrolyser. [g] Required energy to hydrogenate toluene. [h] Based on the energy efficiencies on various natural gas liquefaction cycles. [i] Includes catalytic steam reforming of methanol: 6.7 kWh $kg_{H_2}^{-1}$ and methanol electrolysis: 15.4–32.4 kWh $kg_{H_2}^{-1}$. The methanol electrolysis study referenced contains experimental data. Energy consumption is expected to decrease as the technology develops, hence the best case is stated. [j] Range varies due to the difference in enthalpies of dehydrogenation listed in the studies. [k] Percentage of end product consumed, either hydrogen or LNG. Calculated by total required energy to produce carrier [kWh $kg_{H_2}^{-1}$] over the specific energy of the end product. Hydrogen specific energy: 33.3 kWh kg^{-1}, LNG specific energy: 15.3 kWh kg^{-1}. [l] LCOP – levelized cost of end product. Does not include hydrogen feed costs or transportation. [m] Includes Capex, Opex for compression and storage. Modelling assumes storage capacity is charged and discharged on a daily basis from tanks of 100 m^3 capacity. Stated cost is base case for the levelized cost of hydrogen. With key actions and improvements in technology, best case range is 0.17–0.21 US$ per kg. [n] Cost to compress and refuel 750 bar storage tank. [o] Includes a range of values taken from conceptual studies. Base-case and best-case cost scenarios are included. [p] Includes the cost associated with hydrogenation and dehydrogenation. [q] Price range includes small- and large-scale methanol plants. Small scale – 350 TPD [MeOH], large scale > 1000 TPD [MeOH]. [r] Includes LOHC production, hydrogenation and dehydrogenation costs. [s] Study quantitively assessed various natural gas liquefaction processes. Costs include production, maintenance and amortized capital costs, excludes feed natural gas costs. The data was converted from $ per GJ to $ per kg using the LHV of LNG [methane, 50 MJ kg^{-1}].

54.6% was used on-board; the rest was lost during storage, loading, or replenishment.

• Safety: liquid hydrogen is not a common global shipping commodity. The lack of safety standards and regulation around hydrogen-based processes (especially at large-scale) could impede the establishment of liquid hydrogen supply chains.[128]

• Scale: currently, the largest single liquefier has a capacity of 32 tonnes per day (TPD), and the total global capacity is 350 tonnes per day. By 2050, the Hydrogen Council has estimated that 10% of total hydrogen demand, or 0.17 million tonnes per day, could be transported by sea.[129] To ship even a modest fraction of this amount as liquid will require a substantial scale-up of liquefaction capacity. Achieving this goal will likely help mitigate the challenges of energy cost and economics.[57] However, the technical challenges of scaling-up the necessary equipment (compressors, turbines and coldboxes) items are significant.

This review details the current state of knowledge, technology, and industrial practice relevant to the liquid hydrogen supply chain. Its objectives are to (i) provide an overview of the main challenges associated with producing and storing liquid hydrogen, and (ii) identify the primary opportunities for improving upon the four limitations detailed above: economics, cryogenic loss, safety and scale. To achieve these objectives the review starts by detailing the properties of molecular hydrogen that are relevant to liquefaction (Section 2), with a focus on the role that the spin isomers *ortho*- and *para*-hydrogen have on the thermodynamics and kinetics of liquefaction. Strengths and deficiencies in the models available for engineering design are identified together with knowledge and data gaps that if addressed would likely lead to process improvements. In Section 3, current approaches to hydrogen liquefaction are summarised before conceptual designs expected to deliver the needed efficiency improvements are reviewed. The storage and transport of liquid hydrogen is covered in Section 4, with a focus on the prediction and minimisation of boil-off losses. The specific challenges associated with safety and scale-up of the liquid hydrogen supply chain are considered in Section 5. Finally, a summative list of research and development priorities is presented.

2 Fundamental properties of molecular hydrogen

2.1 Mixture of *ortho*- & *para*-hydrogen

Molecular hydrogen occurs in two isomeric forms, *ortho*-hydrogen and *para*-hydrogen, differentiated by the nuclear spin

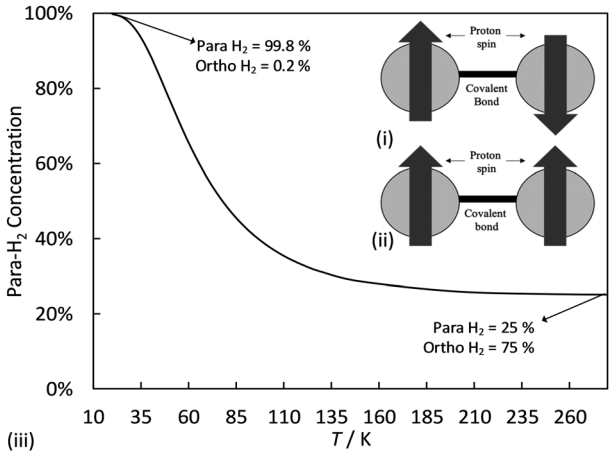

Fig. 2 (i) *para*- and (ii) *ortho*-hydrogen spin isomers. (iii) *para*-Hydrogen content of hydrogen at equilibrium as a function of temperature.

state of the protons in each hydrogen atom. Fig. 2 shows a schematic representation of these two nuclear spin isomers, together with a curve showing the fraction of *para*-hydrogen in an ensemble of H_2 molecules at equilibrium as a function of temperature. For a given temperature, the equilibrium ratio of *ortho*- to *para*-hydrogen concentrations ($c_{oH2}^{(eq)}$ and $c_{pH2}^{(eq)}$, respectively) is given by:[130]

$$K_{OP} = \frac{c_{oH2}^{(eq)}}{c_{pH2}^{(eq)}} = \frac{3 \times \sum_{L=1,3,5,\ldots} \left[(2L+1)\cdot \exp\left(-\frac{F}{kT}\right)\right]}{\sum_{L=0,2,4,\ldots} \left[(2L+1)\cdot \exp\left(-\frac{F}{kT}\right)\right]} \quad (1)$$

Here L is the molecule's rotational quantum number, with even values associated with *para*-hydrogen and odd values with *ortho*-hydrogen; k is the Boltzmann constant, T is the hydrogen temperature and F is the energy of the rotational state, which is given by eqn (2).[130]

$$F = B_0 L(L+1) - D_0 L^2 (L+1)^2 + H_0 L^3 (L+1)^3 \quad (2)$$

where B_0 = 7.36 meV is the rotational constant of hydrogen, and D_0 = 5.69 × 10^{-3} meV and H_0 = 6.45 × 10^{-6} meV are the rotational energy distortion constants.

With decreasing temperature, the probability of a molecule being in a *para*-hydrogen state increases because of its lower energy, and consequently the equilibrium *ortho–para* ratio approaches zero. Intermolecular forces between two *ortho*-hydrogen molecules are slightly stronger than those between two *para*-hydrogen molecules because of the former's larger total nuclear spin. The *ortho–para* ratio thus affects the magnetic, optical, volumetric and thermal properties of the hydrogen.[131]

Accordingly, thermodynamic descriptions of hydrogen's properties at equilibrium should ideally represent the substance as a mixture with a temperature dependent composition. However at temperatures where a liquid phase can exist (<33 K), the substance may be well-approximated as pure *para*-hydrogen, while at ambient temperatures and above a pseudo-pure substance known as normal hydrogen consisting of 75% *ortho*-hydrogen and 25% *para*-hydrogen provides an excellent representation of the fluid.

When normal hydrogen is cooled appreciably, care must be taken with both the modelling approach and any physical handling of the substance. Quantum mechanical selection rules related to the conservation of molecular angular momentum mean that the transition from *ortho*- to *para*-hydrogen is forbidden and cannot occur spontaneously without an external interaction, such as a molecular collision in the presence of an inhomogeneous magnetic field as discussed below. In the absence of a suitable catalyst to facilitate the conversion, if normal hydrogen is rapidly cooled from ambient to cryogenic temperatures the time required before the equilibrium composition is reached can be of the order of days or weeks. Moreover, the conversion from normal to *para*-hydrogen is exothermic, releasing 525 kJ kg^{-1} of heat, which is larger than the enthalpy of vaporisation at liquid hydrogen's normal boiling point (448 kJ kg^{-1}).[131–133]

Thus, the effective and efficient conversion of *ortho*- to *para*-hydrogen is extremely important to industrial-scale applications of hydrogen liquefaction and storage. If insufficient time is allowed for the kinetics of the *ortho–para* conversion reaction to occur, normal hydrogen that is liquefied too rapidly will generate excessive amounts of boil-off gas. Excessive amounts of boil-off gas may cause over-pressurisation of the cryogenic storage tank, leading to serious safety issues. Even if the pressure build up is not rapid, the slow transformation of *ortho*- to *para*-hydrogen is one of the barriers to long-term liquid hydrogen storage given that the heat of conversion can evaporate more than 70% of the stored liquid hydrogen.[133]

Consequently, so-called catalyst materials are integrated into the construction of industrial hydrogen liquefaction processes. In the presence of such catalysts the kinetics are approximately first order with full conversion achieved in minutes.[134–136] The principle cost to their use is an increased pressure drop across the liquefier.

2.2 Thermodynamic property descriptions for hydrogen liquefaction

Thermodynamic models for pure hydrogen. The liquefaction of a fluid requires an adequate knowledge of its thermodynamic properties, starting with its critical point. The slow rate at which *ortho*-hydrogen converts to *para*-hydrogen in the absence of a catalyst means it is possible to determine experimentally a critical point for both normal hydrogen[89,137,138] and *para*-hydrogen.[139,140] Table 3 lists the critical point conditions for *para*-, *ortho*- and normal hydrogen determined by Leachman *et al.*[141]

Table 3 Critical properties of *para*-, *ortho*- and normal hydrogen

	T_c/K	p_c/MPa	ρ_c/kmol m^{-3}
p-H_2	32.938	1.2858	15.538
o-H_2	33.22	1.31065	15.445
n-H_2	33.145	1.2964	15.508

Leachman *et al.* developed a reference equation of state (EOS) for *para*-, *ortho*- and normal hydrogen, valid from the triple point temperature of each fluid ($\approx$14 K) to 1000 K at pressures to 2000 MPa. Within this EOS, the reduced Helmholtz energy of each fluid is represented by a function that contains approximately 30 terms that are either polynomial, exponential, Gaussian or logarithmic functions of the reduced density and inverse reduced temperature. Each of the 30 terms has between one and seven adjustable parameters that were determined *via* non-linear least squares regression to the primary experimental data sets.

With this degree of flexibility, the Leachman EOS for *para*-hydrogen has an estimated expanded uncertainty (95% confidence interval) of 0.1% in density at temperatures up to 250 K and pressures to 40 MPa. Calculated heat capacities, speeds-of-sound and vapour pressures for *para*-hydrogen have estimated uncertainties of 1%, 0.5% and 0.1%, respectively at pressures below 100 MPa. The reference EOS for normal hydrogen has a similar performance over the same ranges and conditions: in the range (250 to 450) K at pressures up to 300 MPa, densities have an estimated uncertainty of 0.04%.

These small uncertainties make the reference EOS of Leachman *et al.* more than sufficient for the purpose of designing and optimising hydrogen liquefaction processes, assuming that the *ortho–para* ratio is known or controlled adequately at each point. Several low-cost or free software packages, including REFPROP 10,[89] TREND 4[142] and ThermoFAST Web,[143] contain implementations of the reference EOS enabling calculations of the enthalpy changes, volumes and vapour–liquid equilibrium conditions needed to size and evaluate the performance of various liquefaction cycles. However, most commercial process simulation software packages do not typically use reference EOS, at least by default, because (i) their high-degree of non-linearity can make the solution of mass and energy balance equations impractically slow; (ii) there is often a need to also consider mixtures at some (early) stage within the process simulation; and (iii) hydrogen is often treated as a pure fluid (normal) with no consideration of the temperature-dependent *ortho–para* ratio. Consequently, commercial process simulation software packages tend to utilise cubic equations of state, such as the Peng–Robinson EOS,[144] to represent pure hydrogen. Cubic EOS typically utilise three fluid-specific parameters based on the substance's critical point and normal boiling point. They then rely on a corresponding-states approach[145,146] to calculate thermodynamic properties for the pure fluid and its mixtures over a wide-range of conditions. However, as discussed by Rowland *et al.*,[147] the corresponding states approach tends to fail for fluids whose critical properties are influenced by quantum phenomena such as hydrogen, helium and neon.[148,149]

When the intermolecular separation is similar to the molecule's de Broglie wavelength, λ_B, quantum effects can influence the fluid's properties significantly: for liquid hydrogen at its normal boiling point, H_2 has a de Broglie wavelength around 0.27 nm and an intermolecular separation of 0.66 nm. Thus the liquefaction of hydrogen provides a rare example of quantum mechanics impacting an industrial process in two separate ways: conversion between the *ortho*- and *para*- quantum states, and the wave-like properties of H_2 molecules at low temperatures.

It is possible to correct the Peng–Robinson model of H_2 for the effects of its de Broglie wavelength by modifying the intermolecular pair potential using the method of Feynman and Hibbs.[150] Essentially, the correction makes the co-volume (size) parameter b in the cubic EOS temperature dependent, which in turn leads to a more robust mathematical representation of the pure fluid's vapour pressure curve. Aasen *et al.*[151] applied this method to develop accurate quantum-corrected cubic equations of state for hydrogen, helium, neon, deuterium and their mixtures. With no new fitting parameters, significant improvements were achieved in the ability of the cubic equation to represent density, heat capacities and enthalpy changes at saturation for normal hydrogen (no consideration is given to *ortho–para* conversion). Perhaps even more significantly, given that the primary utility of cubic models is the description of vapour–liquid equilibrium (VLE) in mixtures, was the ability of the quantum-corrected Peng–Robinson EOS to represent the experimental VLE data for helium-neon and hydrogen-helium. This could be an important tool in the development and simulation of next-generation liquefaction processes that achieve higher efficiencies through the use of ''quantum refrigerant mixtures'' with varying ratios of (He + Ne + H_2).

Mixtures with hydrogen and refrigerants. There are two general reasons for fluid mixture property predictions in the design of hydrogen liquefaction processes:

The first reason relates to the pre-treatment processes where impurities must be separated from the hydrogen prior to liquefaction to avoid solids forming in the cryogenic heat exchangers. The nature of the likely impurities depends upon the source of the hydrogen: if it is produced by SMR, then CH_4, H_2O, CO and CO_2 should be considered, while if it is produced by electrolysis then H_2O, O_2, N_2 and Ar might need to be removed before or during liquefaction. The state-of-the-art for describing the thermodynamic properties of such mixtures is the GERG-2008 EOS,[152] which provides a framework for calculating the Helmholtz energy of mixtures containing up to 21 components, including normal H_2 and the seven impurities listed above. However, the GERG-2008 EOS was developed for natural gas mixtures, with the primary focus being CH_4 dominant systems with H_2 considered only as an impurity. Furthermore the priority of the original GERG-2008 EOS was accurate calculations at pipeline conditions, with less weighting given to cryogenic temperatures (leading to the development of EOS-LNG[153] in 2019).

To help address the resulting deficiencies of property calculations for multi-component hydrogen dominant mixtures, Beckmüller *et al.*[154] have developed new Helmholtz EOS for binary mixtures of H_2 + CH_4, H_2 + N_2 H_2 + CO_2 and H_2 + CO that can be used within the GERG-2008 framework. They replaced the pure-fluid model for H_2 used in the original GERG-2008 model with the reference EOS of Leachman *et al.* for normal hydrogen, and also developed a new binary-specific departure functions to represent the available mixture data. The most significant of the improvements resulting from the new models

of Beckmüller *et al.* is the accurate representation of the available low temperature VLE data, particularly for $H_2 + CO_2$ at $T \leq 296$ K, $H_2 + CH_4$ at $T \leq 140$ K, $H_2 + N_2$ at $T \leq 110$ K, and $H_2 + CO$ at $T \leq 95$ K; for these systems phase boundary predictions around or above 10 MPa made using the original GERG-2008 EOS are in substantial error. While only normal hydrogen is considered, the new Helmholtz models are valid over the same ranges of temperature and pressure as the original GERG-2008 (60 K $\leq T \leq$ 700 K, $p \leq$ 70 MPa).

The second reason that fluid mixture property predictions are needed for hydrogen liquefaction process design is the selection and optimisation of mixed refrigerants (MRs). Conceptual studies have found that using MRs containing between two and five components can significantly improve the liquefaction cycle efficiency as detailed below. Common MR compositions can include hydrogen, nitrogen, neon, helium, and hydrocarbons ranging from methane to butane.[155] The aforementioned quantum-corrected cubic EOS by Aasen *et al.*[151] are one option for use in liquefaction simulations; these should provide reasonably accurate estimates of the cryogenic refrigerant mixture VLE properties. However, the changes in refrigerant enthalpies central to liquefaction cycle design are not so well represented by cubic EOS. Multi-parameter mixture Helmholtz energy models are the most accurate option for such calculations and should be used where available. Tkaczuk *et al.*[156] have reported accurate Helmholtz energy EOS models with binary-specific functions for helium and neon, helium and argon and neon and argon mixtures. For refrigerant mixtures that include hydrogen with the noble gases, an extension of the work by Beckmüller *et al.* is underway; however, this approach will be limited by the use of normal rather than equilibrium hydrogen within the GERG-2008 framework. While this may not be problematic for predictions of phase equilibria and density it is an issue for calculations of the caloric properties needed for energy balances.

2.3 Transport properties and experimental data needs

The thermodynamic models for hydrogen are roughly one order of magnitude less accurate than those available for other fluids like methane or nitrogen, primarily because of the significantly more limited experimental data.[157] Jacobsen *et al.*[158] reviewed the experimental thermodynamic data available for normal and *para*-hydrogen and suggested a range of priority measurements needed to advance hydrogen property predictions at conditions of industrial interest. To improve the simulation of liquefaction processes, Jacobsen *et al.*[158] recommended new measurements of density, speed of sound and heat capacity for normal hydrogen in the gaseous and liquid phases be acquired at temperatures below 50 K, while such measurements for *para*-hydrogen be conducted above 100 K because this would help resolve the contributions due to *ortho*-hydrogen. To acquire data with sufficiently low uncertainty, state-of-the-art experimental techniques for thermodynamic property measurements should be utilised, together with the ability to monitor the *ortho–para* ratio as a function of time (*e.g.* using Raman spectroscopy).[159]

For hydrogen-rich mixtures, new data are required to improve upon and extend the approach of Beckmüller *et al.*[154] For the four binaries they considered, the greatest data need identified was single-phase density data, especially for the normal $H_2 + CO$ system. However, particularly for the temperature range (30 to 150) K, (ternary) mixture measurements of equilibrium hydrogen with various other compounds likely to be present as either impurities in hydrogen production or components in mixed refrigerants should be prioritised. For mixed refrigerant candidates, enthalpy, heat capacity and/or speed of sound data should be acquired in addition to vapour–liquid equilibrium measurements, while for likely impurity compounds, the focus should be on solubility measurements as a function of temperature and concentration.

Both the experimental data situation and, consequently, the accuracy of predictive models are worse for the transport properties of hydrogen and its mixtures. Models for the viscosity and thermal conductivity of hydrogen are needed to estimate, respectively, pressure drops and heat transfer coefficients in various unit operations within the liquefaction process (*e.g.* cryogenic heat exchangers). Advances in fundamental theory[160] have produced *ab initio* calculations of dilute gas transport properties for *para*-, *ortho*- and normal hydrogen from (20 to 2000) K[161] that are as or more accurate than available measurements;[162] however, these are only relevant for calculations involving low density gases. At higher densities, a reference viscosity model only exists for normal hydrogen[163] in part because only one definitive data set for the viscosity of *para*-hydrogen exists.[164]

Muzny *et al.*[163] suggest that *para*-hydrogen's viscosity is essentially equivalent to that of normal hydrogen provided the density is the same; for a given temperature, this correction can be facilitated using the Leachman *et al.* equations of state. The reference viscosity correlation for normal hydrogen has an estimated uncertainty of around 4% over the range (14 to 1000) K at pressures to 200 MPa, except in the critical region (where it is worse) and at pressures around 0.1 MPa (where it is better).

The thermal conductivity of *para*-hydrogen is nearly 30% larger than that of normal hydrogen at 140 K because of the heat capacity difference between the *ortho* and *para* spin isomers; this results from the higher rotational energy levels of the former.[165] Assael *et al.*[166] have developed reference correlations for the thermal conductivity of both normal and *para*-hydrogen, valid from the triple point to 1000 K and pressures to 100 MPa. Both correlations utilise the theoretical calculations of Mehl *et al.*[161] for the dilute gas contribution. Critical enhancement contributions to thermal conductivity are more significant and wide-ranging ($\approx$15 K from the critical temperature) than they are for viscosity, and these are explicitly modelled for both normal and *para*-hydrogen. Thirteen data sets were considered primary for normal hydrogen, although only three extend below 273 K, and only one was measured below 77 K. For *para*-hydrogen, the data situation is worse with only two primary data sets, both measured by Roder[167,168] covering (17 to 153) K and (99 to 274) K, respectively. Assael *et al.* estimated the relative combined expanded uncertainties of these correlations as follows: normal hydrogen – 4% for temperatures above 100 K

at pressures to 100 MPa, and 7% from the triple point to 100 K at pressures to 12 MPa, except in the critical region; *para*-hydrogen – 4% from the triple point to 300 K at pressures to 20 MPa, except in the critical region, and 6% at temperatures above 400 K. Differences in thermal conductivity have been used as a basis for measurements of the *ortho–para* ratio in a sample of hydrogen, particularly in the temperature range (50 to 250) K.

2.4 Conversion of *ortho*-hydrogen to *para*-hydrogen

In the absence of a heterogeneous catalyst, the *ortho–para* conversion occurs *via* a homogeneous auto-catalytic mechanism. In general, the conversion requires the presence of an inhomogeneous magnetic field (a magnetic field gradient), which exerts a torque upon the H_2 molecule inducing the required 'spin-flip'. Given that *para*-hydrogen is non-magnetic, while *ortho*-hydrogen has a net local magnetic field, the rate of homogeneous *ortho*-to-*para* conversion is dictated by collisions between *ortho*-hydrogen molecules. The resulting transition rates are therefore dependent on the concentration and temperature of the *ortho*-hydrogen molecules present, and follow a second-order rate equation:[169,170]

$$\frac{\mathrm{d}y_{ortho}}{\mathrm{d}t} = -ky_{ortho}^2 + k'y_{ortho}(1 - y_{ortho}) \tag{3}$$

$$\tau = \frac{1}{k} \cdot \frac{1 - y_{ortho}^{eq}}{y_{ortho}^{eq}} \cdot \ln\frac{(y_{ortho}^{i} - y_{ortho}^{eq}) \cdot y_{ortho}^{f}}{(y_{ortho}^{f} - y_{ortho}^{eq}) \cdot y_{ortho}^{i}} \tag{4}$$

Here τ is the time needed to convert an initial *ortho*-hydrogen fraction, y_{ortho}^{i}, to a final fraction, y_{ortho}^{f}, which is necessarily larger than the equilibrium fraction y_{ortho}^{eq}; k and k' are the rate constants for the forward (*ortho*-to-*para*) and reverse (*para*-to-*ortho*) transitions, respectively. Milenko *et al.*[169] measured k and k' for liquid and gaseous hydrogen from (16.65 to 120) K, at pressures up to 70 MPa. The conversion constants can be correlated:

$$k = A_0T^n\rho + (C_0 + D/T^m)\rho^q \tag{5}$$

and

$$\frac{k'}{k} = \frac{y_{ortho}^{eq}}{1 - y_{ortho}^{eq}} \tag{6}$$

For k in unit of 10^{-3} h^{-1}, A_0 = 18.2 ± 1.6 cm^3 kg^{-1} h^{-1} K^{-n}; n = 0.56 ± 0.02; C_0 = (38.5 ± 1.5) cm^{3q} h^{-1} g^{-q}; D = (4.605 ± 0.445) K^m cm^{3q} 10^4 h^{-1} g^{-q}; m = 2.5 ± 0.2 and q = 3.6 ± 0.6. Fig. 3 shows the data of Milenko *et al.* together with the correlations presented in eqn (5) and (6). For the supercritical states relevant to hydrogen liquefaction, these results illustrate that while the conversion rate increases with both density and temperature, the time constants of the homogenous reaction are slow; the rate constants determined by Milenko *et al.* were determined from the time required to convert hydrogen samples from 75% to 68% *ortho*-hydrogen. Depending on the temperature and pressure, this degree of conversion took between 12 and 48 hours.

Such a slow conversion rate is unviable for industrial liquefaction processes, and thus heterogeneous catalyst materials are used to ensure that the *ortho–para* conversion occurs sufficiently quickly as the hydrogen is cooled down to 20 K. Solid catalysts convert the spin-isomers *via* one of several mechanisms; at the low temperatures relevant to hydrogen liquefaction, non-dissociative mechanisms where adsorbed hydrogen remains in its molecular form are of primary relevance. The two catalytic *ortho–para* conversion mechanisms most relevant to liquefaction processes are (i) spin-conversion at paramagnetic surfaces, and (ii) spin-conversion at magnetically ordered surfaces. The former involves the interaction of

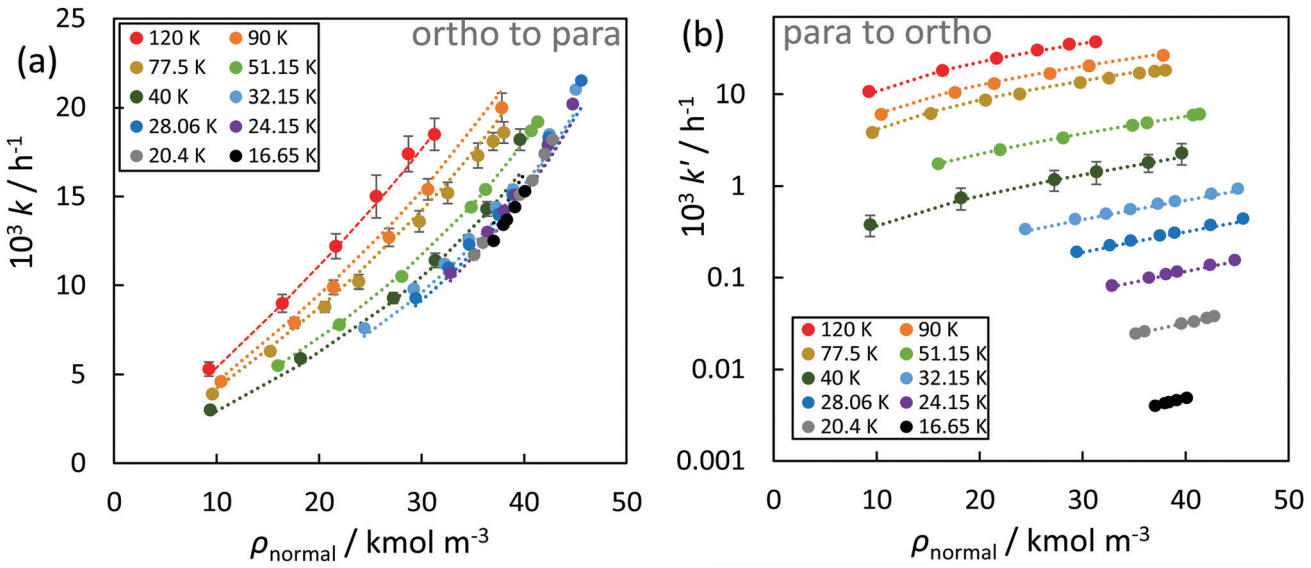

Fig. 3 Autocatalytic homogenous *ortho*-to-*para* (a) & *para*-to-*ortho* (b) conversion rate constants as a function of normal hydrogen molar density systems. The dashed curves correspond to values calculated with the empirical correlation shown in eqn (5) and (6).

hydrogen spin isomers with dilute paramagnetic species, such as Cr_2O_3, dispersed on high surface area materials such as alumina Al_2O_3. Chapin *et al.*[171] found that the time constants of the *ortho–para* conversion reaction for H_2 at 77 K and pressures to 10 MPa increased by an order of magnitude in the presence of about 0.1 wt% Cr_2O_3 on Al_2O_3. Misono and Selwood[172] showed how the application of external magnetic fields up to 0.8 T could further accelerate the conversion rate achieved with 0.003 wt% Cr_2O_3 on Al_2O_3 by a factor between 40 and 90 at 298 K and 173 K, respectively. Spectron Gas Control Systems previously offered a paramagnetic surface catalyst OXISORB® based on CrO for commercial applications. However since chromium has been banned for use in multiple jurisdictions as a result of safety considerations, it is no longer commercially available.

IONEX® is a commercially available catalyst used widely by industry for *ortho–para* conversion that functions *via* the mechanism of spin conversion at magnetically-ordered surfaces. Supplied by Molecular Products,[173] IONEX® is a porous particulate catalyst composed of Fe_2O_3 with a surface area around 216 $m^2\ g^{-1}$ and particle (mesh) sizes between 0.3 and 0.6 mm.[134] Activation to remove adsorbed water is required prior to use *via* heating to 110–150 °C under vacuum or dry H_2 at 1 bar for one day. Exposure to trace impurities during operation can result in catalyst poisoning (H_2S, mercaptans) or gradual deactivation (N_2, H_2O, CO_x, NO_x).[174] Such impurities are, generally removed upstream by adsorption as they might otherwise freeze-out and cause a blockage.

Generally the kinetics of the *ortho–para* conversion in the presence of a heterogeneous catalyst are adequately described by first order kinetics of the form:[175–180]

$$r = k \cdot c_{H_2} \cdot \left(y_{ortho} - y_{ortho}^{\text{Equil.}} \right) \quad (7)$$

Adaptation of eqn (7) using the Langmuir-Hinshelwood approach to account for the adsorption and desorption of hydrogen on the catalyst surface did not provide any significant improvement in agreement with experimental conversion data.[175–180] Inclusion of external and internal mass transfer contributions to the overall reaction rate has been attempted *via* the inclusion of a catalyst effectiveness factor [*e.g.* Wakao *et al.*[181]] but this is an area requiring further investigation.

A few estimates of the inventory of catalyst required to convert a given amount of hydrogen are available in the open literature. Karlsson[134] used 37.5 kg of IONEX® catalyst to convert 24 kg of normal hydrogen in a flow loop at 20 K to 99.8% *para*-hydrogen within 4.75 minutes. Zhuzhgov *et al.*[174] estimated that approximately 65 L (or 80 kg) of an Fe_2O_3 catalyst (like IONEX®) is required to convert 100 kg h^{-1} of normal hydrogen to 99% *para*-hydrogen at 21 K in a continuous flow reactor. They tabulate average rate constants which allow calculation of the catalyst volume (or mass) required in a fixed bed reactor to treat a given feed flow of hydrogen to a specified outlet concentration of *para*-hydrogen. These average volume rate constants, which range from 0.24 mol $s^{-1}\ L^{-1}$ at 78 K for $Co(OH)_3$ to 2.5 mol $s^{-1}\ L^{-1}$ at 22 K for a NiO on Al_2O_3 catalyst, assumed first order kinetics and accounted for mass transfer limitations (and thus particle size) using the approach of Wakao *et al.*[181] Assuming a fixed bed containing 65 L of an Fe_2O_3 catalyst at 21 K with a void fraction of 0.38, Zhuzhgov *et al.*[174] determined that a residence time of 4 s (liquid) and 400 s (gas) was required for effectively full conversion. This is a rate up to five orders of magnitude greater than that of the homogenous self-conversion reaction based on the data shown in Fig. 3. It is in fact likely that the *ortho–para* conversion kinetics in many practical scenarios are limited by heat transfer in terms of the removal of the heat of conversion.

Several research efforts focussed on improving *ortho–para* conversion efficiencies have been reported. One approach is to focus on alternative catalyst materials or properties. For example, Hutchinson[179] and Wilhelmsen *et al.*[182] found that a nickel oxide–silica catalyst doubled the catalytic activity of iron(III) oxide and reduced the cooling power consumption of the heat exchanger by 9%.[182] Reducing the pressure drop associated with catalyst use within the liquefaction process is also an area of opportunity.[183] Park *et al.*[184] studied the pressure drop in a catalyst-packed heat exchanger using a cylinder filled with commercial IONEX® catalyst. It was found that the pressure drop is almost linearly dependent on space velocity (up to 1 bar pressure drop at velocity of 5 m s^{-1}) and approximately five times lower than that predicted using the Ergun equation. Reducing such catalyst-induced pressure drops may prove to be a crucial feature of increased liquefaction efficiency.

Spectroscopic mechanisms of inducing the *ortho–para* conversion might also be worth considering. According to eqn (2), the smallest energy difference between the *para-* and *ortho-*states is approximately $2B_0$ which corresponds to electromagnetic radiation with a frequency of 3.6 THz and a wavelength of 0.083 mm. It might then be possible to use the Purcell effect,[185] which is an enhancement of a molecule's spontaneous emission rate by its environment, to accelerate the conversion of *ortho-* to *para*-hydrogen by incorporating the H_2 molecules within a cavity of length-scale 83 microns. In typical catalyst packings, many such micro-cavities are formed within the porous material. However, the cavities need to be electromagnetically resonant, and consideration would need to be given to the comparatively rapid diffusive motion of the gaseous hydrogen molecules and the associated effects such as Doppler linewidth broadening.

3 Hydrogen liquefaction

3.1 Fundamentals of hydrogen liquefaction

A generic hydrogen liquefaction process block diagram is shown in Fig. 4. Several recent publications cover hydrogen liquefaction methods[131,186–190] so only a brief summary of the fundamentals is provided. If the hydrogen feed to the process is provided at comparatively low pressure, the first step of the process is pre-compression.[190] The hydrogen then undergoes an optional pre-cooling stage to 80 K and an adsorption stage to remove impurities that may freeze out during cryogenic

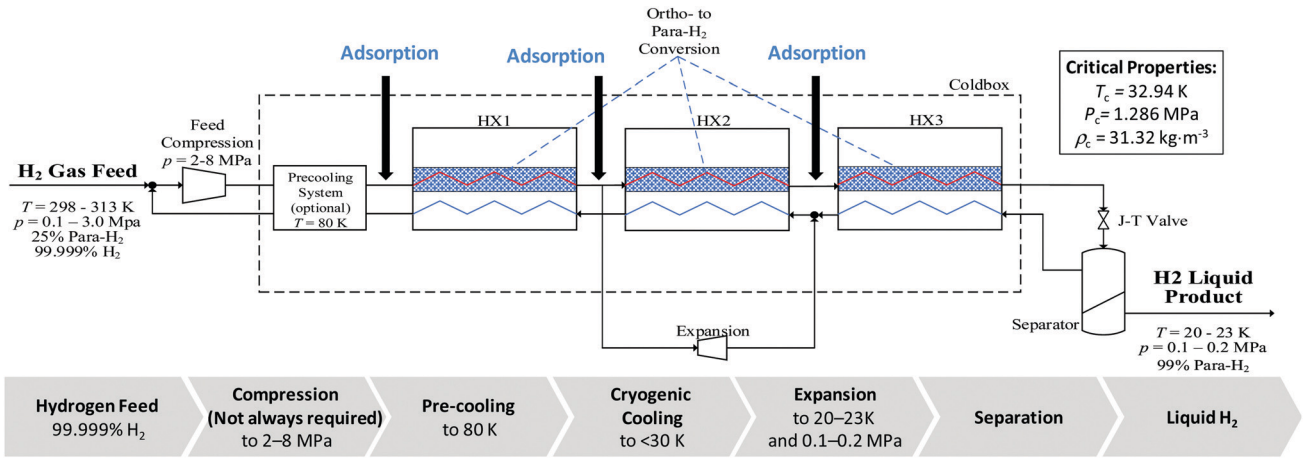

Fig. 4 Simplified schematic diagram of the hydrogen liquefaction process based on simple Claude cycle. Critical properties of *para*-hydrogen are shown in this schematic.

liquefaction.[126] The hydrogen is then cooled to temperatures less than 30 K,[191] using a closed-loop cryogenic refrigeration cycle. This cycle involves continuous or batch catalytic conversion of *ortho* to *para*-hydrogen.[192] The final step is typically adiabatic expansion, which either takes the form of Joule–Thompson or turbine expansion.[131] LH_2 is usually stored at 20–23 K (0.1–0.2 MPa) with a *para*-hydrogen fraction greater than 98%.[192]

Liquefaction cycles. Three dominant types of hydrogen liquefaction system design or cycle are discussed in the literature:[193–198] (i) Linde–Hampson cycle; (ii) Claude cycle; and (iii) Brayton refrigeration cycle. The Linde–Hampson is one of the oldest (1895) cycles used to liquefy gases and is characterised by low efficiency compared with other systems; it is only considered appropriate for small-scale (<2 TPD) systems.[131,199] The initial gas compression provides the work used to liquefy the gas, which is cooled at near constant pressure by two heat exchangers, before undergoing Joule-Thompson expansion. The cold flashed vapour is used as a self-refrigerant in the second heat exchanger before being recycled to the feed. The Claude cycle[190] improves the performance of this self-refrigeration process through the addition of an expander to cool part of the feed and increase the hydrogen coolant flow through the second heat exchanger.[200] The Claude cycle is considered appropriate for large-scale systems (>2 TPD).[131,191] Several modifications exist both in industry and the literature, which improve efficiencies by increasing the number of heat exchangers and/or through the use of nitrogen pre-cooling.[131] The Brayton refrigeration cycle uses a closed refrigeration loop containing nitrogen, helium, or a mixed refrigerant (MR) as the working fluid to cool the hydrogen stream.[199] Historically, the Brayton refrigeration cycle has only been considered appropriate for small-scale plants; however, more recent literature has considered its expanded use in larger- scale systems.[124,131]

Efficiency parameters. The specific energy consumption (SEC) of a given cycle is defined as the energy consumption per unit mass of hydrogen liquefied:[131]

$$w = W/\dot{m} \tag{8}$$

where w is specific energy consumption, W is net power consumption of the cycle, and $\dot{m}$ is the mass flow rate of product LH_2.

The second law of thermodynamics establishes that there exists a minimum possible SEC, related to the specific enthalpy change Δh and the associated specific entropy change Δs of the hydrogen as follows:

$$w_{\text{ideal}} = \Delta h - T_0 \Delta s \tag{9}$$

where T_0 is the ambient temperature. This evaluates to 3.9 kWh $kg_{LH_2}^{-1}$ given the following specifications:[126]

- Inlet and outlet hydrogen pressure: 0.101 MPa;
- Inlet hydrogen temperature: 303 K;
- Ambient temperature: 298 K, and
- Inlet and outlet *para*-hydrogen mole fractions: 25% and 99.8%.

Exergy efficiency is a quantitative measure of the process efficiency and relates the actual SEC to the theoretical minimum value from eqn (9):[201]

$$\mu_{\text{ex}} = \frac{w_{\text{ideal}}}{w} \tag{10}$$

where μ_{ex} is the exergy efficiency of the liquefaction process or stage. An example distribution of total exergy for different stages in a hydrogen liquefaction process operating at various pressures is shown in Fig. 5[202] where most of the exergy is consumed in the cryogenic cooling stage.

Process simulation. The impact of thermodynamic property uncertainty on process simulations has been studied by multiple authors. A general conclusion is that new, high-quality data for multicomponent refrigerant mixtures are needed to improve the reliability of the equations of state used in process simulations, which in turn could reduce design margins and cost.[203–206] Process simulation studies of conceptual liquefaction processes often use a variety of EOS[144,207–209] with varying degrees of simplicity and computational efficiency traded-off with accuracy.

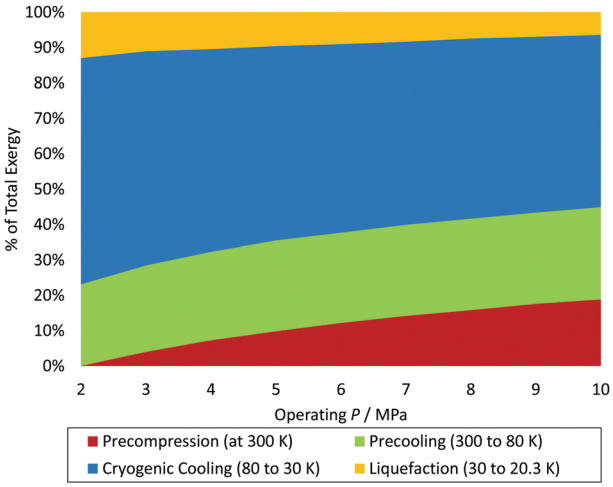

Fig. 5 Distribution of exergy requirements for each stage of hydrogen liquefaction based on operating pressure.

These studies have mostly been undertaken using commercial process simulation tools which permit detailed analysis of steady-state plant operation and the estimation of capital and operating costs for different design scenarios. For example, Cardella *et al.* optimized plant design using UniSim simulations incorporating a kinetic model for *ortho–para* conversion.[210] Yin and Ju,[186] Asadnia and Mehrpooya[200] and Ansarinasab *et al.*[187] all used Aspen HYSYS simulations to explore process optimisation and the economics of hydrogen liquefaction. Yang *et al.*,[211] also using HYSYS, modelled the combined process of hydrogen production by steam methane reforming and liquefaction. Generally, the choice of simulation platform is less important than the fidelity of the models used to represent the physical properties of the hydrogen and refrigerant fluids, and the performance of key items of process equipment such as heat exchangers, turbines and compressors.

Valenti *et al.* assessed the influence of thermodynamic modelling on hydrogen liquefaction simulation outcomes of the Claude cycle.[212] The study focused on the EOS for *para*-hydrogen and calculations of the heat capacity of equilibrium hydrogen (or *para*-hydrogen). The study found the following:

- Different EOS and heat capacity calculation methods yield significant differences in entropy (up to 11%) and exergy values (up to 13%).
- Adopting *para*-hydrogen models for the simulation of equilibrium hydrogen liquefaction may lead to errors greater than 10%.
- Densities calculated from the Peng–Robinson and Helmholtz-energy EOS models differed by up to 10%, with the largest differences found at low temperatures.

Collectively, heat capacity and density calculations had a major effect on the predicted cooling curves and are crucial for accurate and robust simulation of hydrogen liquefaction and subsequent equipment design.[212] Furthermore, uncertainties in density at high pressure and/or liquid states result in uncertainties in volumetric flows. Erroneous volumetric flow predictions can lead to, for example, a mismatch of blade angles in turbo machinery, lowering efficiencies and, potentially leading to mis-predictions of operational range.

To demonstrate further the impact of thermodynamic property uncertainty on overall SEC, we have simulated a hydrogen liquefaction cryogenic process (hydrogen capacity: 5 TPD, T: 104 K to 20 K, p: 3 MPa) employing a basic Brayton refrigeration cycle with pure gaseous helium as the refrigerant (T: 104 K to 19 K, p: 8 MPa). The simulation determines the helium minimum flow rate needed to provide the required cooling, which significantly influences total compression power and thus SEC. Two different EOS have been applied for helium: the PR EOS[213] and the reference Helmholtz EOS of Ortiz-Vega *et al.*[214,215] The helium mass flow rate and SEC calculated using the two different EOS were 91 TPD vs 110 TPD (21% difference) and 5.5 kWh kg^{-1} *vs.* 6.8 kWh kg^{-1} (23% difference), respectively. These significant deviations are mainly caused by the different temperature drop determinations (18.4 K vs 16.6 K) of helium across the vapour expander (isentropic efficiency: 78%), as obtained by the two EOS.

3.2 Industrial liquefaction processes and technology

The SEC of existing industrial hydrogen liquefiers ranges from (10 to 15) kWh $kg_{LH_2}^{-1}$ or (35 to 45) % of the lower heating value of hydrogen,[124–126] with exergy efficiencies ranging from 20–30%. This high energy demand is partially due to the relatively small size (capacity) of the existing liquefiers (less than approximately 32 TPD per liquefaction train), the design of which has focussed on lower capital cost (CAPEX) rather than high efficiency. This adds considerably to the cost and carbon intensity of the end-use hydrogen.[216] More than fifty industrial hydrogen liquefaction plants have been constructed since 1952, with more than fifteen industrial plants constructed or proposed since 2000, as shown in Table 4. Recently-constructed plants are based on modified Claude cycles and use catalyst-packed heat exchangers (for continuous *ortho–para* conversion). Commercial catalysts are used in both the pre-cooling stage (where LN_2 is often used as the refrigerant) and the cryogenic stages before the final expansion. Only a small number of existing liquefiers are discussed in detail in the literature: examples include the Linde hydrogen liquefier at Leuna[217] and Praxair large liquefaction plants[218] in the USA.

Linde–Leuna. The Linde hydrogen liquefier (Fig. 6) at Leuna,[217] Germany, is a modified pre-cooled Claude cycle where liquid nitrogen and hydrogen recycle stream are used in the pre-cooling and cryogenic stages, respectively. It reaches higher efficiency than a similar decommissioned plant at Ingolstadt.[219] The improvements are due to the use of continuous *ortho–para* conversion, oil-free advanced dynamic gas bearing turbines and an ejector to re-liquefy boil-off gas and flash-gas. The cryogenic cooling system includes three turbines in series that operate between (0.52 and 2.0) MPa at 102 000 rpm.[192,217] The reported SEC for the Leuna plant is 11.9 kWh $kg_{LH_2}^{-1}$ and the exergy efficiency is 23.6%.[131,217]

Praxair. Praxair has five hydrogen liquefaction plants, all located in the USA, with capacities between 18 and 32 TPD.[218] These plants also implement modified pre-cooled Claude cycles

Table 4 Hydrogen liquefaction plants constructed within the last 20 years

Location	Operator	Capacity [TPD]	Constructed	Additional information
Kimitsu, Japan[222]	Nippon Steel Corporation	0.2	2004	Pilot plant, separate H_2 from coke oven gas
Saggonda, India[223,224]	Andhra sugars	1.2	2004	Constructed by Linde
Osaka, Japan[189,225]	Iwatani [hydro-edge]	10	2006	Total capacity split between two units[a]
Leuna, Germany[217]	Linde	5	2008	
Chiba, Japan[104,225]	Iwatani	5[a]	2009	Constructed by Linde
Yamaguchi, Japan[104,225]	Iwatani and Tokuyama	5[a]	2013	Constructed by Linde
Akashi, Japan[104,226]	Kawasaki Heavy Industries	5	2014	Japan's first domestically produced facility
Yamaguchi, Japan[227]	Iwatani and Tokuyama	10	2017	Capacity of existing plant doubled[a]
Port of Hastings, Australia[228]	HESC	0.25	2020	Australia's first H_2 liquefaction facility
Las Vegas, USA[56,229]	Air liquide	27.2[b]	2020[c]	Located in Apex Industrial Park
Leuna, Germany[230]	Linde	10	2021	Capacity of existing plant doubled
La Porte, USA[231]	Air products	27.2[b]	2021	
La Porte, USA[232]	Praxair	27.2[b]	2021	Praxair's 5th H_2 liquefaction plant
California, USA[233]	Air products	*	2021	
Ulsan, Korea[234]	Hyosung and Linde	13	2022	Constructed by Linde

*Source did not state a value. [a] Production capacity: 3000 L hour^{-1} per unit. [b] Sources state US tons per day, values have been converted to metric tonnes per day. [c] Construction was set to begin in 2020, source does not state an on-stream date.

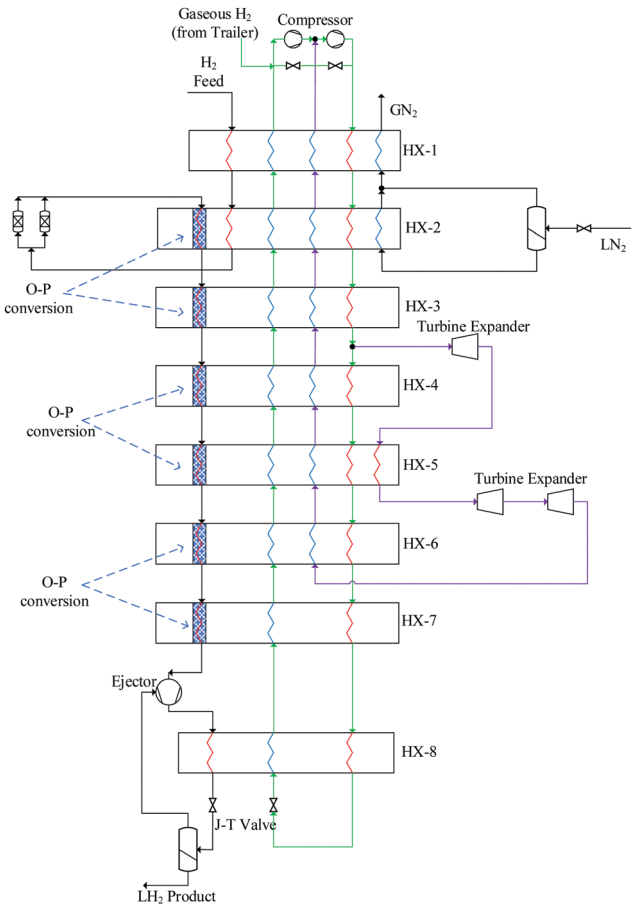

Fig. 6 Process block diagram for the Linde hydrogen liquefier at Leuna.

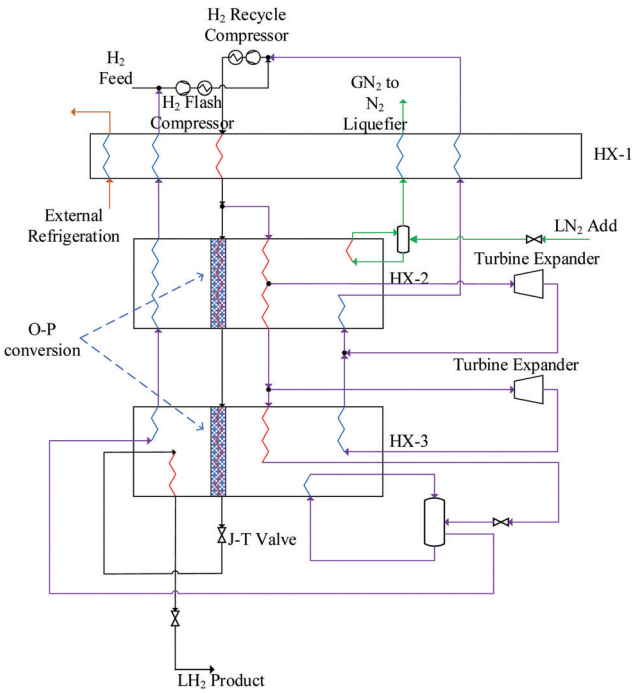

Fig. 7 Process block diagram for a typical Praxair plant.

that include three heat exchangers (Fig. 7): the first cools the hydrogen feed with both nitrogen gas and a refrigerant from an external cycle, the second uses liquid nitrogen and the hydrogen recycle stream as coolants, while the third exchanger is cooled with the hydrogen recycle stream alone.[189] The cryogenic cooling system includes two turbines, before a final isenthalpic (J–T) expansion. The plant includes continuous *ortho* to *para* conversion. Typical SEC values for the Praxair plants are between (12.5 and 15) kWh $kg_{LH_2}^{-1}$ and the exergy efficiency is between (19.3 and 24)%.[125]

3.3 Conceptual liquefaction processes and technology

Over 25 theoretical hydrogen liquefaction processes have been developed conceptually since 1987.[200] The capacity of these conceptual plants ranges from (5 to 864) TPD. The SEC range of conceptual hydrogen liquefaction plants is 4–14 kWh $kg_{LH_2}^{-1}$. The objective of these conceptual models is to demonstrate theoretically how the efficiency of the liquefaction process can be optimised. Conceptual models do not in general fully

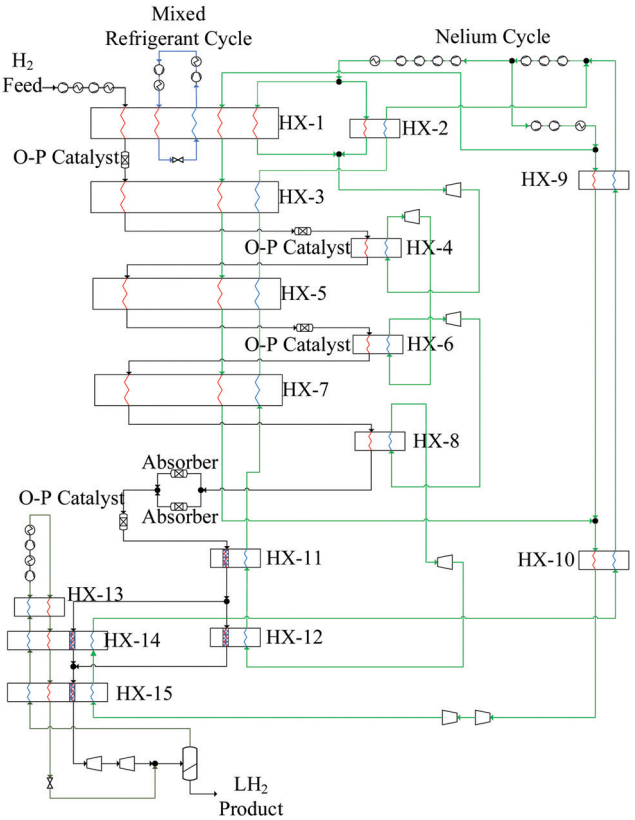

Fig. 8 Process block diagram for IDEALHY project.

consider total cost, operability or technical readiness.[220] Large-scale hydrogen liquefaction methods and different configurations of hydrogen liquefaction cycles were reviewed by Aasadnia and Mehrpooya.[131] Three of these conceptual designs proposed for large-scale hydrogen liquefaction process pants plants are summarised below.

Idealhy. The IDEALHY project[192,221] (Fig. 8) is a conceptual design of a 50 TPD liquefier based on an MR pre-cooled 'nelium' (75% helium, 25% neon) mixed refrigerant in a dual Brayton refrigeration cycle. Compression of the feed from (2 to 8) MPa occurs in two reciprocating piston compressors. Pre-cooling to 130 K is then achieved in four heat exchangers using a MR comprising nitrogen, methane, ethane, propane, and n-butane. Cryogenic cooling is performed by two overlapping Brayton cycles using nelium. *Ortho* to *para* conversion occurs during the pre-cooling stage (130 to 85) K in four adiabatic converters and then continuously in subsequent catalyst-packed heat exchangers (<85 K). Final expansion of the hydrogen stream to the liquid phase is achieved through two expansion turbines from (8 to 0.2) MPa. The outlet stream of the final turbine includes hydrogen flash gas. The SEC and exergy efficiency of this process are 6.7 kWh $kg_{LH_2}^{-1}$ and 32%, respectively. According to Cardella, the SEC increases to approximately 7.8–8.2 kWh $kg_{LH_2}^{-1}$ if the feed compression from (0.1 to 2) MPa is considered.[126] The IDEALHY project found that heat integration with an adjacent LNG import and regasification terminal could reduce the SEC by 0.62 kWh $kg_{LH_2}^{-1}$.[221]

Kuendig *et al.* The model shown in Fig. 9[235] is a conceptual design of a 50 TPD liquefier based on a Claude cycle with pre-cooling by LNG and nitrogen gas. LNG was selected as the working fluid because of its potential availability at the liquefaction site and its possible use for hydrogen production *via* steam methane reforming. The concept also exploits the idea of using LNG re-gasification at an import terminal to provide pre-cooling and therefore reduce the SEC of the hydrogen liquefaction process. The hydrogen feed undergoes pre-cooling from 300 K to 80 K *via* three heat exchangers with

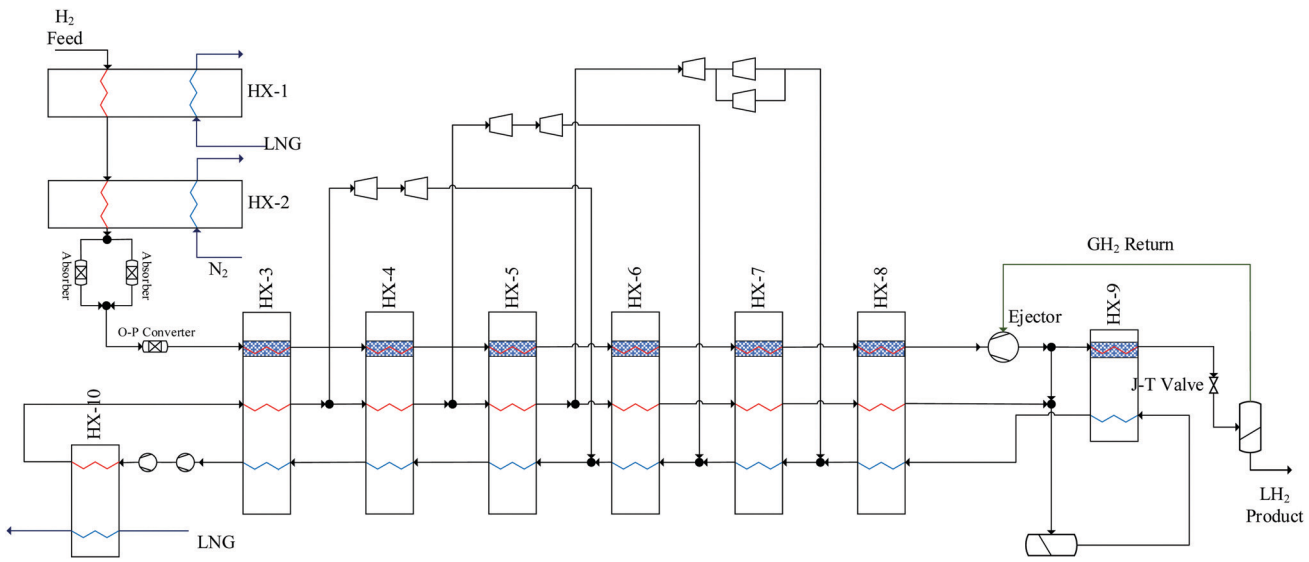

Fig. 9 Process block diagram for the Kuendig model. Simplifications have been implemented based on the original PFD: (i) N_2 compressor system and N_2 cold box are combined as HX-2; (ii) H_2 compressor system is represented by HX-10; two individual cold streams through HX3–HX7 are combined as one cold stream.

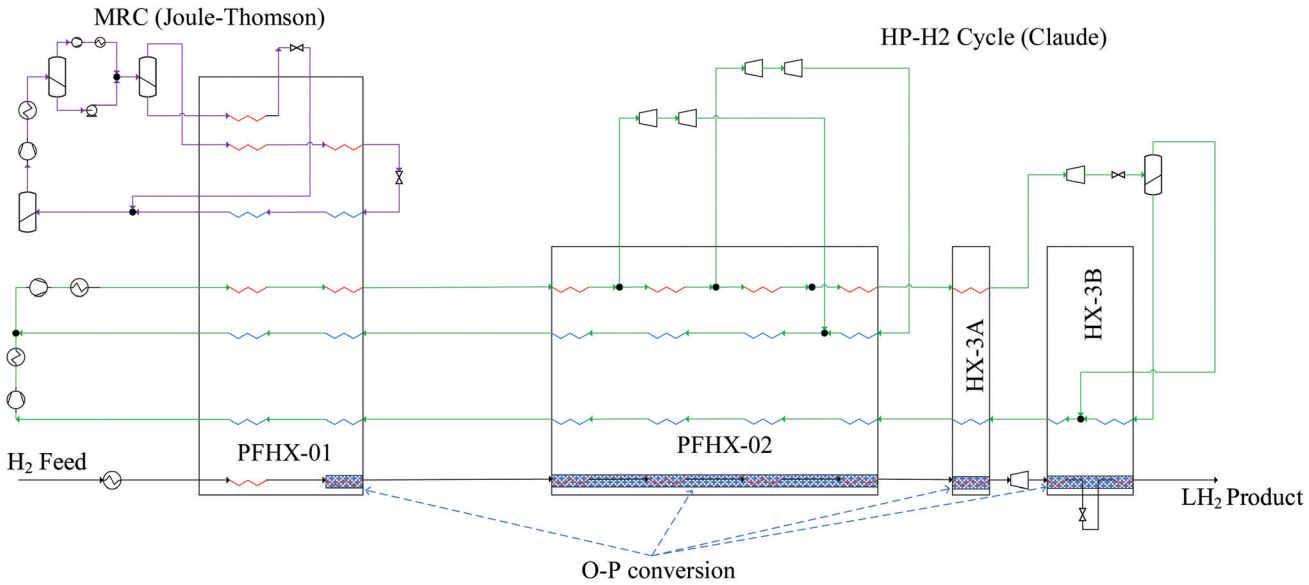

Fig. 10 Process flow diagram for the HP-H_2 Cycle model.

(1) LNG, (2) nitrogen gas, and (3) liquid nitrogen. Hydrogen then passes through a final purification stage before entering an *ortho–para* conversion reactor (from ~25% to 42.7% *para*-hydrogen). Further cooling to 26 K is achieved in five catalyst-packed heat exchangers and seven hydrogen-gas-bearing turbines arranged in three strings. The SEC efficiency of this process is 4 kWh $kg_{LH_2}^{-1}$. The concept is dependent on the availability of LNG, its requirement to be regasified on site, and that it may be used at no additional cost. A similar concept using LNG for pre-cooling was proposed by Shigekiyo.[236]

HP-H_2 cycle with MRC. This 100 TPD hydrogen liquefaction process concept proposed by Cardella *et al.*[210] (Fig. 10) is designed with a mixed-refrigerant Joule–Thomson precooling cycle and a high-pressure hydrogen Claude cycle for cryogenic cooling and liquefaction. This modifed Claude cycle design is optimised for large-scale liquefaction using available oil-free hydrogen reciprocating piston compressors. High-speed oil or gas bearing cryogenic hydrogen turbo expanders can be implemented into this design with the option of energy recovery *via* turbine-generators. The refrigerant compositions were optimized using 4 components and were comprised of a blend of nitrogen with up to three C1 to C5 hydrocarbons. The SEC and exergy efficiency of this process are 6.2 kWh $kg_{LH_2}^{-1}$ and 43%, respectively. According to Cardella *et al.*,[210] a specific energy consumption below 6 kWh $kg_{LH_2}^{-1}$ could be achieved while reducing the specific liquefaction costs by 67% compared to smaller scale 5 TPD LH_2 plants; this process could be implemented in the next few years making it one of the most promising conceptual design currently available. A similar process design was proposed by Berstad *et al.*[237] for a 125 TPD hydrogen liquefier.

Other reported conceptual designs include the WE-NET process[190,210] with a nitrogen pre-cooling stage and a SEC of 8.72 kWh $kg_{LH_2}^{-1}$. This is a complex liquefaction process where a large supporting nitrogen liquefaction system is required to liquefy gaseous nitrogen after its use in the pre-cooling process. Krasae-in[238] proposed a 100 TPD liquefier based on four cascaded hydrogen Brayton refrigeration cycles and a pre-cooling stage (to 80 K) using a five component refrigerant mixture. Cardella notes that, owing to the large number of refrigeration cycles, the likely viability of this process for industrial applications is low.[126] Quack proposed a conceptual design[239] for a 170 TPD liquefier based on propane pre-cooling and helium-neon Brayton refrigeration cycles. Challenges have been identified in determining the true efficiency of the process, owing to the high energy requirements of propane refrigeration. SINTEF reported a modified version of the process model[189,240] proposed by Quack where pre-cooling of the hydrogen stream is achieved by an MR comprising C1–C5, ethylene, nitrogen, neon, and R14. Valenti and Macchi proposed a conceptual design[216] for a 864 TPD liquefier based on four cascaded Brayton refrigeration cycles using a helium refrigerant. However, this is a complex process requiring a large number of compressor stages (hence higher CAPEX) due to the low molar mass of helium.

3.4 Technical gap between actual and conceptual units

Conceptual plants are designed to provide lower SEC and higher exergy efficiency, as summarised in Fig. 11.[126] However, limited consideration is given to total installed and operational costs or the technical maturity and ability to scale-up the component unit operations. This is particular true with respect to selection of the appropriate compressor type and the size of the required cold box.[220] Current designs for approved future hydrogen liquefiers do not exceed the single liquefaction train capacity of approximately 30 TPD. Conceptual plants designed to be larger than 50 TPD thus help identify the required knowledge gaps and technological advances required for hydrogen liquefaction production at these elevated scales with improved SEC and exergy efficiency.

A selection of potentially feasible conceptual hydrogen liquefaction processes are detailed and compared in Table 5.

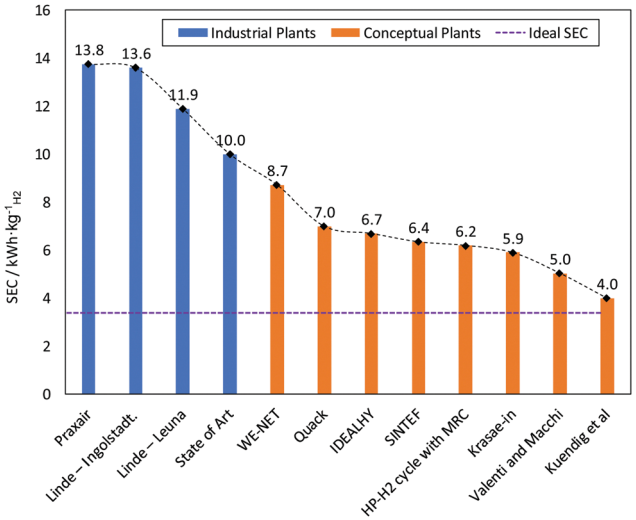

Fig. 11 Performance of industrial and conceptual hydrogen liquefiers. Feed and product conditions of ideal SEC calculation are: 1.01 bar, 303 K, 25% *para*-H_2; 1.01 bar, 20 K, 99.8% *para*-H_2. Purple dashed line corresponds to theoretical minimum.

The following criteria were used to screen proposed processes for inclusion in Table 5:

- Scale $\geq$50 TPD,
- SEC between 4 and 10 kWh $kg_{LH_2}^{-1}$,
- Exergy efficiency >23%, and
- Inclusion of novel but attainable technologies.

The key equipment needed for these most prospective large-scale conceptual are as follows:

Coldbox. The purpose of a coldbox is to minimise heat leakage into the cryogenic equipment. As a result, a coldbox is typically vacuum insulated with multi-layer superinsulation.[126] Industrial coldboxes are cylindrical or rectangular vessels designed to store the main cryogenic equipment such as plate-fin heat exchangers; turbine expanders; adsorber and phase separation vessels. Realistically attainable coldbox dimensions can, however, be a constraint on the large-scale liquefiers proposed by conceptual studies. Large insulated coldboxes can be erected in the field, however, vacuum-insulated coldboxes are typically pre-fabricated off-site and transported to the liquefier construction site; transportation weight and size limits can thus determine the possible coldbox size.[126]

Compression. Compression to higher feed pressures can reduce the work needed downstream;[202] however, feed conditions are limited by the maximum allowable operating pressure of available heat exchangers.[202] Compressors used for both feed compression and in the refrigeration cycle account for the largest proportion of overall power consumed (90% or more).[126,192] Stage efficiency, number of stages, compressor types, intercooling temperatures, and pressure losses, therefore, have a large influence on total power consumption.[241] Hydrogen feed gas is delivered from an SMR or an electrolysis plant typically at pressures greater than 1.5 MPa so that further compression is not generally required, particularly given the complexity and CAPEX it would add. Conceptual studies consider feed pressures in the range (0.1 to 2.5) MPa and compressor discharge pressures in the range (2.1 to 8) MPa, with feed temperature typically set to ambient.[192] Compressors used in the refrigeration cycle depend on the type of refrigerant used.

From Table 5, it is evident that piston and turbo/centrifugal compressors are widely considered in conceptual processes. Whilst piston compressors are state-of-the-art for industrial liquefiers, they are expensive and limited in attainable flow rate and efficiency.[126] Turbo-compressors generally have higher efficiency and greater throughput than piston compressors and are more suitable for large scale liquefaction. However, turbo-compressors are only really feasible for use with gases with molar masses above approximately 6 g mol^{-1}.[192] For pure hydrogen, a large number of turbo-compressor stages are required to reach the desired pressure as shown by Quack[81] and Valenti and Macchi,[216,239] and thus would incur higher capital expenditure. For example, the compression of hydrogen gas from atmospheric pressure to 8 MPa using a turbo-compressor would require at least 24 stages.[202] Turbo-compressors are better suited to installation on the refrigerant side of the liquefaction process, as the refrigerant typically has a higher molar mass than hydrogen.[239] There is no evidence of turbo compressors currently being used in industrial hydrogen liquefaction plants.[192]

Pre-cooling. This is commonly used in both established and conceptual designs to improve liquefaction efficiency.[155] Krasae-in found that the addition of a pre-cooling stage reduced the compressor power required by the Claude cycle by (5 to 10)%; however, additional heat exchangers and a more expensive expander were required.[155] Pre-cooling is a hallmark of all industrial and conceptual process in Table 5. While nitrogen is the only pre-cooling fluid used in known commercial hydrogen liquefaction plants, conceptual cycles use nitrogen, propane, MRs, and LNG as the relevant working fluid.

Heat exchangers. Plate-fin heat exchangers (PFHE, Fig. 12) are used in industrial hydrogen liquefiers because of their high flexibility concerning the number of process channels (and hence capacity), large heat exchange surface area (>2000 m^2 m^{-3} possible[242]) coupled with comparatively small footprint, and comparatively low CAPEX.[188,216,243] Process passages in the heat exchangers are often packed with particulate *ortho–para* conversion catalysts. Aluminium is the most common material used for these cryogenic heat exchangers, due to its comparatively high thermal conductivity and strength at low temperatures.[192,243,244] Such plate and fin heat exchangers are typically designed for pressures up to approximately 13 MPa.[192]

A larger heat exchange surface area and volume can deliver higher exergy efficiency but imposes higher capital expenses.[245,246] The overall heat exchanger size is, however, limited primarily by the size of the accommodating coldbox and, to a lesser extent, the design pressure. Conceptual plants designed for large scale may need to address potential challenges with respect to process fluid pressure drop through the catalyst packings.[183,184,246,247] Linde reported that the maximum size for LH_2 industrial heat exchangers is approximately 8.2 m × 3.4 m × 1.5 m, with a core volume of 15 to 30 m^3 and a specific surface of (500 to 2000) m^2 m^{-3}.[242] These reported maximum

Table 5 Conceptual and established hydrogen liquefaction processes developed within the last 20 years, sorted according to capacity

Project	Linde – Leuna, 2007[127,217,218]	Praxair – USA[125,189,218]	IDEALHY, 2013[192,221]	Berstad *et al*, 2010[127]	Krasae-in, 2014[238]	QUACK, 2002[127,239]	WE-NET, 2004[190,210]	HP-H_2, 2017[210]
Maturity[a]	Established	Established	Conceptual	Conceptual	Conceptual	Conceptual	Conceptual	Conceptual
Liquefaction cycle	LN_2 pre-cooled Claude	N_2 pre-cooled Claude[b]	MR pre-cooled Brayton	MR Brayton	MR pre-cooled Brayton[c]	MR Brayton	LN_2 pre-cooled Claude	MR pre-cooled Claude[d]
Capacity [TPD]	5	20–36[e]	50	86	100	170	300	100
SEC [kWh $kg_{LH_2}^{-1}$][f]	11.9	12.5–15	6.7	6.15–6.51	5.91	6.93	8.53	6.2
Exergy efficiency	23.6%	19–24%	32%	44.7–47.1%	39.1%	56.8%	46%	43%
Hydrogen feed								
Pressure [MPa]	2.4	*	2	2.1	2.1	0.1	0.1	2.5
Temperature [K]	313	*	293	310	298	300	300	303
para-H_2[g]	*	25%	25%	25%	25%	25%	25%	25%
Compression								
Pressure [MPa]	—	*	8	8	—	8	3.04	—
Compressor type	—	*	Piston [2-stage]	*	—	Piston	Centrifugal	—
Efficiency [h]	—	*	85%[i]	85%[j]	—	85%[j]	80%[i]	—
Pre-cooling								
Refrigerant	Nitrogen	Nitrogen	Multi-component[k]	Propane/MR	Multi-component[k]	Propane/MR[l]	Nitrogen	MR
Refrigerant cycle	LN_2 evaporation	GN_2 & LN_2 evaporation[b]	MR closed loop	3 stage MR	2 stage MR	Vapour compression	LN_2 evaporation[m]	MRC[n]
Temperature [K]	80	80	130	75	80	220/73[l]	80	100
Cryogenic cooling								
Refrigerant	Hydrogen	Hydrogen	Helium/Neon	Helium/Neon	Hydrogen	Helium/Neon	Hydrogen	Hydrogen
Refrigeration cycle	Claude	Claude	Brayton	Brayton	Brayton	Brayton	Claude	Claude
Temperature [K]	*	*	26.8	26.5	20	25	*	*
Compressor type	Piston	*	Turbo	Turbo	*	Turbo	Centrifugal	Piston
Compressor stages	2 × 2	*	6	15	8	8	15/25[o]	2[p]
Efficiency	65–70%[q]	*	85%[i]	85%[j]	90%[j]	85%	80%[i]	76–85%
Expander type	Turbo	*	Turbo	Turbo	*	Turbo	Centrifugal	Turbo
No. of expanders	3	*	5	2	4	6	2	*
Expander efficiency	>85%[j]	*	80%[i]	90%[j]	*	90%[j]	85%[i]	78–88%[j]
O–P conversion	Continuous	Continuous	Batch and continuous	Continuous	6 stages	Continuous	Partially continuous	Continuous
Expansion								
Expansion device	J–T[r]	J–T[r]	Expander	J–T[r]/Expander[s]	Expander	Expander & J–T[r]	2 stage J–T[r]	Expander
Isentropic efficiency	N/A	N/A	80%[i]	N/A/ 85%	*	85%	N/A	78–88%
Liquid H_2 product								
Pressure [MPa]	0.13	0.1	0.2	0.1	0.13	0.1	0.1	0.2
Temperature [K]	21	20.2	22.8	20.2	19.5	20.2	20.4	22.8[t]
para-H_2[g]	>95%	>95%	>98%	>98.5%	95%	> 99%	>95%	>98%

*The study did not provide data for this value. [a] Conceptual – presented in research, not yet proven. [b] Modified pre-cooled Claude cycle with 3 heat exchangers. The first: nitrogen gas [GN_2] and an external refrigeration system, second: liquid nitrogen [LN_2] and H_2 recycle stream, third: H_2 recycle stream. Established – process has been implemented at scale. [c] Four cascaded hydrogen Joule–Brayton cycles pre-cooled with a multi-component refrigerant. [d] The largest capacity plant is a double-train liquefier. [e] Includes auxiliary plant energy requirements. [f] Dead-state temperature modified from 288.15 K to 300 K. [g] *para*-hydrogen percentage composition. [h] Main compressor stage efficiency assumed where source has not specifically stated a value. [i] Unknown category of efficiency. [j] Isentropic efficiency. [k] Multi-component mixture contains five components: hydrogen, nitrogen, methane, ethane and butane. [l] Two vapour compression refrigeration cycles used, propane to cool to 220 K and MR to cool to 73 K. [m] Liquid nitrogen at 0.12 MPa. [n] 15 stages required for low pressure and 25 required for high pressure. [o] Isothermal efficiency. [p] Polytropic efficiency. [q] J–T – Joule–Thomson valve. [r] J–T valves produce a SEC and an exergy efficiency of 6.5 kWh kg^{-1} and 44.7%, respectively. Liquid expanders produce a SEC and an exergy efficiency of 6.15 kWh kg^{-1} and 47.1%, respectively.

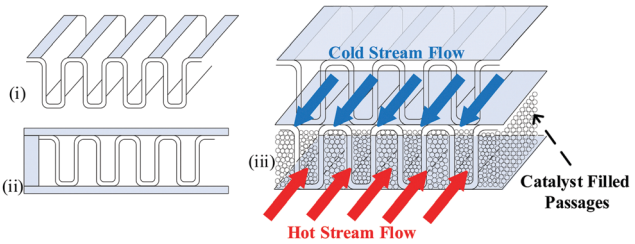

Fig. 12 Illustration of the (i) fins, (ii) empty channels and (iii) catalyst-filled channels in a plate-fin heat exchanger with cold and warm streams flowing through.

feasible geometrical dimensions represent a potential limitation to up-scaling of efficient hydrogen liquefaction processes.[175] However, PFHE remain the preferred technology for large-scaled hydrogen liquefaction. Skaugen *et al.*[246] considered the use of spiral-wound heat exchangers for LH_2 production with a capacity of 125 TPD. The lower surface density area and heat transfer coefficients in the spiral-wound heat exchangers meant their required weights are 2 to 14 times higher than those of the plate-fin heat exchangers.

Recently-built industrial hydrogen liquefiers and most conceptual processes in the literature employ continuous catalytic *ortho–para* conversion. A more thermodynamically efficient conversion that maintains the *ortho–para* ratio close to its equilibrium value can be achieved in such continuous catalytic conversion arrangements because both sensible and conversion heat are removed concurrently in the heat exchanger, resulting in higher exergy efficiency.[248]

Key limitations regarding heat exchanger design are excessive pressure drop through the catalyst bed and the ability to model quantitatively conversion kinetics while incorporating relevant heat and mass transfer limitations. Some conceptual processes use multiple stages of batch conversion to mimic continuous conversion largely because of the difficulty in quantifying the conversion kinetics.

Refrigerants. Existing liquefiers only use nitrogen in the pre-cooling stage while a hydrogen recycle stream is used in the cryogenic stage. Nitrogen is often a readily available fluid because hydrogen liquefiers are frequently sited close to air separation plants.[182] When liquid nitrogen is not readily available and the power required to produce liquid nitrogen is considered (<0.5 kWh kg^{-1} [249]), the efficiency advantage of liquid nitrogen pre-cooling decreases.[250] For example, Van Hoecke *et al.*[251] estimated that 30% of the energy required for the liquefaction of hydrogen is used to produce liquid nitrogen. A challenge with using nitrogen is, however, the large temperature differential between its cooling curve and that of the pre-cooled hydrogen gas which limits heat recovery.[240] Conceptual processes have accordingly explored the use of helium, neon, LNG[235] and mixed refrigerants[127,200,210,238] in both pre-cooling and cryogenic stages.[252] Mixed refrigerants (MRs) are advantageous because the evaporation curve can be designed to closely match the cooling curve of the hydrogen gas by altering the refrigerant mixture's composition (Fig. 13).[155] The resulting minimisation of temperature difference improves thermodynamic efficiency.[155] Mixtures may also have better heat transfer properties and compression features than pure refrigerants.[200] Common MR compositions include hydrogen, nitrogen, neon, helium, and hydrocarbons ranging from methane to butane.[155] However, achieving the desired hydrogen effluent temperature of 80 K in one stage, and the potential freeze-out of the heaviest components in the refrigerants are limitations.[202] Thus conceptual processes have proposed a higher pre-cooling temperature, for example, 130 K,[221] with multi-stage cascaded removal of components based on temperature.[127] While implemented in LNG liquefaction, this can be challenging given the need to control and optimise the composition of the MRs throughout the cooling process.[202] Improved thermodynamic modelling of novel mixed refrigerants is needed to compare their performance with simple conventional refrigerants. Based on LNG experience, research into the optimal blending of these fluids and methods aimed at preventing the refrigerant mixture components from segregating is required.[253]

Expansion. Cooling can be achieved *via* Joule–Thompson expansion through a throttle valve or by turbine expansion

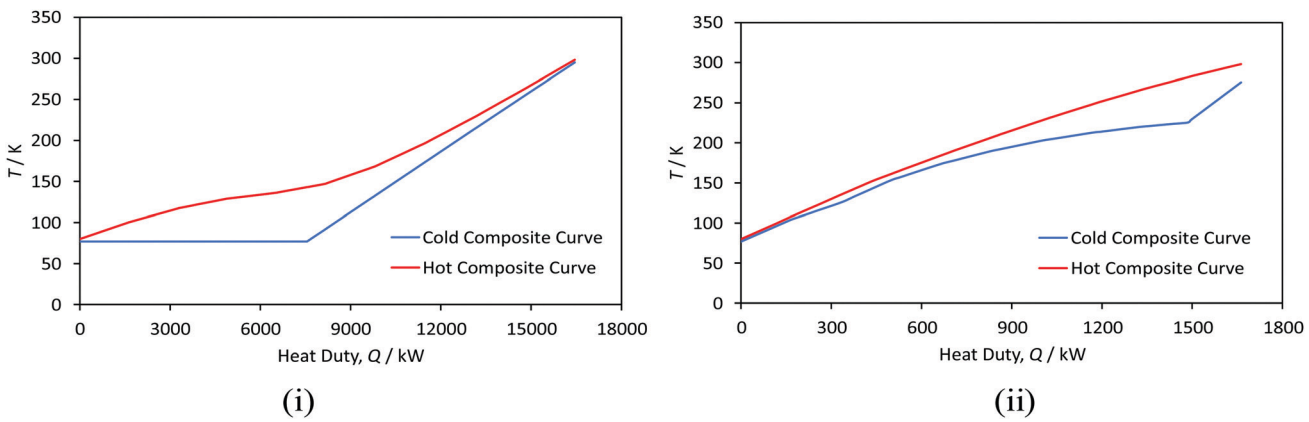

Fig. 13 Hydrogen (10 TPD feed) pre-cooling composite curves with different refrigerants: (i) conventional nitrogen and (ii) MR (nitrogen 18.7%, methane 26.4%, ethane 20.3%, propane 16.9%, i-butane 17.8%) using the PRICO system. Hydrogen feed condition: T = 298.15 K, p = 3 MPa. Hydrogen intermediate condition: T = 80 K, p = 3 MPa. Minimum temperature approach of heat exchanger = 3 K.

which enables further cooling with increased CAPEX. The use of turbine expanders results in higher exergy efficiency[247] because mechanical energy from the rotation of the turbine can be recovered and a larger cooling effect is achieved. This could potentially reduce specific energy consumption by about 7% or more.[237] Radial flow turbines and axial flow turbines are used for industrial liquefier expansion on the refrigeration side.[254] Reported cryogenic expander efficiencies in the literature are between (80 and 90)%.[192] Axial turbines have a higher efficiency than radial turbines (at $Re > 10^6$), but attract a higher capital cost.[255] Radial turbines are advantageous in that the work recovered from a single stage is equivalent to that of two or more stages in an axial turbine.[255]

Oil-bearing and gas-bearing turbine technologies are considered state-of-the-art for hydrogen liquefiers.[126,256] Oil-bearing systems require a continuous oil supply, oil pumps, and additional infrastructure for safe shutdown in the case of cycle failure.[192] This additional equipment and power requirement increases their capital and operational expenditure above those of gas-bearing turbines. Gas-bearing turbines eliminate the risk of oil contaminating the hydrogen (because they use a gas film in the bearings), have higher isentropic efficiencies than oil-bearing turbines, reduced footprint, and provide greater turbine reliability.[126,256]

Most of the conceptual processes identified in Table 5 utilise a turbine expander both on the hydrogen and refrigeration side; however little detail as to the type to be deployed is provided. Valenti and Macchi estimated power recovery from expanders in their helium Brayton cycle to be greater than 1 kWh $kg_{LH_2}^{-1}$.[216] There is certainly potential to use large oil-free turbines in large-scale liquefiers;[257] however, turbine expanders are both complex and attract a higher capital expenditure.[104,258] Alternatively, exposing hydrogen to external magnetic fields can cause a temperature change and potentially liquefy it.[259–261] Consequently, recent studies have considered the use of magnetic refrigeration as a final cooling stage in place of expansion to liquefy the hydrogen.[262,263]

Liquefaction cycles. To date, industrial liquefiers has been limited to pre-cooled Claude cycles. Conceptual liquefaction processes employing Brayton refrigeration cycles with high compressor and expander efficiencies (Berstad *et al.*, Valenti & Macchi, IDEALHY, Krasae-in) are often characterised by higher exergy efficiencies and lower SEC. The use of MRs on the working fluid side, as opposed to hydrogen, has been found to reduce the overall exergy destruction[187] by 7%.[182] Further research into the viability of large scale Brayton cycles is warranted.

3.5 Cost gap between existing and conceptual plants

Energy use accounts for around 30% of the total liquefaction cost of current liquefiers. These are dependent mainly on the liquefier efficiency[189] which is in turn highly dependent on the energy consumption of the selected liquefaction process and electricity price. Liquefaction capacity also plays a major role in the cost breakdown. While existing liquefiers produce liquid hydrogen at (2.5 and 3) US$$ per kg_{LH_2}, some conceptual designs are projected to produce liquid hydrogen below 1 US$$ per kg_{LH_2}. Literature liquefaction cost estimates, as shown in Table 6 and Fig. 14, provide insight into plausible target costs. The Asia Pacific Energy Research Centre (APERC) report includes a projected hydrogen liquefaction price between (0.5 and 0.8) US$$ per kg_{H_2}.[94] This cost is much smaller than current liquefiers and is based on the IDEALHY system which estimates an energy consumption of approximately 6.4 kWh $kg_{H_2}^{-1}$.

To date, such efficiency has not yet been achieved in commercial liquefiers. In comparison, Kawasaki Heavy Industries has stated a liquefaction price of approximately 9.8 JP¥ per Nm^3 (1.1 US$ per kg_{H_2}).[102] Wijayanta *et al.*[98] projected a smaller liquefaction cost by 2030 of approximately 7.3 JP¥ per Nm^3 (0.76 US$ per kg_{H_2}). Other cost estimates are detailed in Table 6. However, none of the cost estimates can be achieved using existing liquefier designs, capacities and technologies. For reference, Connelly *et al.*[109] estimated a liquefaction cost of 2.75 US$ per kg_{LH_2} for a 27 TPD plant in California (USA), which is based on current commercially available technology used in existing industrial liquefiers. As shown in Fig. 14, specific liquefaction costs generally decrease with increasing plant capacity; however, this depends largely on the electricity cost which varied between (40 and 120) US$ per MW h across these studies. This observation is consistent with the work published by Cardella *et al.* who found that SLC decreased by almost 60% with a 50 TPD plant or by 67% with a 100 TPD plant, compared with a 5 TPD plant.[93,264]

3.6 Development potential of large-scale LH_2 plants

From the above review of industrial and conceptual hydrogen liquefaction plants, key challenges were identified across the liquefaction process; these are summarised in Table 7. Obviously, for a new generation of large-scale plants (>100 TPD), there is a need to increase efficiency while managing overall total cost – a SEC target of 6 kWh kg^{-1} and a SLC less than 1 US$ per kg should be achievable.

A specific power requirement range between (6 and 8) kWh kg^{-1} is a plausible target, as shown in Fig. 14 by various conceptual studies, for scaled-up liquefiers without the need for novel technologies. However, this should be obtained *via* identifying rational and economically-viable means for improving efficiency which necessitates more advanced and integrated process designs that can increase exergy efficiency and thus reduce specific power requirements.[237] Different design features should be considered in comparison to traditional large-scale hydrogen liquefaction processes, such as:

- Use of liquefaction cycles with new cryogenic refrigerant mixtures of helium/neon/hydrogen to enable the use of turbo compressors, which are generally well suited and scalable to very high capacities. This, and the potential for higher compressor efficiency, could be important elements when scaling-up liquefaction plants.
- Similarly, use of MR/LNG in the pre-cooled cycle instead of nitrogen to potentially cool down the hydrogen to around (80–110) K. Although some consideration is still required with respect to potential freeze-out and optimized composition, this

Table 6 Hydrogen liquefaction costs reported in literature – ordered by increasing amount

Study/report	Year	Country of study	Liquefaction cycle	Scale [TPD]	Liquefaction units/Individual capacity	SEC [a] [kWh kg^{-1}]	Electricity cost [b] [$$ per MW h]	Liquefaction cost [b] [$ per kg$_{H_2}$]	Status
APERC[94]	2018	APEC[c]		800	16 × 50 TPD	6.4	68[d]	0.53–0.78	Conceptual (2030)
Heuser *et al.*[95]	2019	ARG	MR pre-cooled Brayton[e]	50		6.78	41	0.64[f]	Conceptual (2018)
Hydrogen Council[96]	2021	SAU		9000–10 300[g]			13–37[h]	0.7–1.0[w]	Conceptual (2030)
Li *et al.*[97]	2020	USA		27–30		12	50–120	0.7–2.0[w]	Conceptual (2030)
Wijayanta *et al.*[98]	2019	AUS		822		15		0.76[w]	Conceptual (2030)
Teichnmann *et al.*[99]	2012	EUR[i]		2822		7	56	0.82	Conceptual (2030)
Ishimoto *et al.*[100]	2020	NOR		500	1 × 500 TPD	6.46	42.56	0.95–1.38	Conceptual (2030)
Watanabe *et al.*[101]	2010	ARG	LN_2 pre-cooled Claude[l]	16 400	55 × 300 TPD	8.72[l]	54.5–77.3[jk]	0.97–1.20[jk]	Conceptual (2010)
Watanabe *et al.*[101]	2010	ARG	LN_2 pre-cooled Claude[l]	16 400	322 × 51 TPD	8.72[l]	72.2–100[km]	1.03–1.40[km]	Conceptual (2010)
CSIRO[37 n]	2018	AUS		210		7.88	26.80	1.07–1.30	Conceptual (2025)
KHI[102 o]	2015	AUS		770		11	39.76	1.1	Conceptual (2030)
Nyberg[103]	2021	NOR		176.2		7.5	46.26	1.68	Conceptual (2030)
CSIRO[37 p]	2018	AUS		50		9.05	40.20	1.72–2.10	Conceptual (2025)
IDEALHY[104–106]	2013	DEU	MR pre-cooled Brayton	50		6.4[q]	112	1.93	Conceptual (2013)
Raab *et al.*[107]	2021	AUS		676.5	3 × 225.5 TPD	7	88.14	1.97	Conceptual (2020)
Reuß *et al.*[108]	2017	DEU	MR pre-cooled Brayton[e]	50		6.78	67.2	2.12–2.22[r]	Conceptual (2015)
DOE[109 s]	2019	USA[t]	LN_2 pre-cooled Claude	27		11.5	42.68	2.75[u]	Established (2018)
European Commission[110]	2020	EUR[i]		27		11.5	30–50[v]	2.76	Established (2019)

[a] SEC – specific energy consumption. [b] Average exchange rate over the last 6 months prior to submission: 0.67 USD = 1 AUD, 1.12 USD = 1 EUR, 1 USD = 107.2 JPY. [c] Asia-Pacific Economic Cooperation is a grouping of 21 member countries including Australia, Canada, China, Japan, New Zealand, and the USA. [d] Utility electricity cost in the USA by 2030. [e] Based on IDEALHY conceptual design. [f] Includes the levelized cost of compressing and transporting *via* pipeline the gas after production to the liquefaction facilities. [g] Cost for at-scale production and transportation for selected transport routes. [h] Assumed levelized cost of electricity by 2030. [i] LH_2 imported into Europe. [j] Electricity generated through windmills with a total capacity of 77 500 MW. [k] Cost calculated with an interest rate of 0.5 and 5%, respectively. [l] Liquefaction plant is based on WE-NET conceptual design. [m] Electricity generated through windmills with a total capacity of 60 400 MW. [n] Projected case. [o] Kawasaki CO_2 free hydrogen supply chain concept. [p] Base case. [q] 6.76 kWh kg^{-1}, including auxiliary energy requirements. [r] Prices account for seasonal changes in hydrogen cavern storage due to higher electricity prices. [s] DOE – Department of Energy. Data from national laboratory models, Hydrogen Delivery Scenario Analysis Model [HDSAM] and Hydrogen Analysis [H2A]. [t] Supply chain developed for urban California market. [u] Overall levelized cost is $2.75 per kg H_2, which includes recurring costs. The capital contribution for a plant of this capacity is $1.41 per kg H_2. [v] Cost assumed to be the same that the levelized cost of electricity of renewables at Chile and Australia as analysed in the study. [w] Cost calculated for a 2030 scenario.

can be largely implemented today. This can be accompanied by the use of expanders to increase efficiency.

• In addition use of, high-efficiency turbo-compressors on the refrigeration side, replacement of the J–T valve at the liquefaction stage by an expansion gas-bearing turbine (to minimize vapor fraction after expansion) whilst also ensuring high feed gas pressures between (1.5 and 3) MPa.

4 Liquid hydrogen storage and transportation

Rising demand for liquid hydrogen in new markets located a long-distance from the production site presents a new set of challenges in terms of transport and storage of this cryogenic fluid. These challenges stem largely from the boil-off losses caused by various heat sources leaking into the liquid, particularly over long periods of time. The severity of the problem was demonstrated in the Space Shuttle program managed by NASA, where over 24 500 tonnes of liquid hydrogen were purchased, of which 45.4% was lost during storage, loading, or replenishing.

4.1 Liquid hydrogen storage

Tank design – shape. Liquid hydrogen is most commonly stored in horizontal or vertical cylindrical tanks. Fig. 15 schematically shows the general features of a traditional LH_2 storage tank regardless of shape or scale. Structural supports can be based on tension (rods or cables) or compression (load bearing pads) depending on the particular tank design. Ullage space is typically $\leq$10% of the internal volume of the tank.

Spherical tanks are used for storing larger volumes[132] because they provide a minimum surface-to-volume ratio, and a more uniform distribution of stresses and strains. NASA operates the largest current storage vessel (3800 m^3) for liquid hydrogen at Kennedy Space Centre, FL, USA with a storage capacity of 263 tonnes (if stored at 22 K and 0.15 MPa).[265] NASA has more recently announced the construction of a 4732 m^3, 327 tonne liquid hydrogen tank.[86] In 2015 the US Department of Energy reported the price for a 3500 m^3 liquid hydrogen tank was US$6.6 million (with a long-term target price of US$3.3 million).[266]

Kawasaki Heavy Industries completed the construction of its LH_2 receiving terminal in the Port of Kobe in July 2020.[267] The

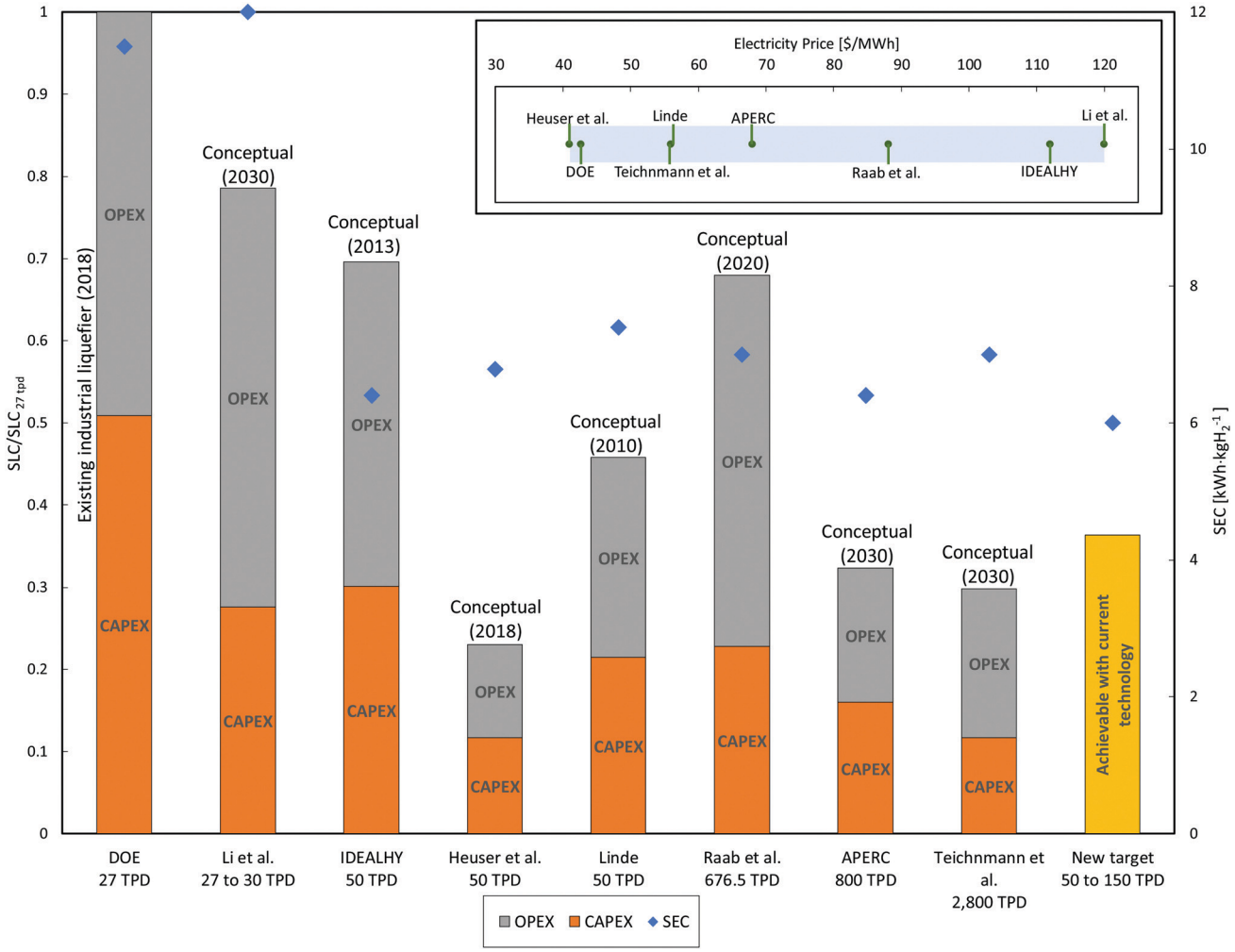

Fig. 14 Specific energy consumption (SEC) and specific liquefaction costs (SLC) relative to a reference 27 TPD LH_2 process ($2.75 per kg H_2) and the various conceptual processes estimated at different electricity costs.

terminal features a 2500 m^3 double-shell spherical storage tank with an outer diameter of approximately 19 m.[267] The tank contains vacuum perlite insulation and is designed for a boil-off rate of less than 0.1% per day.[267] Linde provides a variety of liquid hydrogen storage tank designs for industrial applications, fuel stations and bulk storage. These range in size from (12 to 300) m^3, with a boil-off rate of $<0.95\%$ per day, depending mainly on the insulation materials used (vacuum-perlite or multi-layer insulation).[268] Linde's large spherical tanks have an inner volume of 1100–2300 m^3 with a storage capacity of 70–145 tonnes LH_2 and a boil-off rate of $<0.1\%$ per day.[268]

Tank design – material. The selection of a suitable tank wall material requires a balance of high strength, high fracture toughness, high stiffness, compatibility with cryogenic temperatures, and low permeation of liquid and gaseous hydrogen.[269] The most appropriate materials for the construction of inner tanks are metallic materials and composites.[269] Metals with acceptable properties from ambient to cryogenic temperatures include austenitic stainless steels, monels, aluminium alloys, titanium, and copper.[269] 300-series stainless-steel alloys are most commonly used in industry for inner vessel walls, with carbon steels used for outer vacuum shells. Ceramic materials offer high specific strength but, owing to their low fracture toughness, are not appropriate.[269]

In applications where weight is an issue, tank designs must also minimise tank weight. Tanks can, for example, exceed 50% of the dry weight of a space vehicle.[270] Typical vessel designs are double-walled, vacuum-jacketed fluid containers.[271,272] However, tanks may also use single walls with constant or variable thicknesses, although these are primarily employed at end-use points such as for rocket propellant tanks, and not for long term storage. High-vacuum insulation ($<10^{-2}$ Pa) is commonly used for small-sized tanks (40 m^3) and low-vacuum insulation (<1 Pa) is used for large tanks.[102] The space between the double-walls serves as an insulation layer to minimise heat transfer to the liquid hydrogen in the inner vessel – traditionally perlite is used in this capacity. Advantages and disadvantages of common insulation methods are set out in Table 8.

A number of composite wall materials have also been investigated, including graphite/epoxy composites and composite

Table 7 Summary of challenges across the hydrogen liquefaction process[126,169,174,192,202,245,246,256]

Stage	Overall	Compression	Pre-cooling
Challenges	• Increase efficiency, decrease energy consumption and cost • Modular limitations • Integration of renewable energy • Translation of conceptual models to industry • Thermodynamic model accuracy for process design and simulation • Hydrogen embrittlement and leakage	• High energy demand • Large number of compression stages required • Flow rate limits of piston compressors • No evidence of turbo-compressors use in industrial LH_2 plants	• High energy demand of producing and recycling LN_2 • Limited industry examples of LNG or MR used for H_2 cooling • MR thermodynamics not well understood • Lack of knowledge on costs and environmental consequences for N_2, LNG and MR cycles

Stage	Cryogenic Cooling	Catalysts and OP conversion	Expansion
Challenges	• Freeze out of impurities from H_2 • Optimising heat exchanger sizes • Accuracy of thermodynamic models	• Accurate OP ratio measurement • Optimizing residence time of H_2 in the heat exchanger • Limited conversion rate data for different catalysts • Catalyst longevity • Pressure drop in heat exchangers	• Maximising work recovery • J–T expansion inefficiency • Large-scale oil-free and efficient turbine expanders • Optimising flow rates for different expansion technologies

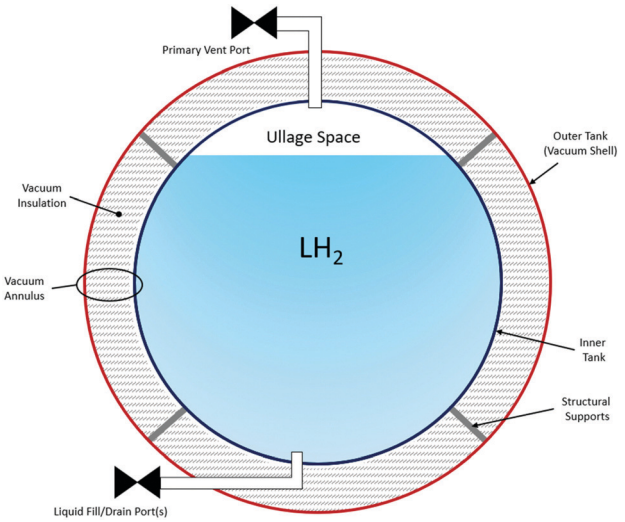

Fig. 15 A schematic showing general features of a LH_2 storage tank.

vessels both with and without liners.[273] Challenges in the application of these materials include significant thermal residual stress in laminates due to coefficient of thermal expansion (CTE) mismatch between fibres and resin, and the embrittlement of resins under cryogenic and thermal cycling conditions.[270] Research is still ongoing into the permeability and microcracking of these materials.[92]

Glass bubble insulation consisting of hollow glass spheres has been proposed. Field demonstration tests at NASA's Kennedy and Stennis Space Centres in 2015 found that boil-off losses were reduced by as much as 46% through the use of this glass bubble insulation in the field, compared to the use of perlite. Aerogel insulation may be feasible for short-term storage.[273] Liquid hydrogen storage vessels manufactured with a liquid nitrogen shield have been proposed. Another design concept is to use the cold hydrogen boil-off vapor to shield the stored liquid hydrogen, resulting in a warmer gas exiting the tank.[274]

At the large scales planned for the future ($>50\,000$ m^3), the biggest issue associated with liquid hydrogen storage is likely to be how to appropriately insulate the vessels. Traditional vacuum-jacketing might not be feasible at this scale. Novel insulation system schemes are needed that don't require a self-supported outer jacket, but which still meet the thermal performance requirements associated with managing boil-off gases, preventing air liquefaction (if exposed to the environment), gas purge requirements, and which do not degrade over time.

Boil off management. Boil-off gas (BOG) production is an unavoidable result of the storage of LH_2.[133,275,276] A certain percentage of liquid hydrogen will enter the gas phase over time depending on factors such as wall material, insulation quality and surface-to-volume ratio of the vessel. While there are analogies with the storage of other industrially important cryogenic liquids, like LNG and LN_2, BOG is much more severe for LH_2 given it is stored at temperatures about 90 K lower. Liquid hydrogen BOG losses can be on the order of 0.4% per day for a 50 m^3 cryogenic tank, and 0.06% per day for a 20 000 m^3 tank.[271] Additionally, heat ingress causes the vapor temperature to increase faster than that of the liquid due to the vapor's higher thermal diffusivity, resulting in heat conduction across the vapor–liquid interface and thus a temperature gradient in the top layer of the liquid phase known as thermal stratification.[277–285]

BOG generation occurs at LH_2 plants and exporting terminal for several additional reasons. These include BOG generation due to depressurisation (flashing), heat ingress into transfer pipes, heat added by equipment such as pumps, and cooling down of LH_2 carrying vessels. For future large-scale LH_2 storage and transport applications involving land-based tanks and

Table 8 Advantages and disadvantages of various insulation methods, listed in order of increasing thermal insulation performance[301]

Insulation method	Advantages	Disadvantages
Foam – outside	+ Currently in use, well established	− Short term storage applications due to high thermal conductivity
	+ Low cost, easy to implement	− Low resistance to thermal radiation
	+ Lightweight and low density	− Potential damage from environmental hazards and CTE mismatching[a]
	+ Provides good thermal resistance under non-vacuum conditions	− Degradation over time if exposed to the environment
Foam – inside	+ Low cost	− Larger structural tank wall required, resulting in increased mass
	+ Structural wall may be not exposed to cryogenic conditions	− Difficult to seal from cryogenic fluid[b]
	+ Reduced CTE[a] mismatch issues because of composite constituents, therefore reduced microcracking	
Vacuum[cf]	+ Convection heat transfer suppressed or eliminated well established	− Heavier tank walls required
		− Costly to implement and maintain
		− Loss of vacuum failure scenario
Aerogel[c] (Bulk fill or blanket)	+ Extremely low thermal conductivity and density[d]	− Limited mechanical properties
	+ Provides excellent thermal resistance under non-vacuum conditions/moderate resistance under vacuum	− Not well established for large vessels
Perlite[c] (Bulk fill)	+ Low cost, well established	− Vacuum required to achieve high performance
	+ Low density	− Compaction can happen with certain tank geometries under thermal cycling and/or dynamic loads
	+ Provides moderate thermal resistance under non-vacuum conditions/good resistance under vacuum	
Glass Bubbles[c] (Bulk fill)	+ Very low density	− Vacuum required to achieve high performance
	+ Simplified installation due to flowability	− Not well established for large vessels
	+ Provides good thermal resistance under non-vacuum conditions/excellent resistance under vacuum	
Multilayer insulation[c] (Blanket)	+ Low density and radiation heat transfer[e]	− High vacuum required
	+ Provides moderate thermal resistance under non-vacuum conditions/superior resistance under high vacuum	− Costly to implement and maintain
		− Near-catastrophic failure upon loss of vacuum
	+ Well established	− Difficult to execute for certain tank geometries

[a] CTE – coefficient of thermal expansion. [b] Fluid infiltration leads to increased thermal conductivity, potential loss of structural wall integrity. [c] These insulation methods are situated between walls. [d] The balance between the structural and thermal properties can be altered and optimized for the application. [e] Multilayer insulation is available in graded form to improve thermal properties and to reduce the density, but at a higher cost. [f] Method must be used in conjunction with an accompanying insulation material in order to achieve proper thermal protection.

sea-borne vessels, the management of such BOG is crucial from both an economic and safety perspective.

Petitpas[276] modified a MATLAB code previously provided by NASA, to estimate the boil-off losses along the entire LH_2 pathway from liquefaction to dispensing. During LH_2 storage, Petitpas found that some temperature gradients may exist across the vessel (thermal stratification). This tendency of the stored liquid hydrogen to thermally stratify in a layer near the liquid-vapor interface causes challenges in propellant utilisation in large liquid-hydrogen fuelled rocket vehicles where pump cavitation is likely to occur which could result in the destruction of the flight vehicle.[278] Fig. 16 shows a comparison between calculations made by their code for a 12.5 m^3 storage vertical tank (90% fill, with initial and final (relief) pressure of 0.137 and 0.31 MPa, respectively) and the super-heated vapour BOG model developed recently at UWA,[286–288] originally for simulating industrial-scale LNG storage. This super-heated vapour model, implemented in the freely-available software package BoilFAST which includes options for LH_2 and NH_3 storage,[289] considers the vapor and liquid phase temperatures to be independent but assumes they are spatially uniform; the liquid phase is assumed to be saturated, while the vapor can become superheated. For each phase, mass and energy balances are solved iteratively to determine phase amount and composition, boil-off rate, and vapor temperature. The BoilFAST results for the 12.5 m^3 LH_2 storage tank were in excellent agreement with those calculated by Petitpas and provided additional predictions such as BOG relief rate. On average, the daily BOG amount was calculated by both methods to be 5 kg (less than 0.5% volume loss per day).

Many studies[290–303] have investigated possible ways to reduce boil-off losses and suggested that top fill (top spray) is probably the most effective way to reduce transfer losses, although more understanding of the underlying physics is needed. NASA have demonstrated the operation of an Integrated Refrigeration and Storage (IRAS)[294] system allowing temperature control of the stored liquid hydrogen. This system employs an integrated heat exchanger together with a cryogenic refrigeration

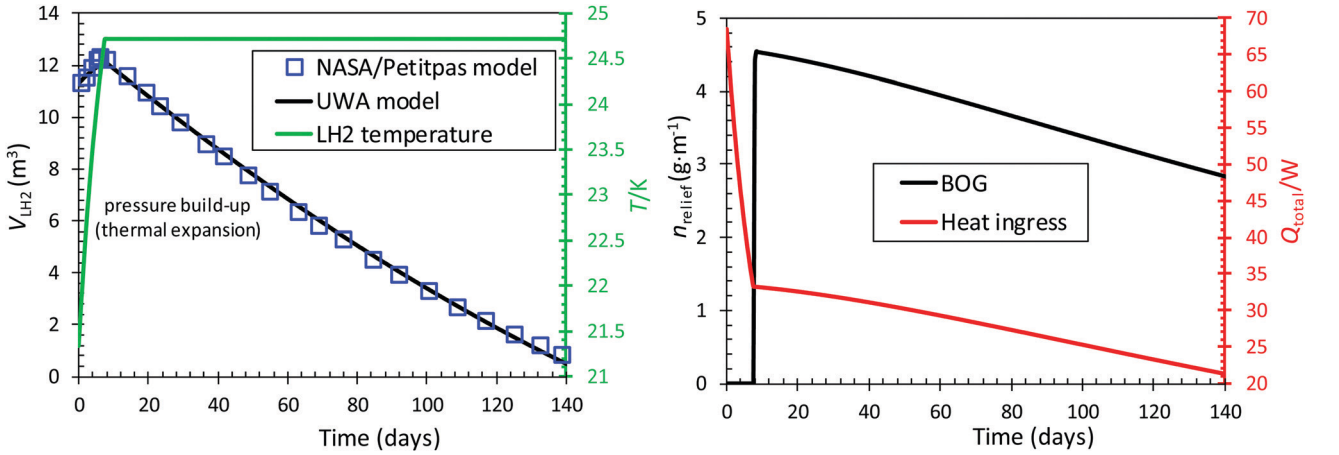

Fig. 16 Change of liquid hydrogen stored volume and boil-off gas rate over time in a 12.5 m^3 storage tank. Symbols correspond to the literature values while solid curves correspond to the value calculated using the model developed at the University of Western Australia (UWA).

system that uses helium as the working fluid. Features of this system include zero boil-off and densified slush hydrogen production (mixture of liquid and solid hydrogen), which is detailed in Section 4.3.

4.2 Liquid hydrogen transport

In addition to selecting suitable materials for tank design, and minimising boil-off gas during transportation,[92,304] another key consideration in liquid hydrogen transport is sloshing.[304] This phenomenon is the movement of the liquid in the vessel due to the motion of the carrier, and it can lead to significant boil-off. Baffles may be installed in the tank to mitigate the effect.[305] The LNG industry has conducted several studies into sloshing and how to minimise it,[306–308] although generally it is avoided in practice by requiring minimum fill levels for vessels before they commence transport. This approach may not be sufficient for LH_2 transport, given the higher rate of boil-off.

To date, transportation of liquid hydrogen occurs predominantly by truck, with capacities up to approximately 60 m^3 ($\approx$4150 kg).[271] The transportation of hydrogen by truck is primarily limited by high boil-off losses and volume capacity, rather than by weight. Safe road transport of liquid hydrogen can be achieved with existing technology; however, this is not at a scale comparable to the existing petroleum fuel distribution network.[309] There exist few examples of liquid hydrogen transported by rail or aircraft.[271] However these methods of LH_2 transportation are limited by high energy use, boil-off losses and/or total capacity.

Transporting liquid hydrogen by marine vessels has historically been limited to fuel supply for the USA and French space programs.[310] In November 2016, the International Maritime Organisation provided endorsement for the transport of liquefied hydrogen in bulk by sea between Australia and Japan.[311] The Hydrogen Energy Supply Chain Project (HESC), which intends to transport liquid hydrogen from the Port of Hastings in Victoria, Australia, to Kobe, Japan, will be the first commercial project to pilot liquid hydrogen maritime transport.[311] The project will inform future amendments to the IGC Code (*International Code for the Construction and Equipment of Ships Carrying Liquefied Gases in Bulk*), including the potential to allow liquid hydrogen to be carried in bulk under the code without the requirement for special agreements.[311]

In December 2019, Kawasaki Heavy Industries launched their liquid hydrogen tanker, designed to carry 1250 m^3 of hydrogen from Australia to Japan. The liquid hydrogen vessel is cylindrical and designed with a vacuum-insulated double-walled structure.[267] The support structure uses glass-fibre-reinforced plastic to minimise heat transfer.[267] A boil-off rate of less than 0.4% per day was reported, with BOG being re-stored without venting to atmosphere.[267] In October 2020, Kawasaki Heavy Industries conducted a successful world-first sea trial of the liquefied hydrogen carrier SUISO FRONTIER. In December 2021, this ship departed from Japan bound for Australia. Conceptual approaches to BOG management have also investigated its use as a fuel, re-liquefying it or burning it.[312]

4.3 Densification and slush hydrogen

The use of liquid hydrogen densification and slush hydrogen are prospective technological approaches for addressing the challenges of storing and transporting LH_2. Reducing the temperature of liquid hydrogen to 13.8 K can increase its density by 8.8% (77.0 kg m^{-3}).[86] Cooling further leads to the creation of slush hydrogen, a mixture of liquid and solid hydrogen at the triple point (13.8 K for *para* hydrogen). The mixture can have a density up to 22% higher than liquid hydrogen at its bubble point.[86] This can offer potential reductions in size and mass of storage systems and transport vessels, and/or enable the transport of larger quantities in a given volume.[297] Densification also allows for longer storage before boil-off, and increases cooling capacity when used as refrigerant.[86] Traditionally, slush hydrogen has only been investigated for use in space missions.[313–316] Slush hydrogen is produced *via* three key methods: (1) the spray method where liquid hydrogen is expanded, thus solidifying it, and mixed with liquid hydrogen; (2) the freeze–thaw method with a Dewar and vacuum pump; and (3) the Augur method (which uses helium refrigeration).[317,318] The production cost of slush

hydrogen is obviously greater than the liquefaction costs of hydrogen.[319]

5 LH_2 supply chains: prospects and challenges

Hydrogen has long been identified as a likely central component of future energy systems. In 1874, Jules Verne described the use of hydrogen and oxygen derived from water as fuels that would replace coal.[320] Waves of enthusiasm for hydrogen have occurred several times in the last 50 years, particularly in the 1970s and early 2000s, largely in response to concerns about energy security. However, the cost of making and using hydrogen at those times ultimately meant these waves of enthusiasm did not lead to the envisaged wide-scale use of hydrogen for energy applications.

Todays' wave of enthusiasm for hydrogen is qualitatively different to those of the last 50 years in at least three ways. It is not only motivated by energy security but also the need to decarbonise the world's energy system. Additionally, the cost of producing renewable energy has decreased substantially, and CCS technologies are also more mature. Finally, the cost of using hydrogen to generate electricity has also dropped dramatically with the development, for example, of fuel cell technologies. These differences provide a basis for optimism regarding the current prospects for hydrogen's ascendance to a prominent and central component of global energy supply chains.

However, if hydrogen is to meet this expectation, a number of significant challenges will need to be overcome. Within the broader context of the hydrogen value chain (Fig. 1) these challenges can generally be classified as relating to cost (*e.g.* \$2 per kg_{H_2} is equivalent to \$16.7 per GJ or more than 4 times the average 2021 Henry Hub natural gas price[321]), scale (*e.g.* the capacity to construct or convert national-scale infrastructure for hydrogen distribution), and the maintenance of social license (*e.g.* managing use conflicts over scarce waterresources). Challenges specific to the LH_2 supply chain may similarly be placed in one or more of the four categories identified in the introduction: economics, cryogenic losses, scale and safety. These categories are clearly inter-related with, for example, safety requirements and the magnitude of cryogenic losses associated with liquid hydrogen storage inherently impacting its economics. Section 4 considered the underlying issues and emerging technical solutions relating to cryogenic losses of LH_2. This section reviews the challenges and prospects associated with the other categories, by first covering the safety of liquid hydrogen supply chains and then considering their economics and scale-up. Comparisons with liquid ammonia, the primary alternative hydrogen vector to LH_2, are then reviewed before a summary is presented of the priority research and development areas needed to advance liquid hydrogen supply chains.

5.1 Safety of liquid hydrogen supply chains

Ensuring the safe operation of hydrogen value chains is a challenge that relates to both cost and the maintenance of social licence. General awareness of the Hindenburg disaster after more than 80 years is a stark example of how easily energy technologies can be substantially tarnished in the mind of the public, even if the accident's root cause had little to do with hydrogen *per se*.[322] The development and application of effective and efficient engineering standards are the central tool to address the challenge of hydrogen safety.

There are several factors that give rise to safety risks inherent to the hydrogen value chain in general and liquid hydrogen in particular. Hydrogen gas has a strong propensity to leak due to its small molecular size and high diffusivity. A number of NASA launches have been halted due to hydrogen leaks, mostly in umbilicals.[86] Hydrogen can also cause embrittlement of many materials, resulting in cracking and catastrophic failure of metals significantly below the yield stress. Furthermore, hydrogen has a high propensity to ignite due to its wide flammability range (4 to 74 vol% in air) and very low ignition energy (0.017 mJ).[251] It has been shown to spontaneously ignite on sudden release from pressurised containers, although the mechanism is not fully understood.[323] Hydrogen flames burn with a hot but near-invisible flame, making them difficult to detect.[323]

For systems producing or handling liquid hydrogen, the materials of construction must be both resistant to hydrogen embrittlement and suitable for use at cryogenic temperatures. Consideration must also be given to the expansion and contraction caused by the changes from ambient to liquid hydrogen temperatures.[323] Liquid hydrogen can cause other gases (such as air and nitrogen) to condense and solidify – this can cause blockages and failures in equipment. As a result, storage tanks should be kept under positive pressure to prevent air ingress and purges of equipment should be followed by refilling with hydrogen, or replacement with helium.[323]

Liquid hydrogen and the associated boil-off gas can produce severe burns upon contact with the skin and delicate human tissue such as the eyes.[323] Until the hydrogen vaporises as it warms, it will accumulate as a substance denser than air. This produces a considerable fire and explosion risk. This has resulted in vent line explosions in the past.[86] In the situation that liquid hydrogen comes into contact with another liquid at a temperature above hydrogen's boiling point, there is a risk of a rapid phase transition explosion.[323] This phenomenon has been observed for spills of LNG on water, but is not well understood for liquid hydrogen.[323]

NASA has observed significant degradation in performance of cryogenic hydrogen storage tanks due to issues with insulation systems.[86] For example, a perlite void resulted in the venting of over 12 000 gallons per day of hydrogen.[86] It was unclear what may have caused the void to form. Vacuum leaks have also posed a significant problem as evidenced by increased boil-off. These leaks resulted in the solidification of air in the storage tank annulus, which subsequently liquefied (as LH_2 was removed from the tank) and cooled the vacuum jacket.[86] This phenomenon decreased the tank wall temperature below its ductility limits, thereby cracking the vacuum jacket;[86] it could have been prevented by draining the tank more slowly whilst heating the outer vessel with water.[86]

PRESLHY[324] is currently conducting experimental work in hydrogen release and mixing, ignition, and combustion with a view to providing enhanced recommendations for safe design and operations of liquid hydrogen technologies.[324–326] Kawasaki Heavy Industries in collaboration with TEN, JAXA, JARI, and the University of Tokyo have conducted experiments into the safety of liquid hydrogen storage including diffusion behaviour and heat leaks through cryogenic tank supporting structures.[267] These tests will help inform the development and strengthening of engineering standards that further increase the safety of planned LH_2 supply chains.

International standards for liquid hydrogen and maritime regulation. International hydrogen standards already exist and continue to be developed[327] both by the International Organisation for Standardization (ISO) and the International Electrotechnical Commission (IEC). A number of international technical committees now are responsible for drafting standards in specific fields.[328] Relevant standards for hydrogen liquefaction and storage include ISO/TC:22[329] (road vehicles), ISO/TC 197[330] (hydrogen technologies), and IEC/TC 105[331] (fuel cell technology).

Most hydrogen-specific transport and storage standards are, however, still in development and targeted primarily at the utilisation stage of the value chain. Long-standing LNG and Liquefied Petroleum Gas (LPG) storage and transport standards may have the potential to cover relevant areas for the export of liquid hydrogen; however, this will require considerable review.[332,333] Whilst the behaviour of LNG and LPG during transport is well understood, liquid hydrogen presents a unique set of challenges, particularly in the understanding of stratification, sloshing, boil-off gas, and pressure build-up. The National Fire Protection Association (NFPA) released a safety code which provides fundamental safeguards for the generation, installation, storage, piping, use, and handling of hydrogen in compressed gas (GH_2) form or cryogenic liquid (LH_2) form.[334]

Standards that govern the handling of liquid hydrogen at the point of use include ISO 13984 (Liquid hydrogen – land vehicle fuelling system interface) and ISO 13985 (Liquid hydrogen – land vehicle fuel tanks).[329] Standards that govern safety regarding liquid hydrogen and associated infrastructure include ISO/TR 15916 (Basic considerations for the safety of hydrogen systems), ISO 26142 (Hydrogen detection apparatus – stationary applications), and IEC EN 60079-10, 14, 17, and 19 (Electrical apparatus for explosive gas atmospheres: classification of hazardous areas, inspection and maintenance, and repair). There are also eleven ISO standards for materials testing, six of which cover hydrogen embrittlement.[335] Specific guidelines and recommendations have been developed by projects funded through the Fuel Cells and Hydrogen Joint Undertaking (FCH JU) (a public-private partnership) including[336] HYPER, HyApproval, HyIndoor, HyFacts, HyResponse and HySEA. The transport of liquefied gases by sea is covered by the International Code for the Construction and Equipment of Ships Carrying Liquefied Gases in Bulk (IGC Code),[337] which is a mandatory code under The International Convention for the Safety of Life at Sea (SOLAS Convention). The International Code of the Construction and Equipment of Ships Carrying Liquefied Gases in Bulk (IGC code) does not currently allow for the transportation of liquid hydrogen.[311]

The current state of standards thus requires first movers to negotiate regulation and permit requirements that are unclear, or not yet adapted for hydrogen use. Risk analysis toolkits, such as HyRAM,[338] have the potential to enable industry and standard development organisations to take a performance-based engineering approach to regulation.

While the development of standards will help with addressing this safety challenge, a gap in the general public's understanding of hydrogen has been identified.[339] Over fifty articles have studied public perceptions of hydrogen across a broad range of applications.[339] Currently, liquid hydrogen is not prominent in the public perception as it is mainly used in industrial applications. However, emerging applications such as its storage and use in domestic refuelling stations, may change this, particularly if an incident occurs where public safety is put at risk.

Several publications studying perceptions of hydrogen have found that public attitudes appear to be generally neutral.[339–345] These studies found that the most frequently identified concerns with the use of hydrogen technologies were safety and cost.[339] A majority of participants identified that they would only be willing to pay for the use of hydrogen technologies if the costs were comparable or less than those of conventional technologies, even if there were clear environmental benefits.[339] Thus even once the challenge of safety has been adequately addressed, the growth prospects for liquid hydrogen supply chains will be acutely dependent on how well the challenges of economics and scale can be addressed.

5.2 Cost and scale-up of liquid hydrogen supply chains

Projections of annual global hydrogen demand in 2050 have reached as high as 621 million tonnes.[129] Near term growth in the liquid hydrogen market is projected to be 5.66% annually in the five years to 2024.[346] For demand to reach these levels, the levelised cost of hydrogen (LCOH) associated with the entire value chain will need to decrease. Most analyses of the pathways by which this cost reduction can be achieved focus on scale up of the process to meet the larger demand. Fig. 17 and Table 9 present a summary of literature studies which have analysed the LCOH of possible liquid hydrogen supply chains, with scales ranging from (27 to 16 400) tonnes per day: the world's current largest single liquefier has a capacity of 32 TPD.

Fig. 17 shows how the LCOH of the liquid hydrogen supply chain was split by each study across four cost components: production, liquefaction, transport and distribution. The scale of the supply chain and the electricity cost assumed for the liquefaction process are also indicated. It is clear that there is significant variation between studies in the contribution of each cost component to the overall LCOH, which can make it difficult to compare different analyses or identify any trends associated with scale. The most variable component across the literature studies is the distribution cost, which ranges from 0 for several studies where it was not considered at all to

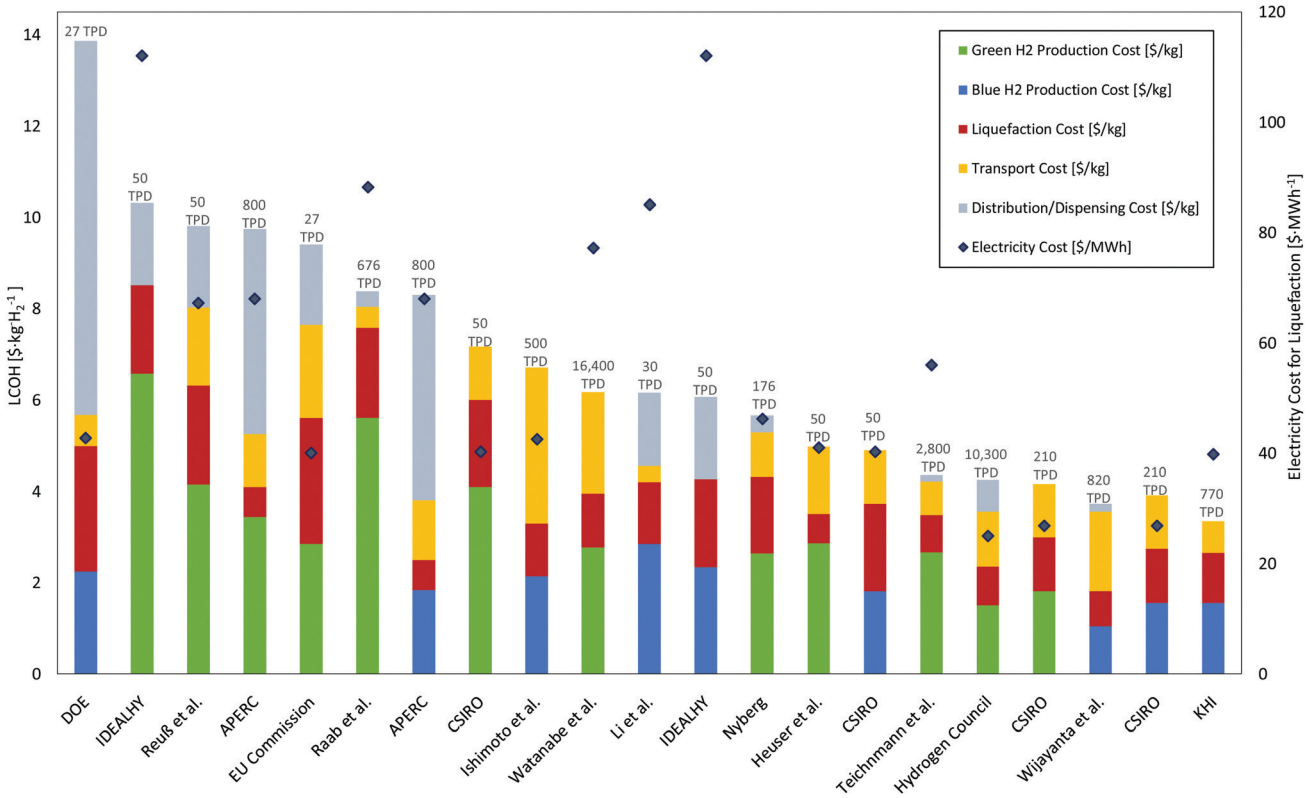

Fig. 17 Levelised cost of hydrogen (LCOH) for proposed liquid hydrogen value chains found in literature.

8.2 US$ per kg_{H_2}. This extreme latter value comes from a 2019 study reported by the DOE,[109] where the distribution cost included the construction of 79 refuelling stations, each dispensing 350 kg day^{-1}, as well as other costs such as taxes, insurance, licensing and permits. Reuß *et al.*[108] have observed that the significant variation of costs for different refuelling stations is caused by site location, station design and capacity. Li *et al.*[97] assessed the cost of various station designs, sizes and configurations. Large-scale hydrogen refuelling stations with a supply capacity of 1000 kg day^{-1} or more have distribution costs in the range (0.9 to 2.3) US$ per kg_{H_2}.

The second most variable component in the LCOH of prospective LH_2 supply chains considered in the literature is the production cost. The comparisons shown in Fig. 17 indicate whether blue or green hydrogen production was assumed; in several studies two different LCOH values were reported with the only difference being the method of production. For example, the APERC[347] conducted a study to calculate the total cost of hydrogen provision in Japan in 2030. Japan has set a target landed price of 3.3 US$ per kg_{H_2} by 2030 and a longer term target of 2.2 US$ per kg_{H_2}).[348] The study considered different international scenarios with an estimated hydrogen production cost from fossil fuel coupled with carbon capture and storage up to 2.8 US$ per kg_{H_2}, and from renewable energy up to 6.6 US$ per kg_{H_2}.[94] The study compared the cost for the liquid hydrogen supply chain in Japan with conventional fuels used directly for electricity generation or in refuelling stations for fuelling FCVs. The APERC study estimated an imported (delivery) cost between (2.5 and 6.8) US$ per kg_{H_2} when used for power generation and a total dispensing cost between (4.5 and 13) US$ per kg_{H_2} when used in refuelling stations.[94] This study concluded that imported hydrogen produced from fossil fuels with CCS can be competitive with power generation from oil by 2030 and with the cost of petrol in Japan if large capacity refuelling stations are utilised.

More recently, Longden *et al.*[349] compared the costs and carbon emissions associated with different modes of hydrogen production. Distributions of costs were collated from 97 estimates across 16 studies that considered both green and blue hydrogen production technologies with various levels of carbon capture and storage. They reported a median cost of hydrogen production from renewables of 3.64 US$ per kg_{H_2}, with a range from (2.13 to 7.79) US$ per kg_{H_2} resulting from the assumed capital cost ($500–2500 per kW), renewable electricity price ($10 to $85 per MW h) and/or electroyser capacity factor (26 to 48%).

The median cost of hydrogen produced by natural gas SMR with at least 90% CCS was 2.09 US$ per kg_{H_2}, with a range from (1.21 to 2.93) US$ per kg_{H_2}. At this level of CCS, the emissions intensity of using the blue hydrogen as a fuel was estimated to be about 22 $kg_{CO_2\text{-e}}$ GJ^{-1}, which is about one third that of using the natural gas directly.

The liquefaction and transport cost components have comparatively smaller variances than those of production and distribution and, based on the averages across the studies considered in Table 9, are the third and fourth largest contributors to the LCOH of the liquid hydrogen supply chains, respectively. The liquefaction

cost component has an average of (1.45 ± 0.66) US$ per kg_{H_2}, where the error bound denotes the standard deviation for the studies listed. The transport cost component of the liquid hydrogen supply chains varies slightly more, depending on the distance considered by the supply chain with an average of (1.32 ± 0.71) US$ per kg_{H_2} across all studies. Supply chains that involve maritime transport over distances of 1000 km or more had average transport costs of 0.14 US$ per kg_{H_2} per 1000 km, while over shorter distances (80 to 500 km) transport costs increased to 4.78 US$ per kg_{H_2} per 1000 km.

Liquefaction costs for the various studies depended on both the energy (electricity) price assumed and the scale of the process. Fig. 18 shows the estimated liquefaction cost component for each study in Table 9 against the scale of the LH_2 supply chains. The scales considered cover a range from just below the largest current LH_2 train in operation to conceptual trains 1000-times as large, with capacities similar to current mega-scale LNG trains. While there is considerable scatter in the estimated liquefaction costs, increasing the supply chain capacity above 100 TPD is expected to bring this component of the LCOH down to around 1 US$ per kg_{H_2}.

At this stage, it is unclear whether increasing the scale of LH_2 production trains beyond 100 TPD would lead to further reductions in unit liquefaction costs.[350–352] It may be that the modularisation of unit operations at a standard size can help lower manufacturing costs by more than the economy of scale benefits that might be achieved in single trains with larger capacities. In either case, up-scaling the equipment required for larger capacity liquefaction trains presents specific technical challenges as discussed in Sections 3 and 4. These include equipment size, process efficiency, cost, safety, boil-off losses and management and insulation methods for large scale storage tanks.

A reduction in liquefaction cost to around 1 US$ per kg_{H_2} or below will nevertheless be essential to the establishment of economically viable, wide-spread liquid hydrogen supply chains. Together with the anticipated reductions in the cost of producing clean hydrogen to 2 US$ per kg_{H_2} or below, this should enable liquid hydrogen supply chains that service fuel cell vehicle (FCV) refuelling networks even with relatively high distribution costs. For example, a report published by the California Energy Commission,[353] estimated the LCOH of hydrogen produced from renewables and used for FCVs in California will decline from around 16 US$ per kg_{H_2} at present to a midpoint of 6 US$ per kg_{H_2} by 2025, and to below 5 US$ per kg_{H_2} by 2050, which is close to the 4 US$ per kg_{H_2} long-term target established by the U.S. Department of Energy.

5.3 Comparison with ammonia

Ammonia is an alternative carrier to liquid hydrogen for storage and transport applications, which in contrast already has international supply chains established. To provide context for the above discussion of prospective liquid hydrogen supply chains, this section considers the use of ammonia as a transport vector in terms of energy consumption, cost and emissions.

Using the conventional Haber Bosch (HB) process, the production of ammonia from H_2 and N_2 consumes power in the range of (2–4) kWh $kg_{NH_3}^{-1}$.[60,74,112,354–356] However, as indicated in Table 2, on a hydrogen mass basis this is equivalent to (11.2–22.5) kWh $kg_{H_2}^{-1}$, which is comparable to or larger than the SEC currently required for hydrogen liquefaction of (11.9–15) kWh $kg_{LH_2}^{-1}$. The primary advantage of ammonia relative to liquid hydrogen is its ease of storage and transport with minimal loss. However, if at the point of end use ammonia must be converted back to H_2 (*e.g.* prior to use in a fuel cell), a further 7.94 kWh $kg_{H_2}^{-1}$ must be used assuming a cracker efficiency of 76% in the best case scenario.[60] In such cases the storage and transport advantages of using NH_3 are greatly ameliorated, with between (57.4 and 90.4)% of the hydrogen stored in the vector being consumed to produce the necessary energy for conversion and (re-)cracking.

Instead of cracking, it is possible to use ammonia as an energy carrier by direct combustion[357] (engine or gas turbine) or, potentially, in fuel cells.[358] The latter technology is still pre-commercial, while the former must deal with challenges such as unwanted NO_X emissions, CO_2 tolerance and the relatively low flammability of ammonia.[357] These challenges have to some extent been addressed through research and development with some demonstration-scale (10–40 kW) turbines and engines. Nevertheless, further research, development and up-scaling is required for these technologies given that the climate impact of ammonia combustion by-products can be multiple times worse than those of CO_2.[359]

While ammonia production, storage and transport are very mature technologies, the associated costs are still important considerations when assessing its use for energy applications (as opposed *e.g.* to food production). Location and plant capacity are two factors influencing ammonia production cost, which range from 0.21–0.40 US$ per kg_{NH_3} in Western Europe to as little as 0.14 US$ per kg_{NH_3} on the US Gulf Coast.[114] This is collectively equivalent to around (0.8–2.2) US$ per kg_{H_2}, considering the content of hydrogen in 1 kg of ammonia. Decomposition back to H_2 adds approximately 0.67 US$ per kg_{H_2}[60] giving a total cost of (1.5–2.9) US$ for each kg of hydrogen transported as NH_3.[37,98,113–115] This is comparable with the sum of the liquefaction and transport costs averaged across *all* the LH_2 studies considered in Table 9 (2.8 ± 0.7) US$ per kg_{H_2}.

Finally the widespread use of ammonia for energy applications has safety challenges potentially comparable to those faced by liquid hydrogen. These include increased rates of corrosion and material wear for containers storing both gaseous and liquid ammonia; high toxicity to biological systems and ammonia's capacity to rapidly dehydrate living tissue; its propensity to form secondary fine ($\leq$2.5 μm) particulate matter upon combustion; and disruption of natural nitrogen deposition cycles.[359] Thus while industry has an established track record of safely storing and transporting NH_3 at commercial scales, significant handling and containment challenges remain if it is to be used on an even larger scale for energy applications.

Table 9 Liquid hydrogen value chains reported in literature ordered by increasing amount of liquefaction cost

Study/report	Scale [TPD]	Green H_2 Production Cost[a] [$ per kg_{H_2}]	Blue H_2 Production Cost[a] [$ per kg_{H_2}]	Liquefaction Cost[a] [$ per kg_{H_2}]	LH_2 Transport mode	Transport Cost[a] [$ per kg_{H_2}]	Distribution Cost[a] [$ per kg_{H_2}]	LCOH[a,b] [$ per kg_{H_2}]
APERC[94]	800	2.55–4.33[d]		0.53–0.78	Road	1.07–1.23	2.3–6.7[e] refuelling station (2.6–0.65 TPD)	6.45–13.04
APERC[94]	800		1.22–2.44[f]	0.53–0.78	Road	1.23–1.40	2.3–6.7[e] refuelling station (2.6–0.65 TPD)	5.28–11.32
Heuser *et al.*[95]	50	2.86[g]		0.64[h]	Maritime (21 400 km)[i]	1.47		4.97
Hydrogen Council[96 k]	9000–10 300[j]	1.5[k]		0.7–1.0	Maritime (8700 km)[l]	1.0–1.4	0.7[m,k] distribution	3.9–4.6[k]
Li *et al.*[97 k]	27–30		2.5–3.2[n,k]	0.7–2.0	Road (200–500 km)	0.2–0.5[k]	0.9–2.3[k] refuelling station (3–1 TPD)	4.3–8.02[k]
Wijayanta *et al.*[98 k]	822		1.04[o,k]	0.76[k]	Maritime (9000 km)[ad]	1.76[k]	0.16[p] distribution	3.72[k]
Teichnmann *et al.*[99]	2822	1.87–3.45[r]		0.82	Maritime (1000–5000 km)[s]	0.37–1.09	0.13–0.15[t] distribution	3.19–5.51
Ishimoto *et al.*[100]	500		2.13	0.95–1.38	Maritime (2539–23 407 km)[u]	2.54–4.28		5.62–7.79
Watanabe *et al.*[101]	16 400	1.97[v]–3.56[y]		0.97[v]–1.40[y]	Maritime (20 000 km)	1.85–2.60[x]		4.79–7.56[w]
CSIRO[37 z]	210	1.53–2.08[aa]		1.07–1.30	Road	1.17[ab]		3.77–4.55
CSIRO[37 z]	210		1.26–1.84[f]	1.07–1.30	Road	1.17[ab]		3.5–4.31
KHI[102 ac]	770		1.55[o]	1.1	Maritime (9000 km)[ad]	0.69[ad,ae]		3.34
Nyberg[103]	176.2	2.63		1.68	Maritime (200–500 km)[af]	0.28–1.68[ag]	0.37 regasification	4.96–6.36
CSIRO[37 ah]	50	3.20–4.98[ai]		1.72–2.10	Road	1.17[ab]		6.1–8.25
CSIRO[37 ah]	50		1.52–2.10	1.72–2.10	Road	1.17[ab]		4.41–5.37
IDEALHY[104–106]	50	3.11–10.04[aj]		1.93			1.80[ak] refuelling station (0.34 TPD)	6.84–13.77
IDEALHY[104–106]	50		1.83–2.84[f]	1.93			1.80[ak] refuelling station (0.34 TPD)	5.56–6.57
Raab *et al.*[107]	676.5	5.6[al]		1.97	Maritime (9250 km)[ad]	0.46	0.34[am] regasification	8.37
Reuß *et al.*[108]	50	4.14[an]		2.12–2.22[ao]	Road (250 km)	1.71[ap]	1.79[a] refuelling station (0.85 TPD)[q]	9.76–10.86
DOE[109 ar]	27		2.24[at]	2.75[au]	Road (80 km)	0.68	8.18[av] refuelling station (0.35 TPD)	14.24[aw]
European Commission[110]	27	1.61–4.07[ax]		2.76	Maritime (14 267–20 972 km)[ay]	1.64–2.43	1.19–2.35[az] refuelling station (>0.6 TPD and <0.6 TPD)	7.2–8.85

[a]Average exchange rate over the last 6 months: 0.67 USD = 1 AUD, 1.12 USD = 1 EUR, 1 USD = 107.2 JPY. [b] Supply cost might include distribution and/or regasification cost, according to data available. [c] Asia-Pacific Economic Cooperation is a grouping of 21 member countries including Australia, Canada, China, Japan, New Zealand, and the USA. [d] Hydrogen produced from hydro and solar PV, respectively. [e] For a large (1200 N m^3 h^{-1} ≈ 2.6 TPD) and small (300 N m^3 h^{-1} ≈ 0.65 TPD) refuelling station, respectively. [f] Hydrogen produced through steam reforming and coal gasification, respectively. In both cases, carbon is captured and stored. [g] Hydrogen produced *via* electrolysis powered by wind. [h] Includes the levelized cost of compressing and transporting *via* pipeline the gas after production to the liquefaction facilities. [i] Includes the cost of storing LH_2 before shipping, based on a maritime route from Patagonia to Japan. [j] Cost for at-scale production and transportation for selected transport routes. [k] Cost for hydrogen produced in 2030. [l] Transportation *via* ship from Saudi Arabia to Rotterdam. [m] Only considers liquid hydrogen distribution with a truck for 300 km, including boil-off losses, port storage cost, and hydrogen refuelling station operating costs. [n] Hydrogen produced through steam reforming and carbon is captured and stored. [o] Cost for hydrogen obtained from coal gasification and CCS. [p] Local distribution/transport. [q] LH_2 imported into Europe. [r] For electrolysis with an electricity price of 0.02 EUR per kWh (22.4 USD per MW h) and 0.05 EUR per kWh (56 USD per MW h, respectively). [s] Transport of hydrogen *via* maritime for a 1000 km and 5000 km trip. [t] Distribution of LH_2 *via* truck for a 20 and 50 km trip, respectively. [u] Maritime transportation from Norway to the Netherlands and Norway to Japan, respectively. [v] Electricity generated through windmills with a total capacity of 77 500 MW. [w] Cost calculated with an interest rate of 0.5 and 5%, respectively. [x] Includes loading, shipping and unloading at the port. [y] Electricity generated through windmills with a total capacity of 60 400 MW. [z] Projected case. [aa] Electrolysis with PEM electrolyser and alkaline electrolyser, respectively. [ab] Cost calculated for a truck that travels 166 330 km per annum as per CSIRO's modelling with a cost of 0.62 USD per km. [ac] Kawasaki CO_2 free hydrogen supply chain concept. [ad] For a trip from Australia to Japan. [ae] Hydrogen transported *via* ships with a capacity of 10 840 tons of LH_2 in a 9000 km trip, including a loading base. [af] Maritime transport within Norway and from Norway to the Netherlands, respectively. [ag] Includes buffer storage costs. [ah] Base case. [ai] Electrolysis with alkaline electrolyser and PEM electrolyser, respectively. [aj] Internal cost of hydrogen produced from wind power by electrolysis. [ak] Internal cost for hydrogen delivery and refuelling for a 100 km round trip transported by road. [al] Assumed a cost of 5 EUR kg^{-1} $H_2{}^{-1}$. [am] Cost for regasification only (in Japan). [an] Hydrogen produced *via* electrolysis. [ao] Prices account for seasonal changes in hydrogen cavern storage due to higher electricity prices. [ap] Cost for delivery *via* a trailer with a capacity of 4300 kg. [aq] Cost for a refuelling station with a design capacity of 850 kg day^{-1} (0.85 TPD). [ar] DOE – Department of Energy. Data from national laboratory models, Hydrogen Delivery Scenario Analysis Model [HDSAM] and Hydrogen Analysis [H2A]. [as] Supply chain developed for urban California market. [at] Hydrogen produced through steam reforming. [au] Overall levelized cost is $2.75 per kg H_2, which includes recurring costs. The capital contribution for a plant of this capacity is $1.41 per kg H_2. [av] Hydrogen delivered *via* trucks, stations are 350 kg day^{-1} (0.35 TPD) and dispensing at 700-bar for the light-duty vehicle market. [aw] Terminal profited cost adds 0.39 $ per kg. [ax] Hydrogen produced in Chile and the North West of Australia, respectively. [ay] Transport *via* ship from Chile to Rotterdam and Australia to Rotterdam, respectively. [az] Cost for large refuelling stations (larger than 20 MW h day^{-1} ≈ 0.6 TPD) and small refuelling stations (smaller than 20 MW h day^{-1} ≈ 0.6 TPD), respectively.

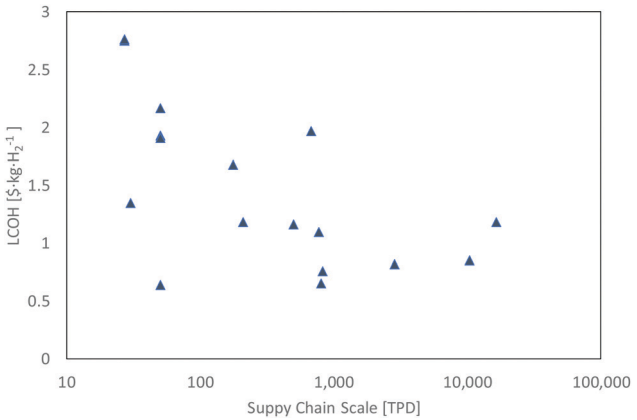

Fig. 18 Liquefaction cost component of the LCOH studies shown in Fig. 17 as a function of the supply chain scale.

Wijayanta *et al.*[98] predicted an imported cost, including hydrogen production from SMR, of ammonia from Australia to Japan by 2030 of around 0.44 US$ per kg_{NH_3} (2.5 US$ per kg_{H_2}) if ammonia can be used directly, and a total cost of 0.563 US$ per kg_{NH_3} (3.2 US$ per kg_{H_2}), when ammonia is decomposed back to hydrogen. They concluded that when highly pure H_2 is needed (such as for fuel cell vehicles), liquid hydrogen is more promising than ammonia and other hydrogen storage methods. Ishimoto *et al.*[360] conducted a hydrogen export value chain analysis over distances ranging from (2500 to 23 407) km for both LH_2 and ammonia. The hydrogen was produced by Autothermal Reforming at the same location for both vectors and the ammonia was cracked back to H_2 at the destination. Using conservative costs for currently available technologies, Ishimoto *et al.*[360] found that the LH_2 supply chain costs ranged from (4.8 to 6.8 US$ per kg_{H_2}), which were generally below those of NH_3 (6.1 to 6.6 US$ per kg_{H_2}), except for the longest distance supply chain. Moreover, the carbon emissions intensity of the LH_2 supply chains were (5 to 7.2) times lower than those using NH_3. Similarly, an analysis by the EU Science Hub – Joint Research Centre[361] found that LH_2 resulted in lower hydrogen delivery cost than NH_3 for supply chain distances up to 22 000 km. Their analysis found that LH_2 also had a supply chain cost below that of either pipelines or liquid organic hydrogen carriers for distances between (3000 and 17 000) km.

5.4 Research, development & demonstration priorities for liquid hydrogen supply chains

The ammonia comparison helps illustrate that liquid hydrogen supply chains have reasonably good prospects relative to (and in conjunction with) those based on alternative vectors. However, practical solutions to multiple challenges in the four categories of economics, cryogenic losses, safety and scale presented in this paper will be required if large-scale LH_2 supply chains are to be established. To address this array of challenges, significant levels of research, development and demonstration will be needed. Table 10 presents a summary of these needs, with a brief discussion of each of the main categories – Liquefaction, Storage & Transport, and Fundamentals – given in the text below. The areas and topics listed in Table 10 are based on the literature review presented in this paper and discussions with industry-based subject matter experts, which provided guidance on prioritisation. Accordingly, the list is non-exhaustive; rather it reflects an informed, yet subjective perspective of technical and engineering needs based on current knowledge.

Liquefaction: increase efficiency & lower cost by scale-up. Significant work needs to be done to reduce the specific energy consumption (SEC) of hydrogen liquefaction to well below 10 kWh $kg_{H_2}^{-1}$ and improve its exergy efficiency. Exploiting economies of scale will be central to achieving this improved energy efficiency while also reducing the specific liquefaction cost (SLC). Particular areas that should be prioritised for research, development and demonstration include:

- The design and fabrication of larger coldboxes (*e.g.* on site), or the viability of hosting cryogenic equipment (*e.g.* heat exchangers) in multiple smaller coldboxes. Work on optimal modular arrangements of coldboxes to insulate different parts of the system while keeping capital costs down is also needed.
- The design of large oil-free turbines for H_2 expansion and the use of turbo-compressors on the working-fluid side of the liquefaction process needs further research regarding their suitability for use in large-scale operations. Owing to the difficulties in compressing hydrogen, research into heavier compressing gases (*e.g.* MRs) used in the pre-cooling and refrigeration cycles should accompany this work. Additionally, the potential of using the electrochemical compression of hydrogen for large-scale operations should be explored given its established high efficiencies (95% for Carnot cycle up to 1 MPa).[362,363]
- Robust optimisation of large-scale liquefaction processes based on Brayton cycles through the use of new mixed-refrigerants, pre-cooling stages, process integration, efficient catalysts, and pressure drop reductions across and between unit operations. Such an optimisation will require robust, accurate and computationally efficient simulation platform for >100 TPD LH_2 plant capable of describing several inherently dynamic (non-steady state) processes in a variety of configurations. Such simulations should use reference thermodynamic and transport properties models for hydrogen and mixed refrigerants, and an accurate kinetic model for *ortho–para* conversion, as recommended in the Fundamentals priority list below.
- The design of improved *ortho*- to *para*-hydrogen conversion reactors that optimise the rate of conversion and heat removal (and hence the management of potential heat spots) as well as the pressure drop experienced by the hydrogen during continuous operation. Currently, the amount of catalyst required for a given flowrate or quantity is specified based on proprietary kinetic data. The development of new catalysts that are easier to integrate into heat exchanger designs and/or work efficiently with trace removal systems (adsorbers) could help reduce both the capital cost (*e.g.* lower equipment counts) or operational cost (pressure drop) of liquefaction processes. The integration of new catalyst materials into vortex tube heat exchangers and/or the development of catalytic coatings are

Table 10 Suggested research, development and demonstration priorities for the liquid hydrogen supply chain

Area	Sub area	R&D opportunities	Potential impact
Liquefaction	Process design	• Cold box modularity and system integration • Liquefier capacity and arrangement optimisation [*e.g.* 10 × 10 TPD *vs.* 1 × 100 TPD] • Optimisation of MR[b] and pre-cooling fluids (techno-economic & environmental) • Large-scale Brayton cycles optimised with robust, accurate dynamic process simulations • Investigate use of electric-drive compressors powered by variable renewable energy profiles	• Enable construction of >100 TPD liquefiers with SEC between (6 and 8) kWh and SLC between (1 and 2) USD $kg_{H_2}^{-1}$
	Equipment design	• Improved heat exchanger designs with integrated catalysts for OP[a] conversion. • Large-scale oil-free turbines and/or large, economical electrochemical compressors for H_2 • Construction with hydrogen-proof materials and effective cryogenic seals to prevent leakage • Optimise trace impurity removal processes (*e.g.* integration with OP conversion process) • Robust sensors for monitoring blockage risk in cryogenic heat exchangers	• Increased equipment efficiency and suitability for large-scale liquefiers, thus enabling construction of >100 TPD liquefiers • Improved operational efficiency with reduced design margin requirements
	Ortho- to *para*-H_2 conversion	• New OP catalysts with improved efficiencies, characterised over wide temperature range • Catalyst performance (kinetics, heat & mass transfer) within dynamic process simulations • Develop catalytic coatings & incorporate catalysts into novel heat exchangers (vortex tubes) • Robust sensors for monitoring OP ratio in process streams over wide temperature range	• Reduced pressure drop in the heat exchangers • Cheaper and/or more efficient heat exchangers • Better monitoring of OP conversion performance allowing real time optimisation
Storage & transport	Tank design & operation	• Vacuum panels, surface coatings, tank wall channels, 3D printed tanks for better insulation • Convert from spherical to cylindrical or conformal tank designs • Efficiently integrate cryo-compressed and slush H_2 storage technologies • Address deficiencies & exploit strengths of existing insulation materials & methods (see Table 8) • Better models for predicting thermal stratification, interfacial heat transfer & resulting boil-off	• Safer storage with reduced boil-off losses • Enable construction of large-scale storage tanks for more cost-effective transport • Improve storage capacity of LH_2
	Shipping & custody transfer	• Leak-free umbilicals and disconnects with good thermal insulation • Improved design & operability of cryogenic hoses, venting systems and flow meters • Design large storage tanks with wide ranges of operating pressure to accommodate boil-off • Optimise ship ballast & sloshing protection requirements to account for low density cargo • Develop operational procedures to keep empty ship tanks cool (or minimise cool-down time)	• Improve safety and minimize boil-off losses • Reliable & safe export infrastructure • Minimise energy wasted during transfer operations
	Safety	• Develop standards for leak-free operations & avoiding material compatibility problems • Leak detection systems with appropriate spatial extent & temporal resolution • Improve detection and develop procedures for stopping "invisible" fires • Long-term cyclic (thermal, pressure) testing of materials & systems in LH_2 supply chain	• Minimise risk of containment failures • Reduce risk of hydrogen fires or explosions • Provide pathways for safe workforce expansion and public utilisation
Fundamentals	Fluids	• EOS[c] based on new (enthalpy) data for fluid mixtures containing H_2 with varying OP ratios • EOS based on new (enthalpy) data for cryogenic MR fluids • Data & models for predicting solubilities, freeze-out kinetics & deposition risk of impurities in H_2 • Data & models for predicting impurity solubility, freeze-out & deposition risk in refrigerants • Improved data & models for transport properties of cryogenic hydrogen & MR fluids	• Helps with liquefaction opportunities listed above for process design and equipment design categories • Helps with storage & transport opportunities listed above for tank design and operation category

Table 10 (*continued*)

Area	Sub area	R&D opportunities	Potential impact
	Catalysts & materials	• Cheaper catalysts with reaction kinetics including heat & mass transfer limitations characterised (*e.g.* particle size effects) over wide ranges of temperature, pressure and initial OP ratio. • Cryogenic adsorption capacities & kinetics of media used for trace impurity removal • High-strength, low cost containment materials compatible with H_2 & cryogenic temperatures • Improved thermal insulation materials with long lifetimes & tolerance for cycling	• Helps with liquefaction opportunities listed above for equipment design and OP conversion categories • Helps with storage & transport opportunities listed above for safety and tank design & operation categories.
	Sensors	• Robust by-line or on-line measurements of OP ratio capable of operating in live plant • Robust by-line or on-line measurements of impurity freeze-out or deposition risk • Effective sensors for hydrogen leaks and/or fires with flexible spatial & temporal resolutions	• Helps with liquefaction opportunities listed above for equipment design and OP conversion categories • Helps with storage & transport opportunities listed above for safety category

[a] OP – *ortho–para*. [b] MR – mixed refrigerant. [c] EOS – equation of state.

promising avenues for further research. Realising any of these opportunities would require a thorough quantification of reaction kinetics (Fundamentals) and their efficient inclusion into reactor models and process simulations recommended above. The development of efficient, standard approaches for the by-line or on-line measurement of *para*-hydrogen content would facilitate the validation of these conversion technologies as well as the real-time optimisation of plant operation.

Storage and transport: reduce cryogenic losses & ensure safety. Boil-off losses associated with the storage, transportation and handling of liquid hydrogen can consume up to 40% of its available combustion energy.[83] Accurate assessment of pressurisation dynamics, thermal stratification and boil-off rates are critical for the design and operation of transfer lines and storage tanks that minimise both LH_2 losses and hazards to safety. Specific areas for research, development and demonstration that will make LH_2 storage and transport more efficient and less risky include:

• Demonstrate innovative insulation schemes and materials to minimise boil-off losses for future large-scale storage tanks and transfer pipelines. As detailed in Table 8, each existing method of insulation has strengths and weaknesses; mechanisms for overcoming the latter and exploiting the former should be investigated, potentially through combinations of different techniques and materials.

• Develop a comprehensive dynamic model able to reliably estimate boil-off rates, thermal stratification, pressurisation and flow dynamics, across a wide range of tank geometries and scales, both during static storage and custody transfer (loading) operations. This model should be validated against data acquired using a range of facilities with instrumentation sufficient to capture the underlying relevant multi-scale phenomena. The ability to describe the impact of sloshing, (auto) *ortho–para* conversion, superheated vapour phases with non-equilibrium *ortho–para* ratios, and boil-off return and re-liquefaction facilities will be important features of such a dynamic model.

• Explore the use of slush hydrogen technologies to simultaneously reduce boil-off rates and increase volumetric energy density. While implementing the additional refrigeration systems required will increase both capital and operational costs, these may be sufficiently offset by efficiencies achieved through system integration and economies of scale.

• Avoiding hydrogen leaks is one of the most difficult but important challenges that must be overcome to ensure sustained safe operations. While the development of standards and operational practice will help mitigate risks associated with de-pressurisation, fire and explosion, technologies that help eliminate and/or correct for human error will be just as important. Intelligent, automated and high-resolution systems for detecting and suppressing leaks or fires across a range of environments (liquefaction plants, ships, domestic fuelling stations) are needed. Additionally, innovations that are potentially ''low-tech'' in comparison, such as leak-free, hydrogen compatible connectors for cryogenic hoses will likely be of significant value.

Fundamentals: improved descriptions of fluids & catalysts. While the underlying science and basic engineering requirements for hydrogen liquefaction are known, significant limitations exist regarding the quantification of key properties needed for improved technical solutions. To progress many of the research and development priorities listed under Liquefaction or Storage & Transport, improved quantitative descriptions of the fluids, catalysts and other key materials used in liquefaction are needed over a wide range of conditions. While much of the basic data required for hydrogen liquefaction processes were obtained over 50 years ago to facilitate the development of rockets and space programs, process efficiency was a relatively low priority compared with the large-scale energy-driven applications now planned.

To reduce the engineering margins applied within LH_2 supply chains, smaller uncertainties are needed in the models used for process design. This provides a motivation to re-visit and extend the underlying database of thermodynamic and kinetic properties. Moreover, measurement technology has

advanced significantly since a large fraction of the original data were acquired. Developing and applying new experimental techniques to reduce the uncertainty and extend the range of property data, both in the laboratory and in the plant *via* new sensors, will assist the establishment of more efficient, large-scale liquid hydrogen supply chains. Research priorities within the Fundamentals category include:

• Thermophysical property data for hydrogen and its mixtures are needed at temperatures from 20 K to 300 K and pressures from ambient to 8 MPa. As detailed in Section 2, a relatively large body of experimental data exists for the density, thermal conductivity and viscosity of hydrogen. However, their coverage of the conditions relevant to liquefaction are in some cases inadequate, and many of the data sets have significant scatter with few of the original articles providing a sufficiently detailed uncertainty analysis. New data should cover wider ranges of *ortho–para* ratios, particularly in the supercritical region (30 K to 100 K); however, it is essential that the *ortho–para* ratio for each data point be measured or well-defined. Importantly, data that provide more direct information about the fluid mixture's enthalpy (*e.g.* heat capacities, sound speeds, vaporisation) would enable significant improvements upon the Helmholtz EOS of Beckmüller *et al.*[154] which only considers normal hydrogen. These more accurate and wider-ranging thermophysical property data would then enable correspondingly improved reference Helmholtz equations of state and transport property models for hydrogen mixtures that are central to process simulations.

• Similarly, new thermophysical property data and improved models are needed for a range of prospective mixed refrigerant fluids likely to be central to the development of hydrogen liquefaction cycles with SECs in the range (6 and 8) kWh $kg_{H_2}^{-1}$. Given their prospective use in both the pre-cooling and cryogenic sections of the plant, there are many mixtures that could help improve overall cycle efficiency (*e.g.* methane + iso-pentane at temperatures as low as 98 K[364]). Again, measurements that provide information about the fluid mixture's enthalpy as a function (T,p) and composition would be of significant value to refrigerant design.

• A more universal kinetic expression for catalyst assisted *ortho–para* hydrogen conversion is required. Fundamental experiments that characterise reaction kinetics, including particle size effects and other heat and mass transfer limitations, over wide ranges of temperature, pressure and initial *ortho–para* ratio will be necessary to validate such an expression. Data on the reverse reaction rate should also be acquired, and a wider range of catalyst materials and morphologies should be investigated to identify potential methods of reducing the cost of conversion. Techniques for accurately and rapidly monitoring *ortho–para* ratios developed for the laboratory should be considered as the basis for improved sensor technologies that can operate in liquefaction plant environments.

• At the cryogenic temperatures encountered in hydrogen liquefaction plants, trace concentrations of impurities can freeze-out and lead to heat exchanger blockages and even plant shutdowns. This risk is similar to that present in the liquefaction of natural gas[365–370] where the concentrations of H_2O, C_6H_6 and CO_2 impurities are controlled to below 0.1, 4 and 50 ppm, respectively. Significant effort has been invested into measuring and modelling the thermodynamic and kinetic aspects of the freeze-out phenomena. However, this problem is likely to be more severe for hydrogen liquefaction given both the additional impurity compounds that may freeze out (N_2, O_2, CH_4, Ar), the even lower (ppb) solubilities in H_2 at cryogenic temperatures, and the catalyst-packed plate and fin heat exchangers used. While existing plants employ adsorbers to remove these impurities, this may not be sufficient for larger plants (>50 TPD), particularly if allowable tolerances on impurity concentrations do not have a robust basis. Accordingly, the void of solubility and freeze-out kinetic data for relevant impurities in cryogenic H_2 should be addressed through laboratory measurements, leading to the development of predictive engineering models. The efficacy of adsorbent materials and processes to remove these impurities to the requisite levels should also be investigated further to identify possible opportunities for optimising cost and performance. Finally, the adaptation of similar sensor technologies developed to provide real-time information on the freeze-out risk of impurities in LNG production[371] should be considered.

6 Conclusions and outlook

Global demand for hydrogen is projected to rise from 75 million tonnes in 2019 to 621 million tonnes in 2050. Hydrogen liquefaction is likely to be a key technology enabling the growth of hydrogen transport and storage needed to meet projected global demand. Whilst it is one several technologies available, including ammonia and liquid organic carriers, LH_2 offers several advantages including being an immediately pure product at the point of use. However, multiple challenges exist to the growth of liquid hydrogen, which can be placed within the broad categories of economics, cryogenic losses, safety and scale. By reviewing the current status of hydrogen liquefaction, from the fundamental physics to current engineering practice, this paper has sought to highlight the key barriers and identify potential solutions needed if LH_2 is to have a substantial role in the world's future energy value chain.

Two key targets for future liquid hydrogen supply chains are (i) reducing the specific liquefaction cost to around (1–2) US$ per kg_{H_2} and (ii) lowering the specific energy consumption of the liquefaction process to between (6 and 8) kWh $kg_{H_2}^{-1}$. These targets should be achievable if liquefaction train capacities can be increased to around 100 TPD or larger. Currently, global liquefaction capacity is around 350 TPD with a further 96 TPD planned; the capacity of the largest single train is 32 TPD. Current commercial processes have SECs from (11.9 to 15) kWh $kg_{H_2}^{-1}$ (or 35 to 45% of the stored energy content), and SLCs around (2.5–3) US$ per kg_{H_2}, which is larger than the current cost of producing blue hydrogen. Achieving these targets will therefore require significant advances in the design and operation of hydrogen liquefaction facilities.

Hydrogen liquefaction plants that achieve these targets will likely use mixed-refrigerants in both the pre-cooling and cryogenic stages of a Brayton cycle, integrated and modular cold box configurations, high-efficiency turbo compressors on the refrigerant-side, and oil-free expanders for the H_2 side. *Ortho–para* conversion will be more efficient using catalysts with better characterised kinetics integrated into heat exchanger designs that reduce the associated pressure drop. Potentially, LH_2 storage and transport systems might utilise densification and slush hydrogen technologies to minimise boil-off losses and increase storage capacity. Improved models for quantitative predictions of thermal stratification, interfacial heat transfer, tank geometry, pressure and the resulting LH_2 boil off rate in large storage tanks will be essential. Finally, if large-scale liquid hydrogen supply chains are to become a reality, addressing the challenge of safety will be vital through a combination of standards development and improved technologies for automatically detecting and eliminating hydrogen leaks and fires.

To help reach these goals, this paper first summarised the current state-of-the-art for knowledge and technology across the LH_2 supply chain, and then presented a list of research, development and demonstration priorities in Table 10. While not exhaustive, over forty opportunities and topics are listed covering liquefaction (*e.g.* process & equipment design, *ortho–para* conversion), storage & transport (*e.g.* tank design, shipping & custody transfer, safety), and fundamentals (*e.g.* fluids, catalysts, sensors). Addressing this range of research, and development opportunities will require a concerted and collaborative effort by both industry and academia, with significant investments of expertise and new infrastructure for laboratory measurements, pilot-scale demonstrations and ultimately industrial-scale deployment.

Abbreviations

Al_2O_3	Aluminium oxide
APEC	Asia Pacific Economic Cooperation
APERC	Asia Pacific Energy Research Centre
Ar	Argon
AUD	Australian dollar
BOG	Boil-off gas
CAPEX	Capital expenditures
CCS	Carbon capture and storage
CG	Coal gasification
CGH_2	Compressed hydrogen gas
CH_4	Methane
CO	Carbon monoxide
$Co(OH)_3$	Cobalt hydroxide
CO_2	Carbon dioxide
CO_X	Oxide of carbon
Cr_2O_3	Chromium oxide
CrO	Chromium oxide
CSIRO	Commonwealth Scientific and Industrial Research Organisation
CTE	Coefficient of thermal expansion
DOE	US Department of Energy
EOS	Equations of state
EU	European union
EUR	Euros
FCH JU	Fuel cells and hydrogen joint undertaking
FCV	Fuel cell vehicle
Fe_2O_3	Iron(III) oxide
GJ	Gigajoule
GN_2	Nitrogen gas
GPD	British pound
H_2	Hydrogen
H_2O	Water
He	Helium
HESC	Hydrogen energy supply chain project
IDEALHY	Integrated design for efficient advanced liquefaction of hydrogen
IEC	International electrotechnical commission
IRAS	Integrated refrigeration and storage
ISO	International organization for standardization
JP¥	Japanese Yen
J–T	Joule–Thomson
K	Kelvin
kg	Kilogram
KHI	Kawasaki heavy industries
kJ	Kilojoule
kWh	Kilowatt-hour
LCOH	Levelised cost of hydrogen
LH_2	Liquid hydrogen
LHV	Lower heating value
LN_2	Liquid nitrogen
LNG	Liquefied natural gas
LOHC	Liquid organic hydrogen carriers
m^3	Cubic meter
MeOH	Methanol
meV	Millielectronvolt
MJ	Megajoule
mm	Millimetres
MPa	Megapascal
MRs	Mixed refrigerants
Mtpa	Million tonnes per annum
MW	Megawatt
N_2	Nitrogen
N_2O	Nitrous oxide
NASA	US National Aeronautics and Space Administration
Ne	Neon
NFPA	National fire protection association
NH_3	Ammonia
NiO	Nickel(II) oxide
Nm^3	Normal cubic meter
NO_X	Nitrogen oxides
O2	Oxygen
OP	*ortho–para*
OPEX	Operating expenses
PFHE	Plate-fin heat exchangers
P_{net}	Net power consumption

ppb	Parts per billion
PV	Photovoltaic
rpm	Revolutions per minute
SEC	Specific energy consumption
SLC	Specific liquefaction cost
SMR	Steam methane reforming
THz	Terahertz
TPD	Tons per day
USA	United States of America
USD	United States dollar
VLE	Vapour–liquid equilibrium
wt%	Percentage by weight

Author contributions

Saif ZS. Al Ghafri: management, literature review, data analysis and writing original draft. Stephanie Munro: literature review and writing original draft. Umberto Cardella: particular section contribution: industrial liquefiers. Thomas Funke: particular section contribution: industrial liquefiers. William Notardonato: particular section contribution: NASA and storage tanks. J.P. Martin Trusler: particular section contribution: thermodynamics and EOS. Jacob Leachman: particular section contribution: thermodynamics and EOS. Roland Span: particular section contribution: thermodynamics and EOS. Shoji Kamiya: particular section contribution: storage tanks and BOG. Garth Pearce: particular section contribution: tanks design and materials. Adam Swanger: particular section contribution: NASA storage tanks and BOG. Elma Dorador Rodriquez: particular section contribution: liquid hydrogen cost analysis. Paul Bajada: particular section contribution: hydrogen production methods. Fuyu Jiao: particular section contribution: fundamentals of hydrogen liquefaction processes. Kun Peng: particular section contribution: ammonia. Arman Siahvashi: particular section contribution: solid freeze-out and impurities. Michael L. Johns: OP conversion, writing, reviewing and editing. Eric F. May: supervision, thermodynamics, writing, reviewing and editing.

Conflicts of interest

There are no conflicts to declare.

Acknowledgements

The authors acknowledge the support of the Australian Research Council through FT180100572 and IC150100019, the DAAD, and the Future Energy Exports CRC (CRCXXI000008), whose activities are funded by the Australian Government's Cooperative Research Centre Program. This is FEnEx CRC Document 2022/RP2-FNX-003. We also thank Dr Neil Robinson for helpful discussions particularly regarding the catalytic mechanisms involved with spin isomer conversion.

References

1 M. Bastos-Neto, C. Patzschke, M. Lange, J. Möllmer, A. Moeller, S. Fichtner, C. Schrage, D. Lässig, J. Lincke, R. Staudt, H. Krautscheid and R. Gläser, *Energy Environ. Sci.*, 2012, **5**, 8294–8303.
2 I. Staffell, D. Scamman, A. Velazquez Abad, P. Balcombe, P. E. Dodds, P. Ekins, N. Shah and K. R. Ward, *Energy Environ. Sci.*, 2019, **12**, 463–491.
3 M. Z. Jacobson, M. A. Delucchi, Z. A. F. Bauer, S. C. Goodman, W. E. Chapman, M. A. Cameron, C. Bozonnat, L. Chobadi, H. A. Clonts, P. Enevoldsen, J. R. Erwin, S. N. Fobi, O. K. Goldstrom, E. M. Hennessy, J. Liu, J. Lo, C. B. Meyer, S. B. Morris, K. R. Moy, P. L. O'Neill, I. Petkov, S. Redfern, R. Schucker, M. A. Sontag, J. Wang, E. Weiner and A. S. Yachanin, *Joule*, 2017, **1**, 108–121.
4 I. Capellán-Pérez, I. Arto, J. M. Polanco-Martínez, M. González-Eguino and M. B. Neumann, *Energy Environ. Sci.*, 2016, **9**, 2482–2496.
5 N. MacDowell, N. Florin, A. Buchard, J. Hallett, A. Galindo, G. Jackson, C. S. Adjiman, C. K. Williams, N. Shah and P. Fennell, *Energy Environ. Sci.*, 2010, **3**, 1645–1669.
6 A. Sartbaeva, V. L. Kuznetsov, S. A. Wells and P. P. Edwards, *Energy Environ. Sci.*, 2008, **1**, 79–85.
7 B. Vogel, T. Feck, J.-U. Grooß and M. Riese, *Energy Environ. Sci.*, 2012, **5**, 6445–6452.
8 B. Parkinson, P. Balcombe, J. F. Speirs, A. D. Hawkes and K. Hellgardt, *Energy Environ. Sci.*, 2019, **12**, 19–40.
9 T. M. Gür, *Energy Environ. Sci.*, 2018, **11**, 2696–2767.
10 United States Department of Energy (DOE), Hydrogen posture plan, 2006, **https://www.hydrogen.energy.gov/pdfs/hydrogen_posture_plan_dec06.pdf**.
11 European Union, Hydrogen Roadmap Europe, 2019, Report 978-92-9246-331-1, 2019.
12 European Commission. Communication from the commission to the European parliament, the European economic and social committee and the committee of the regions. A hydrogen strategy for a climate-neutral Europe, 2020, **https://ec.europa.eu/energy/sites/ener/files/hydrogen_strategy.pdf**.
13 Ministry of Economy, Trade and Industry. Summary of the strategic road map for hydrogen and fuel cells, 2014, **http://www.meti.go.jp/english/press/2014/pdf/0624_04a.pdf**.
14 N. Behling, M. C. Williams and S. Managi, *Econ. Anal. Policy*, 2015, **48**, 204–221.
15 COAG Energy Council. Australia's National Hydrogen Strategy, 2019, **https://www.industry.gov.au/sites/default/files/2019-11/australias-national-hydrogen-strategy.pdf**.
16 Federal Ministry for Economic Affairs and Energy: The National Hydrogen Strategy, 2020, **https://www.bmwi.de/Redaktion/EN/Publikationen/Energie/the-national-hydrogen-strategy.html**.
17 Department of Energy and Climate Change. UK starts work on public-private roadmap for hydrogen fuel cells, DOI: **10.1016/S1464-2859(16)30061-X**.
18 J. Zhang, H. Meerman, R. Benders and A. Faaij, *Energy*, 2021, **224**, 120049.

19 A. McFarlan, *Sustainable Energy Technol. Assess.*, 2020, **42**, 100821.
20 K. Sapkota, A. O. Oni and A. Kumar, *J. Nat. Gas Sci. Eng.*, 2018, **52**, 401–409.
21 S. Shiva Kumar and V. Himabindu, *Mater. Sci. Energy Technol.*, 2019, **2**, 442–454.
22 M. Sankir and N. D. Sankir, *Hydrogen Production Technologies*, Wiley, Somerset, United States, 2017.
23 M. Bui, C. S. Adjiman, A. Bardow, E. J. Anthony, A. Boston, S. Brown, P. S. Fennell, S. Fuss, A. Galindo, L. A. Hackett, J. P. Hallett, H. J. Herzog, G. Jackson, J. Kemper, S. Krevor, G. C. Maitland, M. Matuszewski, I. S. Metcalfe, C. Petit, G. Puxty, J. Reimer, D. M. Reiner, E. S. Rubin, S. A. Scott, N. Shah, B. Smit, J. P. M. Trusler, P. Webley, J. Wilcox and N. Mac Dowell, *Energy Environ. Sci.*, 2018, **11**, 1062–1176.
24 S. Cloete, M. N. Khan and S. Amini, *Int. J. Hydrogen Energy*, 2019, **44**, 3492–3510.
25 G. Collodi, G. Azzaro, N. Ferrari and S. Santos, *Energy Procedia*, 2017, **114**, 2690–2712.
26 C.-C. Cormos, *Int. J. Hydrogen Energy*, 2012, **37**, 5637–5648.
27 B. Angelo, D. Francesco, T. Jianhua and T. N. Vezirolu, *Hydrogen Production, Separation and Purification for Energy, Institution of Engineering and Technology*, 2017.
28 I. M. Karp, *Energy Technol. Resource Saving*, 2020, **2**, 4–13.
29 J. Chi and H. Yu, *Chin. J. Catal.*, 2018, **39**, 390–394.
30 A. Ugurlu and S. Oztuna, *Int. J. Hydrogen Energy*, 2020, **45**, 35269–35280.
31 M. Minutillo, A. Perna and A. Sorce, *Appl. Energy*, 2020, **277**, 115452.
32 N. Sunny, N. Mac Dowell and N. Shah, *Energy Environ. Sci.*, 2020, **13**, 4204–4224.
33 R. Carapellucci and L. Giordano, *J. Power Sources*, 2020, **469**, 228391.
34 G. Locatelli, S. Boarin, A. Fiordaliso and M. E. Ricotti, *Energy*, 2018, **148**, 494–505.
35 H. Tebibel, *International Conference on Wind Energy and Applications in Algeria (ICWEAA)*, 2018, DOI: **10.1109/ICWEAA.2018.8605079**.
36 Global CCS Institute, Global Status of CCS, 2019, **https://www.globalccsinstitute.com/wp-content/uploads/2019/12/GCC_GLOBAL_STATUS_REPORT_2019.pdf**.
37 T. M. Bruce, S. Hayward, J. Schmidt, E. Munnings, C. Palfreyman and D. Hartley, *National Hydrogen Roadmap*, CSIRO, Australia, 2018.
38 A. L. Hoskins, S. L. Millican, C. E. Czernik, I. Alshankiti, J. C. Netter, T. J. Wendelin, C. B. Musgrave and A. W. Weimer, *Appl. Energy*, 2019, **249**, 368–376.
39 R. R. Bhosale, *Fuel*, 2020, **277**, 118160.
40 S. Sadeghi and S. Ghandehariun, *Int. J. Hydrogen Energy*, 2020, **45**, 28426–28436.
41 C. Acar, I. Dincer and G. F. Naterer, *Int. J. Energy Res.*, 2016, **40**, 1449–1473.
42 H. Wang, J. Xu, L. Sheng, X. Liu, Y. Lu and W. Li, *Int. J. Energy Res.*, 2018, **42**, 3442–3453.
43 B. Pandey, Y. K. Prajapati and P. N. Sheth, *Int. J. Hydrogen Energy*, 2019, **44**, 25384–25415.
44 J. Baeyens, H. Zhang, J. Nie, L. Appels, R. Dewil, R. Ansart and Y. Deng, *Renewable Sustainable Energy Rev.*, 2020, **131**, 110023.
45 F. Safari and I. Dincer, *Energy Convers. Manage.*, 2020, **205**, 112182.
46 M. Shaner, H. Atwater, N. Lewis and E. McFarland, *Energy Environ. Sci.*, 2016, 9.
47 A. Grimm, W. A. de Jong and G. J. Kramer, *Int. J. Hydrogen Energy*, 2020, **45**, 22545–22555.
48 J. R. Bartels, M. B. Pate and N. K. Olson, *Int. J. Hydrogen Energy*, 2010, **35**, 8371–8384.
49 J. I. Levene, *Economic analysis of hydrogen production from wind*, National Renewable Energy Laboratory, Golden, CO, 2005.
50 International Energy Agency (IEA), Electrolyser capacity installed by year, 2010-2018, **https://www.iea.org/data-and-statistics/charts/electrolyser-capacity-installed-by-year-2010-2018**, (accessed December, 2019).
51 A. Buttler and H. Spliethoff, *Renewable Sustainable Energy Rev.*, 2018, **82**, 2440–2454.
52 O. Schmidt, A. Gambhir, I. Staffell, A. Hawkes, J. Nelson and S. Few, *Int. J. Hydrogen Energy*, 2017, **42**, 30470–30492.
53 M. Götz, J. Lefebvre, F. Mörs, A. McDaniel Koch, F. Graf, S. Bajohr, R. Reimert and T. Kolb, *Renewable Energy*, 2016, **85**, 1371–1390.
54 C. Zhang and L. D. Anadon, *Environ. Sci. Technol.*, 2013, **47**, 14459–14467.
55 J. A. Turner, *Science*, 2004, **305**, 972.
56 Y. Kuang, M. J. Kenney, Y. Meng, W.-H. Hung, Y. Liu, J. E. Huang, R. Prasanna, P. Li, Y. Li, L. Wang, M.-C. Lin, M. D. McGehee, X. Sun and H. Dai, *Proc. Natl. Acad. Sci. U. S. A.*, 2019, **116**, 6624.
57 International Energy Agency (IEA), The Future of Hydrogen, **https://www.iea.org/reports/the-future-of-hydrogen**.
58 Air Liquid, Inauguration of the world's largest PEM electrolyze, **https://www.airliquide.com/magazine/energy-transition/inauguration-worlds-largest-pem-electrolyzer**.
59 R. J. Detz, J. N. H. Reek and B. C. C. van der Zwaan, *Energy Environ. Sci.*, 2018, **11**, 1653–1669.
60 S. Giddey, S. P. S. Badwal, C. Munnings and M. Dolan, *ACS Sustainable Chem. Eng.*, 2017, **5**, 10231–10239.
61 P. Nikolaidis and A. Poullikkas, *Renewable Sustainable Energy Rev.*, 2017, **67**, 597–611.
62 M. Liszka, T. Malik and G. Manfrida, *Energy*, 2012, **45**, 142–150.
63 F. Dawood, M. Anda and G. M. Shafiullah, *Int. J. Hydrogen Energy*, 2020, **45**, 3847–3869.
64 R. S. El-Emam and H. Özcan, *J. Cleaner Prod.*, 2019, **220**, 593–609.
65 C. Acar and I. Dincer, *J. Cleaner Prod.*, 2019, **218**, 835–849.
66 A. X. Y. Mah, W. S. Ho, C. P. C. Bong, M. H. Hassim, P. Y. Liew, U. A. Asli, M. J. Kamaruddin and N. G. Chemmangattuvalappil, *Int. J. Hydrogen Energy*, 2019, **44**, 5661–5675.
67 M. Kaur and K. Pal, *J. Energy Storage*, 2019, **23**, 234–249.
68 J. O. Abe, A. P. I. Popoola, E. Ajenifuja and O. M. Popoola, *Int. J. Hydrogen Energy*, 2019, **44**, 15072–15086.

69 A. Finkel, *Griffith Rev.*, 2019, **64**, 134–142.
70 R. Moradi and K. M. Groth, *Int. J. Hydrogen Energy*, 2019, **44**, 12254–12269.
71 M. H. McCay, S. Shafiee and T. M. Letcher, *Future Energy (Third Edition)*, Elsevier, 2020, pp. 475–493, DOI: 10.1016/B978-0-08-102886-5.00022-0.
72 Q.-L. Zhu and Q. Xu, *Energy Environ. Sci.*, 2015, **8**, 478–512.
73 M. Niermann, S. Drünert, M. Kaltschmitt and K. Bonhoff, *Energy Environ. Sci.*, 2019, **12**, 290–307.
74 C. Smith, A. K. Hill and L. Torrente-Murciano, *Energy Environ. Sci.*, 2020, **13**, 331–344.
75 C. Weidenthaler and M. Felderhoff, *Energy Environ. Sci.*, 2011, **4**, 2495–2502.
76 Z. Yanxing, G. Maoqiong, Z. Yuan, D. Xueqiang and S. Jun, *Int. J. Hydrogen Energy*, 2019, **44**, 16833–16840.
77 S. Alavi and J. A. Ripmeester, *Mol. Simul.*, 2017, **43**, 808–820.
78 Q. Lai, M. Paskevicius, D. A. Sheppard, C. E. Buckley, A. W. Thornton, M. R. Hill, Q. Gu, J. Mao, Z. Huang, H. K. Liu, Z. Guo, A. Banerjee, S. Chakraborty, R. Ahuja and K.-F. Aguey-Zinsou, *ChemSusChem*, 2015, **8**, 2789–2825.
79 J. Bellosta von Colbe, J.-R. Ares, J. Barale, M. Baricco, C. Buckley, G. Capurso, N. Gallandat, D. M. Grant, M. N. Guzik, I. Jacob, E. H. Jensen, T. Jensen, J. Jepsen, T. Klassen, M. V. Lototskyy, K. Manickam, A. Montone, J. Puszkiel, S. Sartori, D. A. Sheppard, A. Stuart, G. Walker, C. J. Webb, H. Yang, V. Yartys, A. Züttel and M. Dornheim, *Int. J. Hydrogen Energy*, 2019, **44**, 7780–7808.
80 V. A. Yartys, M. V. Lototskyy, E. Akiba, R. Albert, V. E. Antonov, J. R. Ares, M. Baricco, N. Bourgeois, C. E. Buckley, J. M. Bellosta von Colbe, J. C. Crivello, F. Cuevas, R. V. Denys, M. Dornheim, M. Felderhoff, D. M. Grant, B. C. Hauback, T. D. Humphries, I. Jacob, T. R. Jensen, P. E. de Jongh, J. M. Joubert, M. A. Kuzovnikov, M. Latroche, M. Paskevicius, L. Pasquini, L. Popilevsky, V. M. Skripnyuk, E. Rabkin, M. V. Sofianos, A. Stuart, G. Walker, H. Wang, C. J. Webb and M. Zhu, *Int. J. Hydrogen Energy*, 2019, **44**, 7809–7859.
81 M. Hirscher, V. A. Yartys, M. Baricco, J. Bellosta von Colbe, D. Blanchard, R. C. Bowman, D. P. Broom, C. E. Buckley, F. Chang, P. Chen, Y. W. Cho, J.-C. Crivello, F. Cuevas, W. I. F. David, P. E. de Jongh, R. V. Denys, M. Dornheim, M. Felderhoff, Y. Filinchuk, G. E. Froudakis, D. M. Grant, E. M. Gray, B. C. Hauback, T. He, T. D. Humphries, T. R. Jensen, S. Kim, Y. Kojima, M. Latroche, H.-W. Li, M. V. Lototskyy, J. W. Makepeace, K. T. Møller, L. Naheed, P. Ngene, D. Noréus, M. M. Nygård, S.-I. Orimo, M. Paskevicius, L. Pasquini, D. B. Ravnsbæk, M. Veronica Sofianos, T. J. Udovic, T. Vegge, G. S. Walker, C. J. Webb, C. Weidenthaler and C. Zlotea, *J. Alloys Compd.*, 2020, **827**, 153548.
82 D. A. Sheppard and C. E. Buckley, *Int. J. Hydrogen Energy*, 2019, **44**, 9143–9163.
83 S. A. Sherif, N. Zeytinoglu and T. N. Veziroğlu, *Int. J. Hydrogen Energy*, 1997, **22**, 683–688.
84 J. Sloop and A. Silverstein, Liquid Hydrogen as a Propulsion Fuel, https://history.nasa.gov/SP-4404/contents.htm, (accessed December, 2019).
85 The NASA History Series. Taming Liquid Hydrogen: The Centaur Upper Stage Rocket 1958-2002, https://history.nasa.gov/SP-4230.pdf.
86 W. Notardonato, presented in part at the Hydrogen Liquefaction & Storage Symposium, Perth, 2019.
87 International Energy Agency (IEA), Energy Technology Perspectives 2020, Paris, France, 2020.
88 Y. Ishimoto, A. Kurosawa, M. Sasakura and K. Sakata, *Int. J. Hydrogen Energy*, 2017, **42**, 13357–13367.
89 E. W. Lemmon, I. H. Bell, M. L. Huber and M. O. McLinden, NIST Standard Reference Database 23: Reference Fluid Thermodynamic and Transport Properties-REFPROP, version 10.0, 2018.
90 J. Zheng, X. Liu, P. Xu, P. Liu, Y. Zhao and J. Yang, *Int. J. Hydrogen Energy*, 2012, **37**, 1048–1057.
91 T. Q. Hua, R. K. Ahluwalia, J. K. Peng, M. Kromer, S. Lasher, K. McKenney, K. Law and J. Sinha, *Int. J. Hydrogen Energy*, 2011, **36**, 3037–3049.
92 J. Andersson and S. Grönkvist, *Int. J. Hydrogen Energy*, 2019, **44**, 11901–11919.
93 U. Cardella, L. Decker and H. Klein, *Int. J. Hydrogen Energy*, 2017, **42**, 13329–13338.
94 K. Sichao, K. Kimura and H. Ishida, *Perspectives on Hydrogen in the APEC Region*, Asia Pacific Energy Research Centre, Tokyo, Japan, 2018.
95 P.-M. Heuser, D. S. Ryberg, T. Grube, M. Robinius and D. Stolten, *Int. J. Hydrogen Energy*, 2019, **44**, 12733–12747.
96 Hydrogen Council, Hydrogen Insights 2021 - A Perspective on Hydrogen Investment, Deployment and Cost Competitiveness, Hydrogen Council, EU, 2021.
97 X. J. Li, J. D. Allen, J. A. Stager and A. Y. Ku, *Clean Energy*, 2020, **4**, 26–47.
98 A. T. Wijayanta, T. Oda, C. W. Purnomo, T. Kashiwagi and M. Aziz, *Int. J. Hydrogen Energy*, 2019, **44**, 15026–15044.
99 D. Teichmann, W. Arlt and P. Wasserscheid, *Int. J. Hydrogen Energy*, 2012, **37**, 18118–18132.
100 Y. Ishimoto, M. Voldsund, P. Nekså, S. Roussanaly, D. Berstad and S. O. Gardarsdottir, *Int. J. Hydrogen Energy*, 2020, **45**, 32865–32883.
101 T. Watanabe, K. Murata, S. Kamiya and K. I. Ota, *Proc. 18th World Hydrog. Energy Conf.*, 2010, **78**, 547–557.
102 S. Kamiya, M. Nishimura and E. Harada, *Phys. Proc.*, 2015, **67**, 11–19.
103 T. Nyberg, Master, Lund University, 2021.
104 T. Funke, presented in part at the Hydrogen Liquefaction & Storage Symposium, Perth, 2019.
105 N. D. Mortimer, C. Hatto, O. Mwabonje and J. H. R. Rix, *Hydrogen Production and Utilisation Report IDEALHY*, EU, 2013.
106 K. Stolzenburg and R. Mubbala, *Hydrogen Liquefaction Report IDEALHY*, EU, 2013.
107 M. Raab, S. Maier and R.-U. Dietrich, *Int. J. Hydrogen Energy*, 2021, **46**, 11956–11968.
108 M. Reuß, T. Grube, M. Robinius, P. Preuster, P. Wasserscheid and D. Stolten, *Appl. Energy*, 2017, **200**, 290–302.

109 Elizabeth Connelly, Michael Penev, Amgad Elgowainy and C. Hunter, *Current Status of Hydrogen Liquefaction Costs*, DOE Hydrogen and Fuel Cells Program Record, 2019.
110 J. Cihlar, A. Villar Lejarreta, A. Wang, F. Melgar, J. Jens and P. Rio, Hydrogen generation in Europe: Overview of costs and key benefits, European Comission, Luxembourg, 2020.
111 S. y. Obara, *Energy*, 2019, **174**, 848–860.
112 K. H. R. Rouwenhorst, A. G. J. Van der Ham, G. Mul and S. R. A. Kersten, *Renewable Sustainable Energy Rev.*, 2019, **114**, 109339.
113 G. Hochman, A. S. Goldman, F. A. Felder, J. M. Mayer, A. J. M. Miller, P. L. Holland, L. A. Goldman, P. Manocha, Z. Song and S. Aleti, *ACS Sustainable Chem. Eng.*, 2020, **8**, 8938–8948.
114 S. Ecuity, Engie, Siemens, Ammonia to Green Hydrogen Project Feasibility Study, 2019.
115 International Energy Agency (IEA), Hydrogen production costs using natural gas in selected regions, 2018, **https://www.iea.org/reports/the-future-of-hydrogen**, (accessed December, 2019).
116 A. Boretti, *Int. J. Hydrogen Energy*, 2013, **38**, 1806–1812.
117 S. Tuomi, A. Santasalo-Aarnio, P. Kanninen and T. Kallio, *J. Power Sources*, 2013, **229**, 32–35.
118 R. Ahluwalia, D. Papadias, J. Peng and H. Roh, *U.S. DOE Hydrogen and Fuel Cells Program 2019 Annual Merit Review and Peer Evaluation Meeting*, 2019.
119 C. Wulf and P. Zapp, *Int. J. Hydrogen Energy*, 2018, **43**, 11884–11895.
120 S. Bano, P. Siluvai Antony, V. Jangde and R. B. Biniwale, *J. Cleaner Prod.*, 2018, **183**, 988–997.
121 A. Ozawa, Y. Kudoh, N. Kitagawa and R. Muramatsu, *Int. J. Hydrogen Energy*, 2019, **44**, 11219–11232.
122 I. Kuz'menko, V. Peredelskii and A. Dovbish, *Chem. Petroleum Eng.*, 2010, 46.
123 J. Zhang, H. Meerman, R. Benders and A. Faaij, *Appl. Therm. Eng.*, 2020, **166**, 114736.
124 K. Ohlig and L. Decker, *AIP Conf. Proc.*, 2013, 1573.
125 Raymond Drnevich, Hydrogen Delivery Liquefaction & Compression, 2003, **https://www1.eere.energy.gov/hydrogenandfuelcells/pdfs/liquefaction_comp_pres_praxair.pdf**.
126 U. Cardella, Doktor-Ingenieurs, Universität München, 2018.
127 D. Berstad, P. Nekså and J. Stang, *Int. J. Hydrogen Energy*, 2010, **35**, 4512–4523.
128 F. Ustolin, N. Paltrinieri and F. Berto, *Int. J. Hydrogen Energy*, 2020, **45**, 23809–23840.
129 Hydrogen Scaling Up, prepared by Hydrogen Council, 2017, **https://hydrogencouncil.com/wp-content/uploads/2017/11/Hydrogen-Scaling-up_Hydrogen-Council_2017.compressed.pdf**.
130 L. Barrón-Palos, R. Alarcon, S. Balascuta, C. Blessinger, J. D. Bowman, T. E. Chupp, S. Covrig, C. B. Crawford, M. Dabaghyan, J. Dadras, M. Dawkins, W. Fox, M. T. Gericke, R. C. Gillis, B. Lauss, M. B. Leuschner, B. Lozowski, R. Mahurin, M. Mason, J. Mei, H. Nann, S. I. Penttilä, W. D. Ramsay, A. Salas-Bacci, S. Santra, P. N. Seo, M. Sharma, T. Smith, W. M. Snow, W. S. Wilburn and V. Yuan, *Nucl. Instr. Methods Phys. Res. Sect. A: Accelerators, Spectrometers, Detectors Associated Equipment*, 2011, **659**, 579–586.
131 M. Aasadnia and M. Mehrpooya, *Appl. Energy*, 2018, **212**, 57–83.
132 H. You, J. Ahn, S. Jeong and D. Chang, *Ships Offshore Struct.*, 2018, **13**, 79–85.
133 S. Gursu, M. Lordgooei, S. A. Sherif and T. N. Veziroğlu, *Int. J. Hydrogen Energy*, 1992, **17**, 227–236.
134 E. Karlsson, Master Thesis, Lund University, 2017.
135 B. Burkholder, Honours Thesis, Oberlin College and Conservatory, 2009.
136 J. White, *Development of High-Activity Para- to Ortho-Hydrogen Conversion Catalysts*, 1989.
137 D. White, A. S. Friedman and H. L. Johnston, *J. Am. Chem. Soc.*, 1950, **72**, 3927–3930.
138 D. White, A. S. Friedman and H. L. Johnston, *J. Am. Chem. Soc.*, 1950, **72**, 3565–3568.
139 R. D. Goodwin, D. E. Diller, H. M. Roder and L. A. Weber, *Cryogenics*, 1961, **2**, 81–83.
140 H. M. Roder, D. E. Diller, L. A. Weber and R. D. Goodwin, *Cryogenics*, 1963, **3**, 16–22.
141 J. W. Leachman, R. T. Jacobsen, S. G. Penoncello and E. W. Lemmon, *J. Phys. Chem. Ref. Data*, 2009, **38**, 721–748.
142 R. Span, R. Beckmüller, T. Eckermann, S. H. S. Herrig, A. Jäger, T. Neumann, S. Pohl, B. Semrau and M. Thol, TREND. Thermodynamic Reference and Engineering Data 4.0.
143 X. Yang, D. Rowland, C. C. Sampson, P. E. Falloon and E. F. May, *Fuel*, 2022, **314**, 123033.
144 D.-Y. Peng and D. B. Robinson, *Ind. Eng. Chem. Fundamentals*, 1976, **15**, 59–64.
145 R. H. Newton, *Ind. Eng. Chem.*, 1935, **27**, 302–306.
146 T. W. Leland and P. S. Chappelear, *Ind. Eng. Chem.*, 1968, **60**, 15–43.
147 D. Rowland, T. J. Hughes and E. F. May, *J. Chem. Eng. Data*, 2017, **62**, 2799–2811.
148 R. D. Gunn, P. L. Chueh and J. M. Prausnitz, *AIChE J.*, 1966, **12**, 937–941.
149 P. L. Chueh and J. M. Prausnitz, *Ind. Eng. Chem. Fundamentals*, 1967, **6**, 492–498.
150 R. P. Feynman, A. R. Hibbs and D. F. Stye, *Quantum Mechanics and Path Integrals*, McGraw-Hill, New York, Emended edn, 2005.
151 A. Aasen, M. Hammer, S. Lasala, J.-N. Jaubert and Ø. Wilhelmsen, *Fluid Phase Equilib.*, 2020, **524**, 112790.
152 O. Kunz and W. Wagner, *J. Chem. Eng. Data*, 2012, **57**, 3032–3091.
153 T. Monika, R. Markus, F. M. Eric, W. L. Eric and S. Roland, *J. Phys. Chem. Ref. Data*, 2019, **48**, 033102.
154 R. Beckmüller, M. Thol, I. H. Bell, E. W. Lemmon and R. Span, *J. Phys. Chem. Ref. Data*, 2021, **50**, 013102.
155 S. Krasae-in, Philosophy doctorate, Norwegian University of Science and Technology, 2013.
156 J. Tkaczuk, I. H. Bell, E. W. Lemmon, N. Luchier and F. Millet, *J. Phys. Chem. Ref. Data*, 2020, **49**, 023101.

157 R. Span, presented in part at the Hydrogen Liquefaction & Storage Symposium, Perth, 2019.
158 R. T. Jacobsen, J. W. Leachman, S. G. Penoncello and E. W. Lemmon, *Int. J. Thermophys.*, 2007, **28**, 758–772.
159 J. Leachman, presented in part at the Hydrogen Liquefaction & Storage Symposium, Perth, 2019.
160 K. Patkowski, W. Cencek, P. Jankowski, K. Szalewicz, J. B. Mehl, G. Garberoglio and A. H. Harvey, *J. Chem. Phys.*, 2008, **129**, 094304.
161 J. Mehl, M. Huber and A. Harvey, *Int. J. Thermophys.*, 2010, **31**, 740–755.
162 E. F. May, R. F. Berg and M. R. Moldover, *Int. J. Thermophys.*, 2007, **28**, 25.
163 C. Muzny, M. Huber and A. Kazakov, *J. Chem. Eng. Data*, 2013, **58**, 969–979.
164 D. E. Diller, *J. Chem. Phys.*, 1965, **42**, 2089–2100.
165 D. Zhou, G. G. Ihas and N. S. Sullivan, *J. Low Temp. Phys.*, 2004, **134**, 401–406.
166 M. J. Assael, J. A. M. Assael, M. L. Huber, R. A. Perkins and Y. Takata, *J. Phys. Chem. Ref. Data*, 2011, **40**, 033101.
167 H. M. Roder and D. E. Diller, *J. Chem. Phys.*, 1970, **52**, 5928–5949.
168 H. M. Roder, Experimental thermal conductivity values for hydrogen, methane, ethane and propane [microform]/H. M. Roder; prepared for NASA-Lewis Research Center, U.S. Dept. of Commerce, National Bureau of Standards; Order from National Technical Information Service, Washington, D.C., Springfield, Va, 1984.
169 Y. Y. Milenko, R. M. Sibileva and M. A. Strzhemechny, *J. Low Temp. Phys.*, 1997, **107**, 77–92.
170 G. Petitpas, S. M. Aceves, M. J. Matthews and J. R. Smith, *Int. J. Hydrogen Energy*, 2014, **39**, 6533–6547.
171 D. S. Chapin and H. L. Johnston, *J. Am. Chem. Soc.*, 1957, **79**, 2406–2412.
172 M. Misono and P. W. Selwood, *J. Am. Chem. Soc.*, 1968, **90**, 2977–2978.
173 IONEX Type OP Catalyst - Molecular Products, **https://www.molecularproducts.com/products/ionex-type-op-catalyst**.
174 A. V. Zhuzhgov, O. Krivoruchko, L. Isupova, O. Martyanov and V. Parmon, *Catal. Ind.*, 2018, **10**, 9–19.
175 P. J. Donaubauer, U. Cardella, L. Decker and H. Klein, *Chem. Eng. Technol.*, 2019, **42**, 669–679.
176 H. L. Hutchinson, *Masters thesis*, University of Colorado Boulder, 1966.
177 H. L. Hutchinson, P. L. Barrick and L. F. Brown, in *Advances in Cryogenic Engineering*, ed. K. D. Timmerhaus, Springer US, Boston, MA, 1965, pp. 190–196.
178 H. L. Hutchinson, P. L. Barrick and L. F. Brown, *Chem. Eng. Progress, Sym. Ser.*, 1967, **63**, 18–30.
179 H. L. Hutchinson, L. F. Brown and P. L. Barrick, in *Advances in Cryogenic Engineering: Proceeding of the 1970 Cryogenic Engineering Conference The University of Colorado Boulder, Colorado June 17–17, 1970*, ed. K. D. Timmerhaus, Springer US, Boston, MA, 1971, pp. 96–103, DOI: **10.1007/978-1-4757-0244-6_12**.
180 D. H. Weitzel, C. Van Valin and J. W. Draper, in *Advances in Cryogenic Engineering*, Springer, 1960, pp. 73–84.
181 N. Wakao, P. W. Selwood and J. M. Smith, *AIChE J.*, 1962, **8**, 478–481.
182 Ø. Wilhelmsen, D. Berstad, A. Aasen, P. Nekså and G. Skaugen, *Int. J. Hydrogen Energy*, 2018, **43**, 5033–5047.
183 J. Essler and H. Ch, *AIP Conf. Proc.*, 2010, **1218**, 305–310.
184 J. Park, H. Lim, G. H. Rhee and S. W. Karng, *Int. J. Heat Mass Transfer*, 2021, **170**, 121007.
185 F. Reif and E. M. Purcell, *Phys. Rev.*, 1953, **91**, 631–641.
186 L. Yin and Y. Ju, *Front. Energy*, 2020, **14**, 530–544.
187 H. Ansarinasab, M. Mehrpooya and M. Sadeghzadeh, *J. Cleaner Prod.*, 2019, **210**, 530–541.
188 A. Alekseev, in *Hydrogen Science and Engineering, 2 Volume Set: Materials, Processes, Systems and Technology*, eds. D. Stolten and B. Emonts, Wiley, Germany, 2016.
189 S. Krasae-in, J. H. Stang and P. Neksa, *Int. J. Hydrogen Energy*, 2010, **35**, 4524–4533.
190 G. Valenti, in *Compendium of Hydrogen Energy: Hydrogen Storage, Distribution and Infrastructure*, eds. R. Gupta, A. Basile and T. Nejat Veziroglu, Woodhead Publishing, Cambridge, 2016, vol. 2.
191 A. Léon, in *Hydrogen Technology: Mobile and Portable Applications*, ed. A. Léon, Springer, Berlin, 2008, p. 98.
192 J. Essler, C. Haberstroh, H. Quack, H. Walnum, D. Berstad, P. Nekså, J. Stang, M. Börsch, F. Holdener, L. Fecker and P. Treite, presented in part at the Report on Technology Overview and Barriers to Energy- and Cost-Efficient Large Scale Hydrogen Liquefaction, 2012.
193 R. W. Moore Jr, *AIChE J.*, 1972, **18**, 1086.
194 R. F. Barron, *Advances in Cryogenic Engineering: A Collection of Invited Papers and Contributed Papers Presented at National Technical Meetings During 1970 and 1971*, Springer US, Boston, MA, 1972, pp. 20–36, DOI: **10.1007/978-1-4684-7826-6_3**.
195 C. Windmeier and R. F. Barron, *Cryogenic Technology, Ullmann's Encyclopedia of Industrial Chemistry*, 2013, 1–71.
196 M. Mukhopadhyay, *Fundamentals of Cryogenic Engineering*, PHI Learning, 2010.
197 G. Walker, *Cryocoolers: Part 1: Fundamentals*, Springer US, 1983.
198 G. Walker, *Cryocoolers: Part 2: Applications*, Springer US, 1st edn, 1983.
199 H. Chang, K. Ryu and J. Baik, *Cryogenics*, 2018, **91**, 68–76.
200 M. Aasadnia and M. Mehrpooya, *Int. J. Hydrogen Energy*, 2017, **42**, 15564–15585.
201 T. Kotas, *The Exergy Method of Thermal Plant Analysis*, Butterworths, Essex, 1985.
202 H. Walnum, D. Berstad, M. Drescher, P. Nekså, H. Quack, C. Haberstroh and J. Essler, presented in part at the 12th Cryogenics 2012 - IIR Conference, Dresden, 2012.
203 F. Dauber and R. Span, *Appl. Energy*, 2012, **97**, 822–827.
204 E. C. Carlson, *Chem. Eng. Prog.*, 1996, **92**, 35–46.
205 A. H. Harvey and A. Laesecke, *Chem. Eng. Prog.*, 2002, **98**, 34–41.
206 C. L. Rhodes, *J. Chem. Eng. Data*, 1996, **41**, 947–950.
207 G. Soave, M. Barolo and A. Bertucco, *Fluid Phase Equilib.*, 1993, **91**, 87–100.

208 G. Soave, *Chem. Eng. Sci.*, 1972, **27**, 1197–1203.
209 K. E. Starling, *Fluid Thermodynamic Properties of Light Petroleum Systems*, Books on Demand, 1973.
210 U. Cardella, L. Decker, J. Sundberg and H. Klein, *Int. J. Hydrogen Energy*, 2017, **42**, 12339–12354.
211 J.-H. Yang, Y. Yoon, M. Ryu, S.-K. An, J. Shin and C.-J. Lee, *Appl. Energy*, 2019, **255**, 113840.
212 G. Valenti, E. Macchi and S. Brioschi, *Int. J. Hydrogen Energy*, 2012, **37**, 10779–10788.
213 D.-Y. Peng and D. B. Robinson, *Ind. Eng. Chem. Fundamentals*, 1976, **15**, 59–64.
214 D. O. Ortiz-Vega, K. R. Hall, J. C. Holste, V. D. Arp, A. H. Harvey and E. W. Lemmon, *J. Phys. Chem. Ref. Data*, 2018, to be submitted.
215 I. H. B. Eric, W. Lemmon, Marcia L. Huber and Mark O. McLinden, *REFPROP 10.0: NIST Standard Reference Database 23*, 2018.
216 G. Valenti and E. Macchi, *Int. J. Hydrogen Energy*, 2008, **33**, 3116–3121.
217 M. Bracha and L. Decker, *Grosstechnische Wasserstoffverflüssigung in Leuna*, Deutsche Kälte-Klima-Tagung, 2008.
218 J. Essler, C. Haberstroh, H. Quack, H. Walnum, D. Berstad, P. Nekså, J. Stang, M. Börsch, F. Holdener, L. Decker and P. Treite, *Report on technology overview and barriers to energy- and cost-efficient large-scale hydrogen liquefaction*, Fuel Cells and Hydrogen Joint Undertaking (FCH JU), Europe, 2012.
219 M. Bracha, G. Lorenz, A. Patzelt and M. Wanner, *Int. J. Hydrogen Energy*, 1994, **19**, 53–59.
220 U. Cardella, L. Decker and H. Klein, presented in part at the Materials Science and Engineering, 2017.
221 K. Stolzenburg, D. Berstad, L. Decker, A. Elliott, C. Haberstroh, C. Hatto, H. Klaus, N. D. Mortimer, R. Mubbala, O. Mwabonje, P. Nekså, H. Quack, J. H. R. Rix, I. Seemann and H. T. Walnum, presented in part at the Energie Symposium, Germany, 2013.
222 Production of Liquefied Hydrogen Sourced by COG, Nippon Steel Corporation, 2004.
223 V. M. Medisetty, R. Kumar, M. H. Ahmadi, D.-V. N. Vo, A. A. V. Ochoa and R. Solanki, *Chem. Eng. Technol.*, 2020, **43**, 613–624.
224 Linde. Liquefaction for highest density - Hydrogen solutions, **https://www.linde-kryotechnik.ch/wp-content/uploads/2016/10/hydrogen_solutions_eng.pdf**.
225 Iwatani's Third Liquid Hydrogen Plant in Japan Completed, **http://www.iwatani.co.jp/eng/newsrelease/detail_50.html**.
226 Accommodating the Energy Supply Needs of the Next Era: Kawasaki's Hydrogen Liquefaction System, **https://global.kawasaki.com/en/stories/articles/vol57/**.
227 Production Capacity of Liquid Hydrogen Doubled, **http://www.iwatani.co.jp/eng/newsrelease/detail_66.html**.
228 A. Bauer, T. Mayer, M. Semmel, M. A. Guerrero Morales and J. Wind, *Int. J. Hydrogen Energy*, 2019, **44**, 6795–6812.
229 North Las Vegas lands $150 million liquid hydrogen plant, 2019, **https://lasvegassun.com/news/2019/nov/11/north-las-vegas-lands-150-million-liquid-hydrogen/**.
230 L. Decker, Latest Global Trend in Liquid Hydrogen Production, **https://www.sintef.no/globalassets/project/hyper/presentations-day-1/day1_1430_decker_latest-global-trend-in-liquid-hydrogen-production_linde.pdf/**.
231 Air Products' New World-Scale Liquid Hydrogen Plant is Onstream at Its La Porte, Texas Facility, 2021, **https://www.airproducts.com/news-center/2021/10/1007-air-products-new-liquid-hydrogen-plant-onstream-at-laporte-texas-facility**.
232 Praxair to Build New Liquid Hydrogen Plant in La Porte Texas, 2018, **https://investors.linde.com/-/media/linde/investors/documents/investors-archive/praxair-archive/news-releases/2018/praxairtobuildnewliquidhydrogenplantinlaportetexas11718final.pdf**.
233 Air Products to Build Second Liquid Hydrogen Production Facility in California, 2019, **http://www.airproducts.ca/Company/news-center/2019/01/0107-air-products-to-build-second-liquid-hydrogen-productions-facility-in-california.aspx**.
234 M. Marray, Linde, Hyosung to build world's largest liquid hydrogen plant in South Korea, 2020, **https://www.theassetset.com/asia-connect/40347/linde-hyosung-to-build-worlds-largest-liquid-hydrogen-plant-in-south-korea**.
235 A. Kuendig, K. Loehlein, G. J. Kramer and J. Huijsmans, Proceedings of the 16th world hydrogen energy conference, 2006, pp. 3326–3333.
236 H. Shigekiyo, *Air Products Liquid Hydrogen Technologies*, Japan Ship Technology Research Association, Japan, 2015.
237 D. Berstad, G. Skaugen and Ø. Wilhelmsen, *Int. J. Hydrogen Energy*, 2021, **46**, 8014–8029.
238 S. Krasae-in, *Int. J. Hydrogen Energy*, 2014, **39**, 7015–7029.
239 H. Quack, *Adv. Cryog. Eng.*, 2002, **613**, 255–263.
240 J. Eckroll, *Master of Energy and Environmental Engineering*, Norwegian University of Science and Technology, 2017.
241 A. Witkowski, A. Rusin, M. Majkut and K. Stolecka, *Energy*, 2017, **141**, 2508–2518.
242 Linde Group. Aluminium plate-fin heat exchangers, **www.linde-engineering.com**.
243 S. Krasae-in, J. Stang and P. Nekså, *Int. J. Hydrogen Energy*, 2010, **35**, 12531–12544.
244 D. Popov, K. Fikiin, B. Stankov, A. Alvarez, M. Youbi-Idrissi, A. Damas, J. Evans and T. Brown, *Appl. Therm. Eng.*, 2019, **153**, 275–290.
245 R. Hånde and Ø. Wilhelmsen, *Int. J. Hydrogen Energy*, 2019, **44**, 15045–15055.
246 G. Skaugen, D. Berstad and Ø. Wilhelmsen, *Int. J. Hydrogen Energy*, 2020, **45**, 6663–6679.
247 T. Kim, B.-I. Choi, Y.-S. Han and K. H. Do, *Trans. Korean Hydrogen New Energy Soc.*, 2020, **31**, 8.
248 J. Meagher, *Master of Science*, State University of New York, 2008.
249 C. Knowlen, A. Mattick, A. Bruckner and A. Hertzberg, SAE Technical Papers, 1998, DOI: **10.4271/981898**.
250 M. Green, *AIP Conf. Proc.*, 2008, **985**, 872–878.
251 L. Van Hoecke, L. Laffineur, R. Campe, P. Perreault, S. W. Verbruggen and S. Lenaerts, *Energy Environ. Sci.*, 2021, **14**, 815–843.

252 R. Bruno, P. Bevilacqua and N. Arcuri, in *Advances in Natural Gas Emerging Technologies*, eds. H. Al-Megren and R. Altamimi, IntechOpen, Croatia, 2017, p. 3.
253 E. May, presented in part at the Hydrogen Liquefaction & Storage Symposium, Perth, 2019.
254 E. Brown, *Expansion Engines for Hydrogen Liquefiers*, 1959.
255 M. Boyce, in *Gas Turbine Engineering Handbook*, ed. M. Boyce, Gulf Professional Publishing, USA, 3rd edn, 2006, pp. 336–337.
256 K. Ohlig and S. Bischoff, *Am. Inst. Phys. Conf. Ser.*, 2012, **57**, 814.
257 J. Y. Chen, X. M. Li, X. B. Dong, C. Lv and J. H. Wu, *IOP Conf. Ser.: Mater. Sci. Eng.*, 2020, **755**, 012033.
258 M. Trusler, presented in part at the Hydrogen Liquefaction & Storage Symposium, Perth, 2019.
259 H. Zhang, R. Gimaev, B. Kovalev, K. Kamilov, V. Zverev and A. Tishin, *Phys. B*, 2019, **558**, 65–73.
260 T. Feng, R. Chen and R. V. Ihnfeldt, *Int. J. Refrig.*, 2020, **119**, DOI: **10.1016/j.ijrefrig.2020.06.032**.
261 R. Li, *Energy Technol.*, 2019, **7**, 1801070.
262 T. Numazawa, K. Kamiya, T. Utaki and K. Matsumoto, *Cryogenics*, 2014, **62**, 185–192.
263 K. Kamiya, H. Takahashi, T. Numazawa, H. Nozawa and T. Yanagitani, presented in part at the International Cryocooler Conference, Boulder, 2014.
264 U. Cardella, L. Decker and H. Klein, presented in part at the Cryogenic Engineering Conference 2017, Madison, USA, 2017.
265 T. Vanessa, L. Sebastian and S. Detlef, *Hydrogen Science and Engineering: Materials, Processes, Systems and Technology*, 2016, pp. 659–690, DOI: **10.1002/9783527674268.ch27**.
266 DOE Technical Targets for Hydrogen Delivery, **https://www.energy.gov/eere/fuelcells/doe-technical-targets-hydrogen-delivery**, (accessed 2 January, 2020).
267 S. Kamiya, presented in part at the Hydrogen Liquefaction & Storage Symposium, Perth, 2019.
268 L. Decker, Liquid Hydrogen Distribution Technology, **https://www.sintef.no/globalassets/project/hyper/presentations-day-2/day2_1105_decker_liquid-hydrogen-distribution-technology_linde.pdf/**.
269 S. Mital, J. Gyekenyesi, S. Arnold, R. Sullivan, J. Manderscheid and P. Murthy, *Review of Current State of the Art and Key Design Issues With Potential Solutions for Liquid Hydrogen Cryogenic Storage Tank Structures for Aircraft Applications, National Aeronautics and Space Administration*, Cleveland, Ohio, 2006.
270 G. Pearce, presented in part at the Hydrogen Liquefaction & Storage Symposium, Perth, 2019.
271 K. Verfondern, Forschungszentrum Jülich GmbH, Institut für Energieforschung Sicherheitsforschung und Reaktortechnik. Safety Considerations on Liquid Hydrogen, 2007, **http://juser.fz-juelich.de/record/1311/files/Energie%26Umwelt_10.pdf**.
272 M. Klell, *Handbook of Hydrogen Storage*, Storage of Hydrogen in the Pure Form, 2010, ch. 1.
273 R. Sullivan, J. Palko, R. Tornabene, B. Bednarcyk, L. Powers, S. Mital, L. Smith, X. Wange and J. Hunter, Engineering Analysis Studies for Preliminary Design of Lightweight Cryogenic Hydrogen Tanks in UAV Applications, National Aeronautics and Space Administration, Cleveland, Ohio, 2006.
274 P. M. Adam, Doctor of philosophy, Washington State University, 2017.
275 A. Abe, M. Nakamura, I. Sato, H. Uetani and T. Fujitani, *Int. J. Hydrogen Energy*, 1998, **23**, 115–121.
276 G. Petitpas, *Boil-off losses along the LH2 pathway*, Lawrence Livermore National Laboratory, 2018.
277 M. Kang, J. Kim, H. You and D. Chang, *Exp. Therm. Fluid Sci.*, 2018, **96**, 371–382.
278 S. Gursu, S. A. Sherif, T. N. Veziroglu and J. W. Sheffield, *J. Energy Resources Technol.*, 1993, **115**, 221–227.
279 S. W. Choi, W. I. Lee and H. S. Kim, *Numerical Heat Transfer, Part A: Appl.*, 2017, **71**, 402–422.
280 J. L. Ferrín and L. J. Pérez-Pérez, *Comput. Chem. Eng.*, 2020, **138**, 106840.
281 J.-J. Ren, J.-Y. Shi, P. Liu, M.-S. Bi and K. Jia, *Int. J. Hydrogen Energy*, 2013, **38**, 4017–4023.
282 A. Saleem, S. Farooq, I. A. Karimi and R. Banerjee, *Ind. Eng. Chem. Res.*, 2020, **59**, 14126–14144.
283 J. Q. Shi, C. Beduz and R. G. Scurlock, *Cryogenics*, 1993, **33**, 1116–1124.
284 A. Mawire, *Appl. Energy*, 2013, **108**, 459–465.
285 N. K. Ghaddar, A. M. Al-Marafie and A. Al-Kandari, *Appl. Energy*, 1989, **32**, 225–239.
286 F. Perez, S. Z. S. Al Ghafri, L. Gallagher, A. Siahvashi, Y. Ryu, S. Kim, S. G. Kim, M. L. Johns and E. F. May, *Energy*, 2021, **222**, 119853.
287 S. Z. S. Al Ghafri, A. Swanger, K. H. Park, V. Jusko, Y. Ryu, S. Kim, S. G. Kim, D. Zhang, Y. Seo, M. L. Johns and E. F. May, *Acta Astronautica*, 2022, **190**, 444–454.
288 S. Z. S. Al Ghafri, F. Perez, K. H. Park, L. Gallagher, L. Warr, A. Stroda, A. Siahvashi, Y. Ryu, S. Kim, S. G. Kim, Y. Seo, M. L. Johns and E. F. May, *Appl. Therm. Eng.*, 2021, **189**, 116735.
289 V. Jusko, S. Z. S. Al Ghafri and E. F. May, BoilFAST v1.0.0, **https://www.fsr.ecm.uwa.edu.au/software/boilfast/**.
290 M. Moran and T. E. D. Nyland, 28th Joint Propulsion Conference and Exhibit, American Institute of Aeronautics and Astronautics, 1992, DOI: **10.2514/6.1992-3063**.
291 M. E. Moran, T. W. Nyland and S. L. Driscoll, in *Advances in Cryogenic Engineering*, ed. R. W. Fast, Springer US, Boston, MA, 1991, DOI: **10.1007/978-1-4615-33**.
292 D. Chato, 29th Joint Propulsion Conference and Exhibit, American Institute of Aeronautics and Astronautics, 1993, DOI: **10.2514/6.1993-1967**.
293 W. Taylor and D. Chato, in 26th Thermophysics Conference, 1991, DOI: **10.2514/6.1991-1379**.
294 W. U. Notardonato, A. M. Swanger, J. E. Fesmire, K. M. Jumper, W. L. Johnson and T. M. Tomsik, *IOP Conf. Ser.: Mater. Sci. Eng.*, 2017, **278**, 012012.
295 W. U. Notardonato, A. M. Swanger, J. E. Fesmire, K. M. Jumper, W. L. Johnson and T. M. Tomsik, *Cryogenics*, 2017, **88**, 147–155.

296 W. U. Notardonato, W. L. Johnson, A. M. Swanger and T. Tomsik, *IOP Conf. Ser.: Mater. Sci. Eng.*, 2015, **101**, 012081.
297 A. M. Swanger, W. U. Notardonato, J. E. Fesmire, K. M. Jumper, W. L. Johnson and T. M. Tomsik, *IOP Conf. Ser.: Mater. Sci. Eng.*, 2017, **278**, 012013.
298 Y. Kim, C. Lee, J. Park, M. Seo and S. Jeong, *Cryogenics*, 2016, **74**, 123–130.
299 L. Wang, Y. Li, C. Li and Z. Zhao, *Cryogenics*, 2013, **57**, 63–73.
300 L. Wang, Y. Li, F. Zhang and Y. Ma, *Cryogenics*, 2015, **72**, 161–171.
301 L. Jin, C. Park, H. Cho, C. Lee and S. Jeong, *Cryogenics*, 2016, **79**, 96–105.
302 K. J. Kim, L. Jin, Y. Kim and S. Jeong, presented in part at the The 27th International Ocean and Polar Engineering Conference, San Francisco, California, USA, 2017/7/31/, 2017.
303 Y. Ma, Y. Li, K. Zhu, Y. Wang, L. Wang and H. Tan, *Int. J. Hydrogen Energy*, 2017, **42**, 8264–8277.
304 K. Maekawa, M. Takeda, Y. Miyake and H. Kumakura, *Sensors*, 2018, **18**, 3694.
305 Z. Zhongqi, J. Wenbing and H. Yonghua, *Cryogenics*, 2018, **96**, 116–124.
306 F. Pistani and K. Thiagarajan, *Ocean Eng.*, 2012, **52**, 60–74.
307 A. Rafiee, F. Pistani and K. Thiagarajan, *Comput. Mech.*, 2011, **47**, 65–75.
308 K. P. Thiagarajan, D. Rakshit and N. Repalle, *Ocean Eng.*, 2011, **38**, 498–508.
309 L. Decker, Liquid Hydrogen Distribution Technology-HYPER Closing Seminar, **https://www.sintef.no/globalassets/project/hyper/presentations-day-2/day2_1105_decker_liquid-hydrogen-distribution-technology_linde.pdf/**.
310 J. Kelley and E. Laumann, *Hydrogen Tomorrow: Demands & Technology Requirements*, NASA, California, 1975.
311 Australia and Japan develop safety standards for shipping liquid hydrogen, Australian Maritime Safety Authority, Australia, 2017.
312 H. Lee, Y. Shao, S. Lee, G. Roh, K. Chun and H. Kang, *Int. J. Hydrogen Energy*, 2019, **44**, 15056–15071.
313 A. Friedlander, R. Zubrin and T. Hardy, *Benefits of Slush Hydrogen for Space Missions*, National Aeronautics and Space Administration, Cleveland, Ohio, 1991.
314 F. Ma, P. Zhang and X. J. Shi, *Int. J. Heat Mass Transfer*, 2017, **110**, 482–495.
315 N. Frischauf, in *Compendium of Hydrogen Energy*, eds. M. Ball, A. Basile and T. N. Veziroğlu, Woodhead Publishing, Oxford, 2016, pp. 87–107, DOI: **10.1016/B978-1-78242-364-5.00005-1**.
316 M. T. Scelzo, L. Peveroni and J.-M. Buchlin, *AIAA Aviation 2020 Forum*, American Institute of Aeronautics and Astronautics, 2020, DOI: **10.2514/6.2020-3037**.
317 K. Ohira, *AIP Conf. Proc.*, 2004, **710**, 27–34.
318 K. Ohira, in *Compendium of Hydrogen Energy*, eds. R. B. Gupta, A. Basile and T. N. Veziroğlu, Woodhead Publishing, 2016, pp. 53–90, DOI: **10.1016/B978-1-78242-362-1.00003-1**.
319 S. Gursu, S. Sheriff, T. Veziroglu and J. Sheffield, *Int. J. Hydrogen Energy*, 1994, **19**, 491–496.
320 J. Verne, *Mysterious island*, Watermill Press, Mahwah, N.J., 1983.
321 International Energy Agency (IEA), Henry Hub Natural Gas Spot Price, **https://www.eia.gov/dnav/ng/hist/rngwhhdm.htm**.
322 N. Ferguson, *Doom: The Politics of Catastrophe*, Penguin Press, 2021.
323 D. Pritchards and W. Rattigan, Hazards of liquid hydrogen position paper, Health and Safety Executive, 2010.
324 T. Jordan, S. Jallais, L. Bernard, A. Venetsanos, S. Coldrick, M. Kuznetsov and D. Cirrone, presented in part at the International Conference on Hydrogen Safety, 2019.
325 K. Lyons, C. Proust, D. Cirrone, P. Hooker, M. Kuznetsov and S. Coldrick, Theory and analysis of ignition with specific conditions related to cryogenic hydrogen, **https://hysafe.info/wp-content/uploads/sites/3/2020/02/200127-WP4_D4_1_Theory-of-cryogenic-hydrogen-V1.2.pdf**.
326 Prenormative Research for Safe Use of Liquid Hydrogen (PRESLHY), **https://preslhy.eu/**.
327 S. Pique, B. Weinberger, V. De-Dianous and B. Debray, *Int. J. Hydrogen Energy*, 2017, **42**, 7429–7439.
328 G. Hinds, *Fuel Cells Bull.*, 2017, **2017**, 14–15.
329 Y. Yang, G. Wang, S. Zhang, L. Zhang and L. Lin, *E3S Web Conf.*, 2019, **118**, 03032.
330 J.-W. Kim, T. H. Lee and J.-W. Choi, *Trans. of the Korean Hydrogen and New Energy Society*, 2016, **27**, 245–255.
331 A. V. Tchouvelev, S. P. de Oliveira and N. P. Neves, in *Science and Engineering of Hydrogen-Based Energy Technologies*, ed. P. E. V. de Miranda, Academic Press, 2019, pp. 303–356, DOI: **10.1016/B978-0-12-814251-6.00006-X**.
332 S. Tomevska, *Hydrogen Technologies Standards Discussion Paper*, Standards Australia, Australia, 2018.
333 S. Tomevska, *Hydrogen Standards Forum Outcomes Report*, Standards Australia, Australia, 2018.
334 National Fire Protection Association. Hydrogen Technologies Code, **https://www.nfpa.org/codes-and-standards/all-codes-and-standards/list-of-codes-and-standards/detail?code=2**.
335 Y. Yang, G. Wang, S. Zhang, L. Zhang and L. Lin, *E3S Web Conf.*, 2019, **118**, 03042.
336 Safety Planning for Hydrogen and Fuel Cell Projects, European Hydrogen Safety Panel, Brussels, 2019.
337 International Maritime Organization. International Code for the Construction and Equipment of Ships Carrying Liquefied Gases in Bulk (IGC Code), **https://www.imo.org/en/OurWork/Environment/Pages/IGCCode.aspx**.
338 Hydrogen Risk Assessment Model (HyRAM), **https://energy.sandia.gov/programs/sustainable-transportation/hydrogen/hydrogen-safety-codes-and-standards/hydrogen-risk-assessment-model-hyram/**, (accessed January, 2019).
339 P. Ashworth and V. Lambert, *The Australian public's perception of hydrogen for energy, S. o. C. Engineering*, The University of Queensland, Queensland, Australia, 2018.
340 L. Garrity, presented in part at the Hydrogen and Fuel Cell Futures Conference, Perth, Australia, 12th–15th September 2004, 2004.

341 T. O'Garra, *Comparative Analysis of the Impact of the Hydrogen Bus Trials on Public Awareness, Attitudes and Preferences: a Comparative Study of Four Cities*, Imperial College, London, 2005.
342 G. Thesen and O. Langhelle, *Int. J. Hydrogen Energy*, 2008, **33**, 5859–5867.
343 R. Zimmer and J. Welke, *Int. J. Hydrogen Energy*, 2012, **37**, 17502–17508.
344 Australian Department of the Environment and Energy, Solar PV and batteries, **https://www.energy.gov.au/households/solar-pv-and-batteries**, (accessed January, 2019).
345 K. Itaoka, A. Saito and K. Sasaki, *Int. J. Hydrogen Energy*, 2017, **42**, 7290–7296.
346 Global Liquid Hydrogen Market Report 2019-2024, Business Wire, Dublin, 2019.
347 Asia Pacific Energy Research Centre (APERC), **https://aperc.or.jp/**.
348 Hydrogen for Australia's Future – A Briefing Paper for the COAG Energy Council, prepared by the Hydrogen Strategy Group, 2018, **http://www.coagenergycouncil.gov.au/publications/hydrogen-australias-future**.
349 T. Longden, F. J. Beck, F. Jotzo, R. Andrews and M. Prasad, *Appl. Energy*, 2022, **306**, 118145.
350 K. Buckland, Why Asia's biggest economies are backing hydrogen fuel cell cars, The Japan Times, 2019.
351 Germany launches world's first hydrogen-powered train, 2019, **https://www.theguardian.com/environment/2018/sep/17/germany-launches-worlds-first-hydrogen-powered-train**.
352 ACLNGF, Hydrogen liquefaction and storage symposium: outcomes report. September 2019., **https://lngfutures.edu.au/hydrogen-liquefaction-and-storage-symposium-outcomes-report-september-2019/**.
353 J. G. Reed, E. E. Dailey, B. P. Shaffer, B. A. Lane, R. J. Flores, A. A. Fong and G. S. Samuelsen, *Final Project Report - Roadmap for the Deployment and Buildout of Renewable Hydrogen Production Plants in California*, California Energy Commission, 2020.
354 J. R. Bartels, *A feasibility study of implementing an Ammonia Economy*, Iowa State University Digital Repository, 2008.
355 European Fertilizer Manufacturers Association, 2000.
356 F. R. D. Velázquez, J. Rodríguez and F. Galindo, Nitrogen+ Syngas, 2013.
357 H. Kobayashi, A. Hayakawa, K. D. Kunkuma, A. Somarathne and E. C. Okafor, *Proc. Combust. Inst.*, 2019, **37**, 109–133.
358 G. Jeerh, M. Zhang and S. Tao, *J. Mater. Chem. A*, 2021, **9**, 727–752.
359 A. Valera-Medina, F. Amer-Hatem, A. K. Azad, I. C. Dedoussi, M. de Joannon, R. X. Fernandes, P. Glarborg, H. Hashemi, X. He, S. Mashruk, J. McGowan, C. Mounaim-Rouselle, A. Ortiz-Prado, A. Ortiz-Valera, I. Rossetti, B. Shu, M. Yehia, H. Xiao and M. Costa, *Energy Fuels*, 2021, **35**, 6964–7029.
360 SINTEF, Presentations from the HYPER closing seminar, **https://www.sintef.no/projectweb/hyper/presentations-from-the-hyper-closeing-seminar/**.
361 EU Science Hub – Joint Research Centre, Assessment of Hydrogen Delivery Options, **https://ec.europa.eu/jrc/sites/default/files/jrc124206_assessment_of_hydrogen_delivery_options.pdf**.
362 R. Maha, T. Marine, D. Florence, D. Jonathan and C. Marian, *Chin. J. Catal.*, 2020, **41**, 756–769.
363 R. Maha, T. Marine, D. Florence, D. Jonathan and C. Marian, *Chin. J. Catal.*, 2020, **41**, 770–782.
364 M. S. Sadaghiani, A. Siahvashi, B. W. E. Norris, S. Z. S. Al Ghafri, A. Arami-Niya and E. F. May, *Energy*, 2022, **250**, 123789.
365 A. Siahvashi, S. Z. S. Al Ghafri and E. F. May, *Fluid Phase Equilib.*, 2020, **519**, 112609.
366 A. Siahvashi, *PhD*, The University of Western Australia, 2019.
367 A. Siahvashi, S. Z. S. Al Ghafri, T. J. Hughes, B. F. Graham, S. H. Huang and E. F. May, *J. Exp. Therm. Fluid Sci.*, 2019, **105**, 47–57.
368 A. Siahvashi, S. Z. S. Al Ghafri, J. H. Oakley, T. J. Hughes, B. F. Graham and E. F. May, *J. Chem. Eng. Data*, 2017, **62**, 2896–2910.
369 C. C. Sampson, P. J. Metaxas, A. Siahvashi, P. L. Stanwix, B. F. Graham, M. L. Johns and E. F. May, *Chem. Eng. J.*, 2021, **407**, 127086.
370 J. P. Kohn and K. D. Luks, *GPA Research Report RR-22: Solubility of Hydrocarbons in Cryogenic LNG and NGL Mixtures*, Gas Processors Association, 1976.
371 M. Hopkins, A. Siahvashi, X. Yang, M. Richter, P. Stanwix and E. May, *Fuel Process. Technol.*, 2021, **219**, 106878.